

Stable Strontium Isotope ($\delta^{88/86}\text{Sr}$) Fractionation in the Marine Realm: A Pilot Study

DISSERTATION

zur Erlangung des Doktorgrades

Dr. rer. nat.

der Mathematisch-Naturwissenschaftlichen Fakultät
der Christian-Albrechts-Universität zu Kiel

Vorgelegt von

André Krabbenhöft

Kiel, 2011

... dedicated to my family

Referent:

Prof.Dr. Anton Eisenhauer

Korreferent:

Priv.Doz.Dr. Thor Hansteen

Tag der mündlichen Prüfung:

22.03.2011

Zum Druck genehmigt:

Kiel, 22.03.2011

Der Dekan

Hiermit erkläre ich, dass ich die vorliegende Doktorarbeit selbstständig und ohne Zuhilfenahme unerlaubter Hilfsmittel erstellt habe. Weder diese noch eine ähnliche Arbeit wurde an einer anderen Abteilung oder Hochschule im Rahmen eines Prüfungsverfahrens vorgelegt, veröffentlicht oder zur Veröffentlichung vorgelegt. Ferner versichere ich, dass die Arbeit unter Einhaltung der Regeln guter wissenschaftlicher Praxis der Deutschen Forschungsgemeinschaft entstanden ist.

Kiel, den 22.3.2011

André Krabbenhöft

Abstract

The determination of the isotopic composition of natural substances is an important field of research within isotope geochemistry. Especially the investigation of the alkaline earth element strontium (Sr) plays an important role in geological and geochemical research. In order to quantify the degree of natural stable Sr isotope fractionation a double spike technique was developed in the frame of this study. This technique allows the precise determination of natural Sr isotope fractionation without normalizing the $^{87}\text{Sr}/^{86}\text{Sr}$ to a fixed $^{88}\text{Sr}/^{86}\text{Sr}$ ratio in order to correct for instrumental mass fractionation. Variations in the stable Sr isotope ratio are presented in the common δ -notation in per mill [‰] deviation from standard material NIST SRM 987 ($\delta^{88/86}\text{Sr}[\text{‰}] = ((^{88}\text{Sr}/^{86}\text{Sr})_{\text{sample}} / (^{88}\text{Sr}/^{86}\text{Sr})_{\text{standard}} - 1) \cdot 1000$). Measurements were carried out at the IFM-GEOMAR in Kiel using a thermal ionization mass spectrometer (TIMS). Long term measurements of the coral standard JcP-1 and the seawater standard IAPSO resulted in $\delta^{88/86}\text{Sr} = 0.194 \pm 0.025\text{‰}$ and $\delta^{88/86}\text{Sr} = 0.389 \pm 0.026\text{‰}$ (2SD), respectively. This corresponds to an improvement of measurement precision of at least a factor of 2 when compared to multi collector inductively coupled plasma mass spectrometer (MC-ICP-MS) measurements using bracketing standard (FIETZKE and EISENHAUER, 2006).

The precise determination of natural Sr isotope fractionation adds a new dimension to the well established radiogenic Sr isotope system. Seawater and marine carbonates show significant differences in their stable Sr isotopic composition which were not accessible by applying the radiogenic $^{87}\text{Sr}/^{86}\text{Sr}$ ratio alone. In order to constrain glacial/interglacial changes in the marine Sr budget the isotope composition of modern seawater and modern marine biogenic carbonates are compared with the corresponding values of river waters and hydrothermal solutions in a triple isotope plot ($\delta^{88/86}\text{Sr}$ vs. $^{87}\text{Sr}/^{86}\text{Sr}$). The Sr sources ($^{87}\text{Sr}/^{86}\text{Sr} \sim 0.7106 \pm 0.0008$, $\delta^{88/86}\text{Sr} \sim 0.31 \pm 0.01\text{‰}$) show a heavier isotopic composition compared to marine carbonates ($^{87}\text{Sr}/^{86}\text{Sr} \sim 0.70926 \pm 0.00002$, $\delta^{88/86}\text{Sr} \sim 0.21 \pm 0.02\text{‰}$), representing the main Sr sink. This reflects isotopic disequilibrium with respect to Sr inputs and outputs. In contrast to the modern ocean, isotope equilibrium between inputs and outputs was achieved during the last glacial maximum (10-30 kyr before present). This can be explained by invoking three times higher Sr inputs from a uniquely "glacial" source: weathering of shelf carbonates exposed at low sea levels. Our data are also consistent with the "weathering peak" hypothesis that invokes enhanced Sr inputs resulting from weathering of post-glacial abundant fine-grained material left exposed by the retreating ice masses (VANCE et al., 2009).

Furthermore, the temperature dependency of $\delta^{88/86}\text{Sr}$ in cultured and temperature controlled (21°C to 29°C) warm water corals (*Acropora* sp.) was investigated. A strict linear trend like reported by (FIETZKE and EISENHAUER, 2006; RÜGGERBERG et al., 2008) could not be confirmed in this study. Our measurements rather revealed a nonlinear relationship between temperature and $\delta^{88/86}\text{Sr}$ ($\delta^{88/86}\text{Sr} = 0.001 \cdot T^2 - 0.039 \cdot T + 0.692$, $r^2 = 0.47$) whereas the Sr/Ca ratio shows the expected linear

trend. Moreover, we determined $\delta^{88/86}\text{Sr}$ -, $\delta^{18}\text{O}$ - and Sr/Ca-ratios of a fossil (15 kyr B.P.) *Porites* sp. coral originating from Tahiti (French-Polynesia). The Sr/Ca as well as the isotope ratios shows a similar seasonal variability. Fossil *Porites* sp. ($\delta^{88/86}\text{Sr}_{\text{mean}}=0.205\pm 0.017\text{‰}$, 2SEM) and recent *Porites* sp. represented in this study by the coral standard JCp-1 ($\delta^{88/86}\text{Sr}_{\text{JCp-1}}=0.194\pm 0.009\text{‰}$, 2SEM) show connatural mean $\delta^{88/86}\text{Sr}$ values. The average $\delta^{88/86}\text{Sr}$ is obviously not affected by enhanced weathering and elevated Sr fluxes from exposed shelves during glacial times like it is the case for Sr/Ca elemental ratios. Therefore, stable Sr isotope fractionation can potentially serve as independent and unbiased parameter for reconstructing paleo-sea-surface-temperatures.

Kurzfassung

Die Bestimmung der isotopischen Zusammensetzung natürlicher Substanzen ist ein wichtiges Forschungsfeld der Isotopengeochemie. Speziell die Untersuchung des Erdalkalielements Strontium (Sr) spielt eine wichtige Rolle in der geologischen und geochemischen Forschung. Um den Grad der natürlichen Sr Isotopenfraktionierung zu bestimmen wurde im Rahmen dieser Arbeit eine Doppelspike Methode entwickelt. Diese Methode erlaubt die präzise Bestimmung der natürlichen Sr Isotopenfraktionierung ohne das $^{87}\text{Sr}/^{86}\text{Sr}$ Verhältnis auf ein konstantes $^{88}\text{Sr}/^{86}\text{Sr}$ Verhältnisses zu normieren, um für die maschinelle Isotopenfraktionierung zu korrigieren. Variationen des $^{88}\text{Sr}/^{86}\text{Sr}$ werden in der üblichen δ -Notation als Abweichung vom Strontiumcarbonatstandard NIST SRM987 in Promille [‰] angegeben ($\delta^{88/86}\text{Sr} [\text{‰}] = ((^{88}\text{Sr}/^{86}\text{Sr})_{\text{Probe}} / (^{88}\text{Sr}/^{86}\text{Sr})_{\text{Standard}} - 1) \cdot 1000$). Die Messungen wurden an einem Thermionen-Massenspektrometer (TIMS) am IFM-GEOMAR in Kiel durchgeführt. Der Korallenstandard Standard JcP-1 und der Meerwasser Standard IAPSO wurden mit $\delta^{88/86}\text{Sr} = 0.194 \pm 0.025\text{‰}$ bzw. $\delta^{88/86}\text{Sr} = 0.389 \pm 0.026\text{‰}$ (2SD) bestimmt. Dies entspricht, verglichen mit Multikollector- induktiv gekoppelter Plasma-Massenspektrometrie (MC-ICP-MS) unter Verwendung der Bracketing Standard Methode (FIETZKE and EISENHAUER, 2006), einer Verbesserung der Messgenauigkeit mindestens um den Faktor 2.

Die präzise Bestimmung natürlicher Sr Isotopenfraktionierung erweitert das etablierte radiogene Sr Isotopensystem um eine zusätzliche Dimension. Dadurch lassen sich marine Carbonate nun isotopisch vom Meerwasser unterscheiden, was aufgrund der Normierung auf ein festes $^{88}\text{Sr}/^{86}\text{Sr}$ Verhältnis vorher nicht möglich war. Um Änderungen im Sr Budget des Ozean während Glazial/Interglazial Übergängen zu untersuchen, werden die Isotopien von rezemem Meerwasser und rezemten biogenen marinen Carbonaten mit den entsprechenden Werten von Flusswasser und Hydrothermalfluiden in einem drei Isotopen Diagramm verglichen ($\delta^{88/86}\text{Sr}$ vs. $^{87}\text{Sr}/^{86}\text{Sr}$). Die Sr Quellen ($^{87}\text{Sr}/^{86}\text{Sr} \sim 0.7106 \pm 0.0008$, $\delta^{88/86}\text{Sr} \sim 0.31 \pm 0.01\text{‰}$) zeigen dabei eine schwerere Isotopie als marine Carbonates ($^{87}\text{Sr}/^{86}\text{Sr} \sim 0.70926 \pm 0.00002$, $\delta^{88/86}\text{Sr} \sim 0.21 \pm 0.02\text{‰}$), welche die wichtigste Sr Senke des Ozeans repräsentieren. Dieser Unterschied zwischen Sr Quellen und Senken zeigt, dass sich der heutige Ozean im isotopischen Ungleichgewicht befindet. Während der letzten Eiszeit (10-30 ka v.h.) befand sich der Ozean im isotopischen Gleichgewicht. Dies kann durch einen ~ 3 Mal höheren Sr Fluss, verursacht durch die Verwitterung freiliegender Schelfe, erklärt werden. Der Unterschied in der radiogenen Signatur der Sr Quelle zum Gleichgewichtswert unterstützt die Hypothese eines „Verwitterungspeak“. Dabei kommt es zu einem zusätzlichen post-glazialen Sr Eintrag durch die Verwitterung des von den Gletschern zurückgelassenen feinen Gesteinssubstrats (VANCE et al., 2009). Ein weiterer Schwerpunkt dieser Arbeit ist die Untersuchung der Temperatursensitivität des $\delta^{88/86}\text{Sr}$. Dazu wurde die Sr Isotopie von Warmwasserkorallen (*Acropora* sp.) aus temperaturkontrollierten Hälterungsexperimenten (21°C bis 29°C) untersucht. Ein streng linearer Zusammenhang zwischen

Wassertemperatur und $\delta^{88/86}\text{Sr}$, welcher zuvor gefunden wurde (FIETZKE and EISENHAEUER, 2006; RÜGGERBERG et al., 2008), konnte hier nicht bestätigt werden. Vielmehr zeigen die $\delta^{88/86}\text{Sr}$ Daten einen quadratischen Zusammenhang mit der Hälterungstemperatur, wohingegen die Sr/Ca Daten den erwarteten linearen Zusammenhang zeigten.

Des Weiteren wurden $\delta^{88/86}\text{Sr}$ -, $\delta^{18}\text{O}$ - und Sr/Ca Verhältnisse einer fossilen (~15 ka) *Porites* Koralle aus Tahiti (Französisch-Polynesien) analysiert. Das Elementverhältnis Sr/Ca sowie die Isotopen zeigen ähnliche saisonale Verläufe. Im Mittel zeigt die fossile *Porites* Koralle eine vergleichbare Sr Isotopie ($\delta^{88/86}\text{Sr}_{\text{mittel}}=0.205\pm 0.017\text{‰}$) wie rezente *Porites* Korallen die in dieser Studie durch den Korallenstandard JcP-1 repräsentiert werden ($\delta^{88/86}\text{Sr}_{\text{JcP-1}}=0.194\pm 0.009\text{‰}$). Im Gegensatz zum Sr/Ca Verhältnis ist das mittlere $\delta^{88/86}\text{Sr}$ offensichtlich nicht durch verstärkte Verwitterung freiliegender Schelfe, wie sie während Eiszeiten stattfindet, beeinflusst. Daher kann $\delta^{88/86}\text{Sr}$ als unabhängiger Parameter zur Rekonstruktion von früheren Oberflächenwassertemperaturen herangezogen werden.

Table of contents

Abstract	I
Kurzfassung	III
Table of contents	V
List of figures	IX
List of tables	X
List of abbreviations	XI
I. General introduction	13
I.1 Non-traditional stable isotope geochemistry	13
I.2 Marine carbonates – A proxy archive	14
I.3 Isotope fractionation	16
I.3.1 Equilibrium isotope fractionation	18
I.3.2 Kinetic isotope fractionation.....	19
I.3.3 Rayleigh fractionation.....	20
I.4 Strontium isotope geochemistry	20
I.4.1 The radiogenic strontium isotope system	21
I.4.2 The stable strontium isotope system.....	25
I.5 Thermal ionization mass spectrometry	29
I.6 Correction methods for instrumental isotope fractionation.....	30
I.6.1 Internal normalization	31
I.6.2 Bracketing standard method	32
I.6.3 The double spike technique.....	34
I.7 Thesis outline	37
I.8 References	39
II. Determination of radiogenic and stable strontium isotope ratios ($^{87}\text{Sr}/^{86}\text{Sr}$, $\delta^{88/86}\text{Sr}$) by thermal ionization mass spectrometry applying an $^{87}\text{Sr}/^{84}\text{Sr}$ double spike	49
II.1 Abstract.....	49
II.2 Introduction	49

II.3	Experimental methods and TIMS measurement.....	51
II.3.1	$^{87}\text{Sr}/^{84}\text{Sr}$ -double spike preparation	51
II.3.2	TIMS multicollector measurement procedure	51
II.3.3	Double spike algorithm.....	53
II.4	Results.....	54
II.4.1	Spike calibration	54
II.4.2	Results of standard measurements.....	56
II.5	Conclusions.....	59
II.6	Tables.....	60
II.7	Acknowledgements	60
II.8	References	61
III. Constraining the Marine Strontium Budget with Natural Strontium Isotope		
Fractionations ($^{87}\text{Sr}/^{86}\text{Sr}^*$, $\delta^{88/86}\text{Sr}$) of Carbonates, Hydrothermal Solutions and River		
Waters..... 63		
III.1	Abstract.....	63
III.2	Introduction	64
III.3	Materials and methods.....	66
III.3.1	River waters	66
III.3.2	Hydrothermal solutions.....	67
III.3.3	Marine carbonates.....	67
III.3.4	Sample preparation	68
III.3.5	TIMS measurements.....	68
III.4	Results.....	69
III.4.1	Sr isotope composition of the marine input.....	69
III.4.1.1	Sr isotope composition of the riverine discharge to the ocean	69
III.4.1.2	Sr isotope composition of the hydrothermal discharge to the ocean	70
III.4.1.3	Sr composition of the combined riverine and hydrothermal input to the ocean	72
III.4.2	Isotope composition of the marine Sr output	72
III.5	Discussion	74

III.5.1	Sr budget of the global ocean	74
III.6	Sr isotope equilibrium in the ocean during the last glacial.....	76
III.7	Sr budget disequilibrium during glacial/interglacial transitions	77
III.8	Conclusion.....	78
III.9	Tables	79
III.10	Acknowledgements.....	82
III.11	Appendix	82
III.11.1	Notation and terminology.....	82
III.11.2	Sr mass fractionation	82
III.11.3	Error notation and propagation.....	83
III.11.4	Calculation of flux-weighted mean global river discharge to the ocean	83
III.11.5	Calculation of flux-weighted mean global input to the ocean	83
III.11.6	Isotope equilibrium.....	83
III.12	References	84
IV.	Strontium Isotope ($\delta^{88/86}\text{Sr}$) Fractionation in Scleractinian Warm Water Corals.....	89
IV.1	Abstract.....	89
IV.2	Introduction	89
IV.3	Materials	90
IV.3.1	Cultured warm water coral (<i>Acropora</i> sp.)	90
IV.3.2	Fossil warm water coral (<i>Porites</i> sp.)	91
IV.4	Methods.....	92
IV.4.1	Sampling, chemical preparation and measurements	92
IV.4.2	Stable strontium ($\delta^{88/86}\text{Sr}$) measurements.....	93
IV.4.3	Sr/Ca and $\delta^{18}\text{O}$ measurements	93
IV.5	Results.....	93
IV.5.1	Temperature- $\delta^{88/86}\text{Sr}$ relationships of <i>Acropora</i> sp.	94
IV.5.2	Temperature- $\delta^{88/86}\text{Sr}$ relationships of a fossil <i>Porites</i> sp. (Tahiti).....	96
IV.6	Discussion.....	99

IV.6.1	Temperature dependence of $\delta^{88/86}\text{Sr}$ in <i>Acropora</i> sp.	99
IV.6.2	Tahiti record IODP Expedition 310 (fossil <i>Porites</i> sp.)	99
IV.7	Conclusion	100
IV.8	Acknowledgements	101
IV.9	References	102
IV.10	Tables.....	103
V.	Summary and outlook.....	107
VI.	Appendix	111
VI.1	Conference Abstracts	111
VI.1.1	AGU Fall Meeting 2008.....	111
VI.1.2	AGU Fall Meeting 2009.....	112
VI.1.3	Goldschmidt Conference 2009	113
VI.1.4	Geologische Vereinigung Annual Meeting 2009	114
VI.2	Data export and evaluation manual	115
VI.2.1	Data export from TIMS	115
VI.2.2	Data reduction with the EXCEL [®] spread sheet	116
VI.2.2.1	Overview.....	116
VI.2.3	Data import to Excel [®]	117
VI.2.3.1	Worksheet “1” – “21”	117
VI.2.3.2	Worksheet “précis”	118
VI.2.4	Data evaluation.....	119
VI.2.5	Standard measurement.....	119
VI.2.5.1	Sample measurement.....	120
VI.2.5.2	Blank measurement.....	120
VI.2.6	Error detection “cookbook”	120
VI.2.7	Further information.....	121
VI.3	The Sr double spike data reduction algorithm	123
VI.4	Acknowledgements	127

VI.5	Curriculum Vitae	128
List of figures		
I. GENERAL INTRODUCTION		
fig.I.1:	The seawater Sr evolution curve modified after (MCARTHUR et al., 2001).	23
fig.I.2:	The range of stable Sr values of different materials measured in different studies.	29
fig.I.3:	Principal of mass fractionation correction via internal normalization. The measured $^{87}\text{Sr}/^{86}\text{Sr}$ ratio is normalized to a fixed $^{88}\text{Sr}/^{86}\text{Sr}=8.375209$ ratio (NIER, 1938).	31
fig.I.4:	Schematic sketch of the double spike technique in a three isotope space.	35
fig.I.5:	Long term reproducibility of the coral standard JCp-1. We determined the stable Sr isotope composition with $0.194\pm 0.025\%$ (2SD).	36
fig.I.6:	Long term reproducibility of the seawater standard IAPSO. We determined the stable Sr isotope composition with $0.389\pm 0.026\%$ (2SD).	36
II. MANUSCRIPT I		
fig.II.1:	Flow Chart of the Sr-double spike algorithm.	52
fig.II.2:	Results of standard (SRM987) measurements with different $^{84}\text{Sr}_{\text{sample}}/^{84}\text{Sr}_{\text{spike}}$ ratios with <i>uncalibrated</i> double spike solution.	55
fig.II.3:	Results of standard (SRM987) measurements with different $^{84}\text{Sr}_{\text{sample}}/^{84}\text{Sr}_{\text{spike}}$ ratios with <i>calibrated</i> double spike solution.	56
fig.II.4:	Longterm session-to-session variations for the SRM987 standard.	56
fig.II.5:	Longterm results of IAPSO seawater standard $\delta^{88/86}\text{Sr}$ measurements.	57
fig.II.6:	Longterm results of JCp-1 coral standard $\delta^{88/86}\text{Sr}$ measurements.	58
III. MANUSCRIPT II		
fig.III.1:	$(^{87}\text{Sr}/^{86}\text{Sr}^*, \delta^{88/86}\text{Sr})_{\text{River}}$ -values of the investigated rivers plotted in a triple isotope plot.	66
fig.III.2:	$(^{87}\text{Sr}/^{86}\text{Sr}^*, \delta^{88/86}\text{Sr})$ -values of hydrothermal fluid samples.	71
fig.III.3:	Triple isotope plot showing the flux-weighted average Sr isotope values of rivers, hydrothermal fluids, marine carbonates and seawater.	75
IV. MANUSCRIPT III		
fig.IV.1:	Sampling location of fossil warm-water coral <i>Porites</i> sp..	94
fig.IV.2:	Sketch of cultured <i>Acropora</i> sp. and results of the heterogeneity test.	96
fig.IV.3:	Linear relationship between $\delta^{88/86}\text{Sr}$ and temperature in the range between 21 and 25°C.	97
fig.IV.4:	Stable Sr and Sr/Ca values of <i>Acropora</i> sp. vs. temperature.	98
fig.IV.5:	Stable Sr data of one annual cycle of a fossil (15 kyr B.P.) <i>Porites</i> sp. from Tahiti.	99
fig.IV.6:	Comparison of Sr/Ca, $\delta^{18}\text{O}$ and $\delta^{88/86}\text{Sr}$ data of fossil <i>Porites</i> sp..	100

V. APPENDIX

fig.VI.1: TIMS data evaluation software.	118
fig.VI.2: Worksheets within the EXCEL [®] spreadsheet for stable Sr data reduction.	119
fig.VI.3: Data import to the EXCEL [®] spreadsheet.	120
fig.VI.4: Free parameters in worksheet 1-21.	121
fig.VI.5: Labeling of the samples.	122
fig.VI.6: Labeling systematic in worksheet “précis”.	123

List of tables
I. GENERAL INTRODUCTION

tab.I.1: Results of stable Sr measurements of selected studies available so far.	28
--	----

II. MANUSCRIPT I

tab.II.1: Original isotopic composition of the Oak Ridge National Laboratory Sr carbonate standards used to mix the double spike.	61
tab.II.2: Sample treatment prior mass spectrometric analysis.	61
tab.II.3: Calibrated Sr isotopic composition of the double spike solution.	61

III. MANUSCRIPT II

tab.III.1: Sr isotope data and annual Sr fluxes of selected rivers.	79
tab.III.2: Mg/Sr and Sr isotopic composition of hydrothermal fluids.	79
tab.III.3: Sr burial fluxes and isotopic composition of the oceans Sr output.	80
tab.III.4: The isotopic composition and fluxes of the oceans Sr sources.	90

IV. MANUSCRIPT III

tab.IV.1: Stable Sr and Sr/Ca data of <i>Acropora</i> sp.	105
tab.IV.2: Stable Sr data of fossil <i>Porites</i> sp. from Tahiti.	106

List of abbreviations

B.P.	–	Before present
CC	–	Calcium Carbonate
DIC	–	Dissolved Inorganic Carbon
MAR	–	Mid Atlantic Ridge
MC	–	Marine Calcifiers
MC-ICP-MS	–	Multi Collector Inductively Coupled Plasma Mass Spectrometer
MOR	–	Mid Ocean Ridge
PPM	–	Parts per Million
RSD	–	Relative Standard Deviation
SD	–	Standard Deviation
SEM	–	Standard Error of the Mean
SIS	–	Strontium Isotope Stratigraphy
SSS	–	Sea Surface Salinity
SST	–	Sea Surface Temperature
SW	–	Seawater
TIMS	–	Thermal Ionisation Mass Spectrometer

Chapter I

GENERAL INTRODUCTION

I. General introduction

I.1 Non-traditional stable isotope geochemistry

The determination of variations in the isotopic composition of elements in different materials arising from chemical, biological or physical processes rather than nuclear processes provides the basis of '*stable isotope geochemistry*'.

Since the invention of the mass spectrometer in the first half of the 20th century the isotopic composition of different materials has been investigated in order to give answers to geological questions. Due to the low resolution of these early instruments, it was not possible to resolve isotopic variations smaller than several hundred per mill [‰]. Only isotope systems with a radiogenic component like the strontium (Sr) isotope system or '*light*' stable isotopes with a large relative mass difference like carbon (C), nitrogen (N), hydrogen (H) or oxygen (O) show natural isotopic variations large enough to be resolved at this early stage of stable isotope geochemistry. Light elements have been investigated since the late 1930's when Alfred O. Nier demonstrated the natural variability of their isotopic composition (NIER, 1938).

The theoretical basis for the mechanisms driving natural stable isotope fractionation was provided by (UREY, 1947) who - in wise foresight - suggested that the natural fractionation of stable isotopes can provide useful geochemical and geological information. He determined the isotope fractionation of several natural substances and also investigated its temperature dependency. Stable isotope geochemistry since then is a continuously growing field of research not only in geochemistry. The investigation of variations in the isotopic composition of '*traditional*' stable isotopes (e.g.: C, N, H, O) in different materials provided important insights into the earth's system and its geological history.

Recent studies also focus their attention on variations in the isotopic composition of the so called '*non-traditional*' stable isotopes, such as e.g. lithium (Li), calcium (Ca), magnesium (Mg) and strontium (Sr). This trend is based on improvements in instrumentation and analytical precision of mass spectrometry. With the advent of new generation mass spectrometers like multi collector inductively coupled plasma mass spectrometers (MC-ICP-MS) and improved thermal ionization mass spectrometers (TIMS) as well as innovative analytical improvements, particularly for elements with four or more stable isotopes, even isotopic variations in the range of a view parts per million [ppm] are now detectable. The progress in this field of research opened new areas of the periodic table for the investigation of natural stable isotope fractionation and paved the way for '*non-traditional stable isotope geochemistry*'. A detailed review of the relatively new field of non-traditional stable isotope geochemistry is given by e.g. (BULLEN and EISENHAUER, 2009; EISENHAUER et al., 2009; JOHNSON et al., 2004).

I.2 Marine carbonates – A proxy archive

A major goal of geochemical research is the reliable reconstruction of changes in past environmental conditions which is essential for accurate predictions of future climate development. The ocean as a major geochemical reservoir reacts very sensitively to environmental changes which are reflected by variations in e.g. the oceans chemical composition, sea surface temperatures (SST) or sea surface salinities (SSS).

Elemental or isotopic ratios that are either directly or indirectly coupled to changes of environmental parameters are termed '*proxies*'. Therefore, a downcore record of a proxy covering a continuous time interval can be utilized to reconstruct variations of environmental conditions. To be suitable for geochemistry, a marine archive has to fulfill specific requirements. It has to be easily accessible, robust (it should not be prone to diagenesis), should record information about environmental parameters continuously and - of course - it should be abundant in the time interval of interest. The preservation of the original geochemical signature is the most important property characterizing such an archive.

Corals meet most of the desired requirements demanded for geochemical research and they are used to extend records of environmental parameters back in time. These attributes combined with rapid growth rates (commonly 10-20 mm/yr), the presence of annual skeletal banding that provides precise chronology (KNUTSON et al., 1972), the longevity of individual colonies (commonly >100 yrs) and the fact that their CaCO₃ skeleton is suitable for high-resolution ¹⁴C and U-Th-series dating make corals exceptional archives of climate conditions for timescales of 10² up to 10⁵ years. Additionally, they are widely distributed in tropical / subtropical zones and cover a variety of different environmental settings. Corals, especially *Porites* spp., yields continuous reconstructions of environmental and climatic parameters, with annual to monthly resolution back to several thousand years ago (FELIS et al., 2000; GAGAN et al., 2000; KUHNERT et al., 2000; PÄTZOLD, 1984; COBB et al., 2008).

During CaCO₃ precipitation (biologically or inorganically) Ca is partly substituted by Sr (and other trace metals like e.g. Mg, Li, Ba) in the crystal lattice which is due to the chemical and physical similarity of these divalent cations. The magnitude of this elemental exchange and subsequently the substitution of Ca by different Sr isotopes chiefly depends on environmental parameters (e.g. temperature).

Therefore, elemental ratios (e.g. Sr/Ca) and potentially stable Sr isotope fractionation in biologically precipitated calcium carbonate (CaCO₃) are interesting in terms of their applicability as paleo-climate proxy.

Biological CaCO_3 mainly occurs in form of calcite (e.g. foraminifera, coccolithophores, brachiopods and some mussels) and aragonite (e.g. corals, green algae and most molluscs) with aragonite having a ten times higher Sr concentration (~10000 ppm) compared to calcite (~1000 ppm) (MILLIMAN, 1974). Variations of the Sr/Ca ratio in marine carbonates are a direct consequence of the temperature dependence of the Sr partitioning coefficient between seawater and aragonite/calcite. In calcite the Sr/Ca ratio mainly depends on precipitation rate and shows only a weak temperature effect (TANG et al., 2008). Therefore, Sr/Ca ratios of marine carbonates have been used for SST reconstruction (BECK et al., 1992; MCCULLOCH et al., 1994; PFEIFFER et al., 2006; SHEN et al., 1996). Skeletal Mg/Ca ratios (MITSUGUCHI et al., 1996) and U/Ca ratios (CARDINAL et al., 2001; MIN et al., 1995) have also been proposed as SST proxies. It was reported that temperature might not be the only controlling parameter of these elemental ratios (CARDINAL et al., 2001). All these elemental ratios are influenced by other parameters beside temperature like e.g. the seawater composition, growth rate or other “vital effects”.

But not only elemental ratios are utilized as proxies for the reconstruction of past environmental conditions. Variations in the stable isotopes composition of marine carbonates also provide important insights in past climate development. The first stable isotope ratio in coral skeletons used for SST reconstruction was $\delta^{18}\text{O}$ (WEBER and WOODHEAD, 1972) (for a definition of the δ -notation see chapter I.4). It was also applied in many other studies like e.g. (CHAKRABORTY and RAMESH, 1993; DUNBAR et al., 1994; FELIS et al., 2000; LEDER et al., 1996) where corals have been employed as paleo-climate archive. The stable isotope ratio $\delta^{18}\text{O}$ the most widely used temperature proxy in corals. The theoretical basis for $\delta^{18}\text{O}$ as a paleo-thermometer was established by (UREY, 1947). Calculations were verified with laboratory experiments of inorganic calcites by (MCCREA, 1950). Because of the seasonal cycle's effect on the $\delta^{18}\text{O}$ of coralline aragonite, early work confirmed that the alternating density bands of coral skeletons often represented annual accumulation (FAIRBANKS and DODGE, 1979). In addition, long term records from modern corals in the tropics record variations in the amplitude and period of the El Nino Southern Oscillation (ENSO; e.g., (COLE et al., 1993a)). The use of $\delta^{18}\text{O}$ as paleo-thermometer on glacial timescales is limited due to its dependency of global ice volume (SHACKLETON, 1967). On shorter timescales $\delta^{18}\text{O}$ is also influenced by the local variability of e.g. salinity and $\delta^{18}\text{O}_{\text{seawater}}$. Nevertheless, $\delta^{18}\text{O}$ values derived from biogenic carbonates are a fundamental tool for reconstructing past climates (ADKINS et al., 2003).

Carbon isotopes ($\delta^{13}\text{C}$) also have been used as proxy for e.g. nutrient availability, biological activity or to identify deep ocean water masses. The work of (MCCONNAUGHEY, 1989) for example showed that the uptake of dissolved inorganic carbon (DIC) by the coral symbiont affects the skeletal carbon isotopic composition. These symbionts preferentially incorporate the light C isotopes leaving the heavier C isotopes for incorporation in the coral skeletons crystal lattice. The interpretation of

seasonal variations of $\delta^{13}\text{C}$ of coral skeletons in environmental terms is still under debate (SWART et al., 1996). Most likely the main driving factor of seasonal variations in zooxanthellate corals is the photosynthetic activity of their symbionts and is therefore related to the seasonal light cycle, cloudiness or water column transparency (FAIRBANKS and DODGE, 1979; MCCONNAUGHEY, 1989; PÄTZOLD, 1984).

Recent studies also focus their attention on the natural fractionation of non-traditional stable isotopes. The isotope fractionation of Ca ($\delta^{44/40}\text{Ca}$) in cultured (*Acropora* sp.) and open ocean tropical reef corals (*Pavona clavus*, *Porites* sp.) are positively correlated with growth temperature as published by (BÖHM et al., 2006). A similar slope was reported for all investigated species to be about 0.02‰/°C. The results are similar to the temperature dependence of $\delta^{44/40}\text{Ca}$ found in cultured foraminifera (*Orbulina universa*, 0.019‰/°C) and inorganically precipitated aragonite (0.015‰/°C) as published by (GUSSONE et al., 2003). The calcium isotope fractionation in another foraminifera species (*Globigerinoides sacculifer*) was investigated by (NÄGLER et al., 2000) who reported a significantly steeper slope of 0.24‰/°C.

Measurements of Lithium (Li) isotopes in planktonic foraminifera (*Globigerinoides* and *Globorotalia*) did not show isotope fractionation during precipitation from seawater (VIGIER et al., 2007). On the other hand, the study of (ROLLION-BARD et al., 2009) revealed significant Li isotopes fractionation between seawater and coral aragonite ($\delta^7\text{Li}_{\text{skeleton}} - \delta^7\text{Li}_{\text{seawater}} = \Delta_{\text{sw-coral}} = -12.8 \pm 0.4\text{‰}$ to $-8.1 \pm 1.1\text{‰}$, 2SD) in warm water corals (*C. caespitosa*) and cold water corals (*D. cristagalli* and *L. pertusa*). These results are in agreement with the experimentally determined lithium isotope fractionation of inorganic calcite (-11.7‰ , (MARRIOTT et al., 2004))

Like mentioned above, the Sr/Ca element ratio is often used as paleo-thermometer. Strontium is the major element that substitutes Ca in the aragonitic skeleton of marine calcifiers (in calcite Mg is the most abundant trace element). Therefore, the stable Sr isotopic composition of biogenetic CaCO_3 represents a new potential geochemical proxy for past environmental conditions. It can provide new and additional insights in geological and biological processes. An introduction to the relatively new field of stable Sr isotope fractionation is given in chapter I.4.2 where an overview of stable Sr literature published so far is provided.

I.3 Isotope fractionation

Atoms of a certain element have identical atomic numbers (Z) which denotes the number of protons forming the atomic nucleus. Therefore, Z denotes the charge number of the atomic nucleus which is characteristic for every element whereas the number of neutrons (N) in their nuclei can differ. Atoms with same Z but differing N are termed *isotopes*. Isotopes of an element show the same chemical behavior and have only minor differences in their atomic radii. Differences in the number of neutrons

in the nucleus result in slight differences in atomic weight ($M=Z+N$) and enables their separation via mass spectrometry. The change in the isotopic composition of an element between two substances or two phases of the same substance due to chemical or physical processes e.g. diffusion or reaction kinetics is called '*isotope fractionation*'. Generally, isotope fractionation can be divided into two branches: (1) '*mass dependent*' isotope fractionation which depends on the relative mass difference of the involved isotopes and (2) '*mass independent*' isotope fractionation which shows no systematic behavior related to the relative mass difference of the involved isotopes. Latter was first reported by (THIEMENS, 1992; THIEMENS et al., 1995) for oxygen isotopes in stratospheric CO_2 .

However, all fractionation processes occurring during sample preparation, mass spectrometric measurements and in nature will be assumed throughout this work to follow the mass dependent exponential fractionation law (RUSSELL et al., 1978):

$$\text{eq.I.1} \quad \left(\frac{X}{Y}\right)_{\text{true}} = \left(\frac{X}{Y}\right)_{\text{meas}} \cdot \left(\frac{m_X}{m_Y}\right)^\beta,$$

Where X and Y are two isotopes of an element, m_X and m_Y are their masses and β is the fractionation factor. The subscripts '*true*' and '*meas*' indicate the true and the measured isotope ratio, respectively. The applicability of other mass-fractionation laws to describe isotope fractionation processes in nature or during mass spectrometric measurements is discussed in detail in (YOUNG et al., 2002) and (ALBARÉDE et al., 2004). Isotopic variations as a consequence of natural isotope fractionation are generally small. For this reason it is impractical to use absolute isotopic ratios when comparing the isotopic composition of two samples. The fractionation of the stable $^{88}\text{Sr}/^{86}\text{Sr}$ ratio is therefore presented in the common δ -notation in per mill [‰] deviation from standard material NIST SRM 987:

$$\text{eq.I.2} \quad \delta^{88/86}\text{Sr} = \left[\frac{\left(\frac{^{88}\text{Sr}}{^{86}\text{Sr}}\right)_{\text{sample}}}{\left(\frac{^{88}\text{Sr}}{^{86}\text{Sr}}\right)_{\text{SRM987}}} - 1 \right] \cdot 1000$$

Note: A $^{88}\text{Sr}/^{86}\text{Sr}$ ratio of 8.375209 corresponds to $\delta^{88/86}\text{Sr}=0$.

Isotope fractionation occurring in nature is interesting in terms of geological research, especially when it is preserved over geological time scales. Due to the similarity, not only in size but also in chemical behavior, Ca is substituted by Sr in Ca-bearing minerals. During precipitation from seawater the light Sr isotopes are preferentially incorporated in the skeletons of marine calcifiers (FIETZKE and EISENHAUER, 2006). Hence, marine carbonates (MC) show a significant isotope fractionation during CaCO_3 precipitation from seawater which is in the order of $\Delta^{88/86}\text{Sr}_{\text{MC}}=-0.2\text{‰}$ (with $\Delta^{88/86}\text{Sr}_{\text{MC}}=\delta^{88/86}\text{Sr}_{\text{MC}} - \delta^{88/86}\text{Sr}_{\text{SW}}$). Natural Sr isotope fractionation has only a small effect on the isotopic composition of different materials compared to natural fractionation of isotopes like e.g. C, N, H or O. This is because of the smaller relative mass difference of the relative heavy Sr isotopes compared to lighter isotopes

and because Sr occurs not in molecules where differences in vibrational energy of covalent bonds are responsible for strong isotope fractionation effects. However, with the improvement of analytical methods and instrumentation even variations in the ppm range are now measurable. There are two main types of isotope fractionation processes which will be introduced in the following chapters: (1) ‘*equilibrium isotope fractionation*’ (chapter I.3.1) and (2) ‘*kinetic isotope fractionation*’ (chapter I.3.2).

I.3.1 Equilibrium isotope fractionation

A chemical reaction is in equilibrium when there is no net change of the concentrations of the reactants and products over time. This usually is the case when the forward chemical process proceeds at the same rate as the reverse reaction. This process is called dynamic chemical equilibrium and can be expressed as:



Where A and B are phases or molecules (with a and b representing their amounts) and superscripts 1 and 2 indicate different isotopes. At *isotopic* equilibrium, the forward and reverse reaction rates of any particular isotope are identical and hence, the isotopic composition of the left and right side of eq.I.3 remains constant until isotopic equilibrium is reached. Equilibrium fractionation is driven mainly by differences in the vibrational energies of molecules and crystals containing different isotopes (UREY, 1947). The vibrational modes are discrete energy levels and hence, equilibrium isotope fractionation is a quantum-mechanical phenomenon. The equilibrium constant K can be expressed by the quotient of two partitioning function (Q) ratios for the isotopic species A and B:

$$\text{eq.I.4} \quad K = \frac{\left(\frac{A^2}{A^1}\right)}{\left(\frac{B^2}{B^1}\right)} = \frac{\left(\frac{Q_{A^2}}{Q_{A^1}}\right)}{\left(\frac{Q_{B^2}}{Q_{B^1}}\right)}$$

The partitioning function is defined as:

$$\text{eq.I.5} \quad Q = \sum_i g_i \cdot e^{-\frac{E_i}{kT}}$$

The summation in eq.I.5 includes all allowed energy levels (E_i) of the molecules, g_i is the statistical weight of the single energy levels (with: $\sum_i g_i = 1$) and k is the Boltzmann constant that relates energy to temperature (T). The partitioning function Q can be separated into three terms corresponding to the different types of energy namely translation energy, rotation energy and vibration energy ($Q=Q_{\text{trans}} + Q_{\text{rot}} + Q_{\text{vib}}$). Differences in translation and rotation energy are negligible. Q_{vib} is related to the vibrational zero-point energy difference ($E_{(\text{vib})_i} = \left(n_i + \frac{1}{2}\right) h\nu_i$, with $n=0$) of

reactants and products in a chemical reaction and mainly accounts for variations in equilibrium fractionation with temperature. For a deeper understanding of the processes driving equilibrium fractionation the reader is referred to reviews of equilibrium fractionation theory e.g. (CHACKO et al., 2001; O'NEIL, 1986; UREY, 1947).

1.3.2 Kinetic isotope fractionation

Isotope fractionation that is chiefly dependent on molecular velocity is termed '*kinetic isotope fractionation*'. This type of mass dependent fractionation is associated with fast, chemically incomplete and unidirectional isotope exchange processes which primarily occur during phase transfer reactions or during chemical reactions where isotopic equilibrium is not achieved. These processes are for example evaporation, dissociation reactions, diffusion and biological mediated reactions like calcium carbonate precipitation (LEMARCHAND et al., 2004). A simple example of kinetic isotope fractionation is the evaporation of a liquid water droplet where H₂O molecules are physically removed from the vicinity of the droplet when entering the gas-phase. Hence, there is no chance for the system to achieve isotopic equilibrium between the vapor-phase and the residual liquid. The molecule containing the lighter isotopes is preferably converting into the gas phase and the residual droplet is continuously increasing its molar mass. For heavy elements like Sr the most common types of kinetic fractionations are those driven by effects of isotopic mass, velocity and diffusivity. At a given temperature the average kinetic energy of all molecules in an ideal gas is the same and given by:

$$\text{eq.1.6} \quad E_{\text{kin}} = \frac{3}{2}kT = \frac{1}{2}mv^2$$

Where m is the mass of the molecule, v is its velocity, T its temperature and k is the Boltzmann constant that relates energy to temperature. Molecules having different isotopic compositions will apparently have different velocities:

$$\text{eq.1.7} \quad \frac{\sqrt{\frac{3kT}{m_1}}}{\sqrt{\frac{3kT}{m_2}}} = \frac{v_1}{v_2}$$

Due to this difference in velocity molecules consisting of light isotopes convert easier from the liquid to vapor-phase or diffuse faster compared to their heavy counterpart. This leads to (physical) kinetic isotope fractionation between different phases of a substance.

Kinetic isotope fractionation can also occur when the rate of a chemical reaction is sensitive to the atomic mass of the involved ions. Unidirectional reactions always show preferential enrichment of the light isotopes in the reaction products which is a consequence of the lower bonding energy of

lighter isotopes compared to heavier isotopes. This phenomenon is termed chemical kinetic isotope fractionation.

1.3.3 Rayleigh fractionation

The Rayleigh fractionation law is an exponential relation that describes the partitioning of isotopes between two reservoirs where one of them decreases in size. This fractionation law is used to describe isotope fractionation processes where (1) material is continuously removed from a mixed system containing molecules of two or more different isotopes and (2) the fractionation taking place during the removal process is described by a constant fractionation factor α . Like mentioned before, the lighter isotopes preferentially convert into the vapor phase during evaporation. They are also enriched in the CaCO_3 crystal lattice when precipitated from seawater. Fractionation processes induced by chemical reactions (or evaporation or condensation processes) where the reaction products are removed from a finite reservoir can be described by Rayleigh fractionation. Under these conditions, the isotopic composition of the residual material (reactant) is described by:

$$\text{eq.1.8} \quad R = R_0 f^{\alpha-1}$$

Where R_0 is the initial isotope composition of the reservoir, R is isotope ratio of the residual reservoir and f being the fraction of residual solution.

Here we have to distinguish between open and closed systems. In a closed system the residual reservoir of the reactants stays in direct contact with the reservoir of the products while the products are removed from the system and not able to re-react with the reactants in an open system. The Rayleigh fractionation law is applicable to open systems where the isotopes are removed at every instant. Furthermore, an "ideal" Rayleigh fractionation process is one where the reactant reservoir is finite and well mixed, and the reservoir does not re-react with the product (KENDALL AND MCDONNELL, 1998).

1.4 Strontium isotope geochemistry

The second column of the periodic table is collectively called the *alkaline earth metal group* consisting of beryllium (Be), magnesium (Mg), calcium (Ca), strontium (Sr), barium (Ba), and radium (Ra). Alkaline earth metals almost always form ions with twofold positive charge (divalent cations). They are sufficiently reactive as elements so they usually occur in nature only in compound form, frequently as carbonates $[\text{CO}_3]^{2-}$, silicates $[\text{SiO}_4]^{4-}$ or sulfates $[\text{SO}_4]^{2-}$. Calcium is by far the most abundant earth alkaline element in the continental crust, followed by magnesium, and in much lesser amounts barium, beryllium and strontium. The determination of variations in isotopic composition of

different materials caused by fractionation or radioactive decay provides the foundation for the field of isotope geochemistry. This field of research can generally be divided into two parts: (1) ‘*radiogenic*’ isotope systems and (2) ‘*stable*’ isotope systems.

The earth alkaline metal strontium is widely distributed in biological and geological reservoirs and with a concentration of 8 ppm it is the 5th most abundant cation in seawater (BROECKER and PENG, 1982). It has four naturally occurring stable isotopes (⁸⁴Sr, ⁸⁶Sr, ⁸⁷Sr and ⁸⁸Sr). Their abundances are approximately 0.56%, 9.87%, 7.04% and 82.53%, respectively. These abundances are variable due to (1) the formation of radiogenic ⁸⁷Sr from the radioactive β^- decay of ⁸⁷Rb with a half-life of $4.88 \cdot 10^{10}$ years (FAURE and MENSING, 2005) and (2) to a much lesser extent due to natural isotope fractionation during chemical or physical processes. Hence, the Sr isotope system combines two important features for geochemical research. The radiogenic Sr isotope ratio (⁸⁷Sr/⁸⁶Sr) is a well established tool in isotope geochemistry. It is characterized by excellent tracer and dating properties and is part of the ‘*traditional*’ isotope systems. The stable Sr isotope ratio (⁸⁸Sr/⁸⁶Sr) is part of the new research field termed ‘*non-traditional stable isotopes geochemistry*’ and mirrors natural Sr isotope fractionation. Both systems for themselves are important tools in isotope geochemistry and will be introduced in the following chapters.

1.4.1 The radiogenic strontium isotope system

Some elements have isotopes that are subject to the radioactive decay either directly (*radioactive* isotopes) or indirectly as end products of the decay chain of an unstable isotope (*radiogenic* isotopes). In this process always two isotopes of different elements are involved. Thus, isotopic variations in radiogenic isotope systems are primarily based on the radioactive decay. This radioactive decay occurs in different ways:

- **α -decay:** The isotopic nucleus emits an alpha particle (He-nucleus). Thus, M decreases by four and Z by two units.
- **β^- -decay:** One neutron of the nucleus transforms into a proton with the emission of one electron and one anti-neutrino.
- **β^+ -decay:** One proton of the nucleus transforms into a neutron with the emission of one positron and one neutrino.
- **K-capture:** One of the orbital electrons, usually from the K electron shell, is captured by a proton in the nucleus, forming a neutron and a neutrino.
- **Spontaneous decay:** The isotopic nucleus decays spontaneously into two unequal halves and emits several neutrons.

One of the Sr isotopes, namely ⁸⁷Sr, is formed by the β^- decay of Rubidium (⁸⁷Rb) with a half-life of $4.88 \cdot 10^{10}$ years (FAURE and MENSING, 2005). In the following the ⁸⁷Sr/⁸⁶Sr isotopic ratio is also referred

to as *radiogenic Sr* or *radiogenic isotope ratio*. This radiogenic component makes the Sr isotope system a useful tool in isotope geochemistry which had been used e.g. for quantifying the hydrothermal activity (PALMER and EDMOND, 1989), as indicator of continental weathering intensity (CAPO and DEPAOLO, 1990), geochronology (FAURE and MENSING, 2005) and strontium isotope stratigraphy (MCARTHUR et al., 2001).

The elemental fractionation of Rb and Sr during magmatic processes leads to large variations in the Rb/Sr ratios of minerals forming different types of magmatic rocks (e.g. basalt (Rb/Sr=0.06), granite (Rb/Sr=0.25), (FAURE and MENSING, 2005)). This elemental fractionation consequently leads to variations in the isotopic composition of different magmatic rocks due to the decay of ^{87}Rb and is the origin of differences of Sr the isotopic composition of the earth's mantle and crust (FAURE and MENSING, 2005).

One major application of the radiogenic Sr system is the investigation and quantification of the oceans Sr budget e.g. (BURKE et al., 1982; DAVIS et al., 2003; ELDERFIELD and SCHULTZ, 1996; HODELL et al., 1990; PALMER and EDMOND, 1989; RICHTER et al., 1992). Strontium is mainly released to the ocean by two sources: (1) Radiogenic Sr from continental weathering which is delivered to the ocean by river- and groundwater discharge and (2) low radiogenic “mantle”-Sr from hydrothermal circulation at mid-ocean ridges (MOR) (PALMER and EDMOND, 1989; TAYLOR and LASAGA, 1999). A minor Sr source is represented by diagenetic alteration and dissolution of seafloor sediments (ELDERFIELD and GIESKES, 1982). The main sink for Sr is the sedimentation and Sr fixation in marine carbonates where Sr substitutes Ca in the crystal lattice of calcium carbonate. The Sr isotopic composition of seawater is controlled by the balance of its Sr sources and sinks characterized by different isotopic compositions and Sr fluxes which are variable with time.

A first approach of evaluating the oceans Sr budget was done by (WICKMAN, 1948). Because continental weathering products have a more radiogenic $^{87}\text{Sr}/^{86}\text{Sr}$ ratio compared to seawater (WICKMAN, 1948) suggested a monotonic increase in seawater $^{87}\text{Sr}/^{86}\text{Sr}$ with time. This suggestion was based on the assumption that continental river discharge is the only source delivering Sr the ocean. Radiogenic Sr measurements of recent marine carbonates collected worldwide show equal $^{87}\text{Sr}/^{86}\text{Sr}$ ratios. This is due to the relatively short mixing time of the oceans (~ 1.5 kyr) compared to the residence time of Sr which is ~ 2.4 Ma (ELDERFIELD, 1986; FAURE and MENSING, 2005; HODELL et al., 1990). This geographical constancy is assumed to be also valid for the geological past. Furthermore, marine carbonates and seawater, where they have been precipitated from, show identical $^{87}\text{Sr}/^{86}\text{Sr}$ values. This is a direct consequence of the internal normalization (chapter I.6.1) to a fixed $^{88}\text{Sr}/^{86}\text{Sr}$ ratio of 8.375209 (NIER, 1938). This procedure is conventionally used to correct for mass-dependent isotope fractionation during mass spectrometry. Any mass-dependent isotope fractionation that may

occur in nature is neglected by applying this technique. Thus, the Sr isotopic composition of marine carbonates directly reflects the isotopic composition of seawater at the time of precipitation.

Therefore, well preserved fossil marine carbonates of different ages can be used to reconstruct the Sr isotopic composition of seawater. Measurements of $^{87}\text{Sr}/^{86}\text{Sr}$ in biostratigraphically well dated marine carbonates (PETERMAN et al., 1970) revealed variations in $^{87}\text{Sr}/^{86}\text{Sr}$ between 0.707 and 0.709 throughout the Phanerozoic and confute the monotonic increase predicted by (WICKMAN, 1948) who did not include hydrothermal activity as another source for Sr to the ocean. A compilation of $^{87}\text{Sr}/^{86}\text{Sr}$ data of marine carbonates covering the Phanerozoic was published by (VEIZER et al., 1999). The general trend of Phanerozoic seawater $^{87}\text{Sr}/^{86}\text{Sr}$ is displayed in fig.I.1.

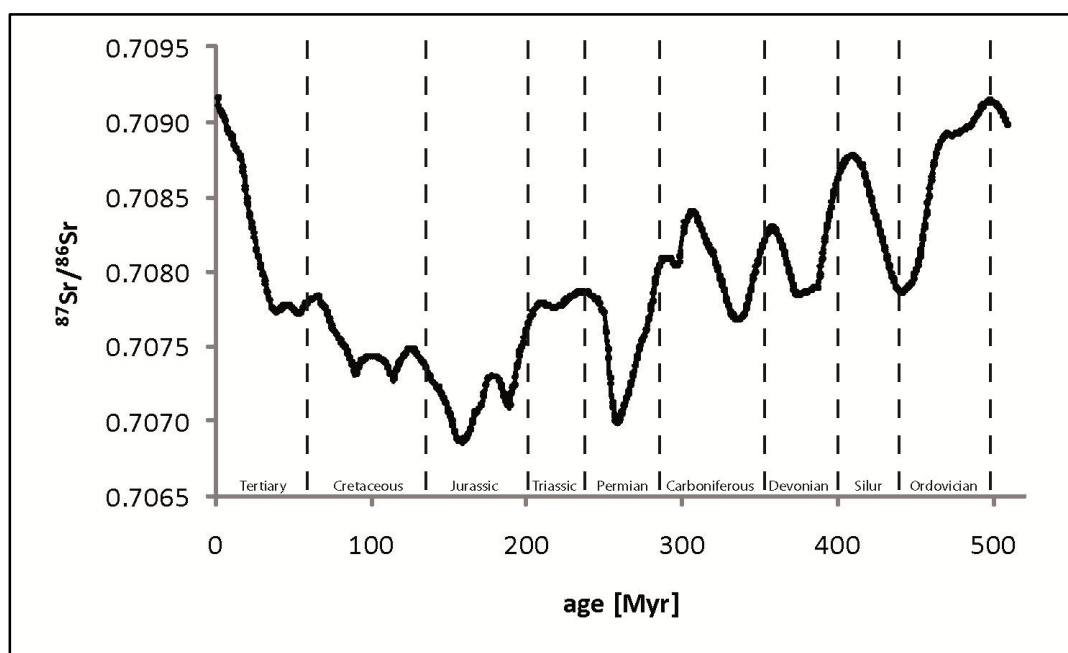


fig.I.1: The seawater Sr evolution curve of the Phanerozoic after (McARTHUR et al., 2001)

The seawater evolution curve tends to decrease from the early Cambrian to the mid Jurassic superimposed by second order variations of the $^{87}\text{Sr}/^{86}\text{Sr}$ with a periodicity of ~ 50 Ma and amplitude of ~ 1000 ppm. Values are increasing almost continuously from ~ 0.7068 in the middle Jurassic to the recent seawater value 0.709241 ± 0.000032 (ELDERFIELD and SCHULTZ, 1996). This monotonous increase implied that the input of relatively radiogenic Sr from the continents cannot be balanced by unradiogenic Sr derived from hydrothermal exchange with the oceanic crust.

The Sr isotope data of (VEIZER et al., 1999) show an increase of seawater $^{87}\text{Sr}/^{86}\text{Sr}$ ratio at a rate of $0.000054 \text{ Myr}^{-1}$ for the past ~ 30 Myr. PALMER AND EDMOND (1989) calculated that a hydrothermal fluid flux of $\sim 1.2 \times 10^{14} \text{ kg yr}^{-1}$ is required to keep the oceanic strontium budget near steady state. This estimate is an order of magnitude higher than other hydrothermal fluid flux predictions of e.g. (ELDERFIELD and SCHULTZ, 1996) ($3\text{-}6 \times 10^{13} \text{ kg yr}^{-1}$). The extent of alteration of oceanic crust measured

in drill cores and ophiolites implies a hydrothermal fluid flux of $\sim 2.3\text{-}4.6 \cdot 10^{13}$ kg yr⁻¹ (DAVIS et al., 2003) which is similar to the results of (ELDERFIELD and SCHULTZ, 1996).

Other modeling advances have been carried out by (GODDERIS and FRANCOIS, 1995; HODELL et al., 1990; RICHTER et al., 1992; VANCE et al., 2009). All these studies only focus on the Sr sources of the ocean because in the radiogenic picture marine carbonates and seawater, where the carbonates have been precipitated from, show identical isotopic composition due to the internal normalization procedure. Hence, $^{87}\text{Sr}/^{86}\text{Sr}$ ratios is a powerful tool for balancing the Sr sources but the radiogenic Sr alone is not providing the full information that is necessary quantify the Sr sink of the ocean. By the determination of stable Sr isotopic ratios ($\delta^{88/86}\text{Sr}$, chapter I.4.2) an additional dimension is added to the radiogenic picture. Seawater and marine carbonates show significant differences in their stable Sr isotope ratio $\delta^{88/86}\text{Sr}$ that were not visible by applying the radiogenic $^{87}\text{Sr}/^{86}\text{Sr}$ ratio alone. The non-traditional stable isotope system of Sr is the subject of chapter I.4.2.

The seawater Sr evolution curve has also been utilized for strontium isotope stratigraphy (SIS). In order to improve this technique (MCARTHUR et al., 2001) compiled and fitted $^{87}\text{Sr}/^{86}\text{Sr}$ data of marine carbonates published in 42 earlier studies (see tab. 1 in (MCARTHUR et al., 2001)). The precision of SIS is limited due to the uncertainty of the age model developed with e.g. biostratigraphy or magnetostratigraphy. Errors of ages derived with this age model range in between 0.15 - 2 Ma. The stratigraphic resolution of SIS is also limited by the slope of the seawater $^{87}\text{Sr}/^{86}\text{Sr}$ -evolution curve (VEIZER et al., 1999). Therefore the seawater Sr isotope curve can only be resolved as a band, due to the uncertainties in biostratigraphy, geochronology and uncertainties in $^{87}\text{Sr}/^{86}\text{Sr}$ determinations due to preservation of sample material (VEIZER et al., 1997). The radiogenic Sr isotope ratio was applied in many studies in stratigraphic terms e.g. (ELDERFIELD, 1986; JENKYNS et al., 2002; MCARTHUR, 1994; MCARTHUR et al., 2001; SMALLEY et al., 1994).

The variation of the $^{87}\text{Sr}/^{86}\text{Sr}$ ratio in different minerals makes the radiogenic Sr an excellent tracer for geological processes. Because of the importance of silicate weathering for the global CO₂ cycle, radiogenic Sr isotope data have been utilized to discriminate between carbonate and silicate weathering e.g. by (HARRINGTON and HERCZEG, 2003; KRISHNASWAMI and SINGH, 1998; OLIVER et al., 2003; QUADE et al., 2003). In the study of (BLUM, 1995) a negative correlation between $^{87}\text{Sr}/^{86}\text{Sr}$ ratio in soils and the soil age was observed, indicating that the $^{87}\text{Sr}/^{86}\text{Sr}$ ratio of Sr released in the early stages of weathering is significantly higher than in later stages. They estimated that this mechanism can increase global riverine $^{87}\text{Sr}/^{86}\text{Sr}$ by an average of 0.0002 during periods of glacial/interglacial cycling. This “weathering peak” hypothesis is discussed in detail in chapter III with respect to stable Sr isotope fractionation. On the other hand, (HENDERSON et al., 1994) reported that their $^{87}\text{Sr}/^{86}\text{Sr}$ data derived from planktonic foraminifera covering the time period of the last 400 kyr show no evidence

for a glacial/interglacial cyclicity. Their data constrain the change in riverine flux between glacial and interglacial periods to be less than 10^{10} mol/yr.

Additionally, the isotopic abundance of ^{87}Sr in a closed system is determined by four parameters: (1) The isotopic abundance of ^{87}Sr at a given initial time, (2) the $^{87}\text{Rb}/^{87}\text{Sr}$ ratio of the system, (3) the decay constant of ^{87}Rb and (4) the time elapsed since the initial time. Hence, the radiogenic component of the Sr isotope system allows to date any material that contains ^{87}Rb (FAURE and MENSING, 2005).

Variations in the $^{87}\text{Sr}/^{86}\text{Sr}$ isotopic ratio originating from the radiogenic in-growth due to the decay of ^{87}Rb are much larger compared to $^{87}\text{Sr}/^{86}\text{Sr}$ variations as a consequence of natural isotope fractionation. Therefore, natural isotope fractionation is negligible when investigating changes in the radiogenic Sr isotope ratio and thus, the normalization to fixed $^{88}\text{Sr}/^{86}\text{Sr}$ is an adequate method to correct for instrumental mass fractionation during mass spectrometric measurements. To determine natural Sr isotope fractionation the stable $^{88}\text{Sr}/^{86}\text{Sr}$ ratio is more applicable because it shows a larger relative mass difference and is not biased by the radioactive decay of another element.

1.4.2 The stable strontium isotope system

The non-traditional stable Sr isotopes recently received much attention in the geochemical science community. It was found that Sr isotopes show significant fractionation during biological and inorganic precipitation of CaCO_3 e.g. (FIETZKE and EISENHAUER, 2006; RÜGGERBERG et al., 2008). It was shown that the light Sr isotopes are preferentially incorporated into the crystals. This was the starting point of one of the newest fields of non-traditional stable isotope research – the investigation of natural stable Sr isotope fractionation. Since then the investigation of stable Sr isotope fractionation is the subject of a growing group of isotope geochemists. Several materials and methods have been tested with respect to Sr isotope fractionation in the recent past. Nevertheless the stable Sr database is still very limited. In the following an overview of recent publications dealing with stable Sr isotope fractionation is given.

A first approach applying a standard bracketing technique for determining stable Sr isotope fractionation using MC-ICP-MS was presented by (FIETZKE and EISENHAUER, 2006). The impetus for their study was the previous observed temperature dependence of Ca isotope fractionation during inorganically and biologically mediated calcium carbonate precipitation published by (GUSSONE et al., 2003; NÄGLER et al., 2000). Fietzke and Eisenhauer found a temperature dependency of stable Sr isotope fractionation in the tropical coral *Pavona clavus* with a positive slope of $(0.033 \pm 0.005\%/\text{°C})$ in the range of 23°C to 27°C and a lower temperature dependency of $\delta^{88/86}\text{Sr}$ in inorganically precipitated aragonite $(0.0054 \pm 0.0005\%/\text{°C})$ in the range of 10°C to 50°C .

The external reproducibility for stable Sr measurements in this study was reported to be better than $\pm 0.05\%$ (2SD). Stable Sr $\delta^{88/86}\text{Sr}$ values of inorganically precipitated aragonite range from $\delta^{88/86}\text{Sr}=0.0\%$ (10 °C) to $\sim 0.2\%$ (50 °C). *Pavona clavus* samples revealed $\delta^{88/86}\text{Sr}$ values between $\sim 0.16\%$ and $\sim 0.31\%$ corresponding to water temperatures of 23°C and 27°C, respectively. The lighter isotopes were found to be preferentially incorporated into the calcium carbonate for both, organically and inorganically precipitated minerals. The same was reported by (RÜGGERBERG et al., 2008) for the cold water coral *Lophelia pertusa* who also applied the bracketing standard method using MC-ICP-MS. They found a temperature sensitivity of $\delta^{88/86}\text{Sr}$ with a positive slope of $0.026\pm 0.003\%/^{\circ}\text{C}$ in the range from 6°C to 9°C. These results are in good accordance with $\delta^{88/86}\text{Sr}$ data derived from *Pavona clavus* in the study of (FIETZKE and EISENHAUER, 2006). The external reproducibility achieved in this study was $\pm 0.05\%$ (2SD) and thus comparable to previous results. These studies indicated the use of stable Sr isotope fractionation as a potential proxy for paleo-sea surface temperature reconstructions.

In the study of (WALTHER and THORROLD, 2006) the relative contributions of water and food to Sr and Ba deposited in otoliths of juvenile mummichogs fishes of the species *Fundulus heteroclitus* was quantified. The water in which the fishes lived was spiked with ^{86}Sr and ^{137}Ba , resulting in an isotopic composition significantly beyond natural values, to obtain distinct isotopic signatures for water and food. Stable strontium isotope ratios in otoliths were obtained by laser ablation ICP-MS and a bracketing standard technique. The relative contributions of water and food sources to otolith aragonite were assessed using a simple linear isotope mixing model resulting in a Sr contribution of water sources of 83%. Their results indicate that water chemistry is the dominant factor controlling the uptake of Sr in the otoliths of marine fish. Thus, chemical signatures recorded in the otoliths of marine fish should preliminary reflect the ambient water Sr isotopic composition at the time of deposition. Reported errors range from $\pm 0.09\%$ to $\pm 0.3\%$ (2SD).

In 2008 (YANG et al., 2008) presented a new technique for the measurement of Sr isotopes by MC-ICP-MS using Zirconium (Zr) as an internal standard in combination with the bracketing standard method (see chapter I.6.2). They reported a 2.5-fold improvement in precision by the use of this technique compared to Sr isotope data which were obtained by the bracketing standard method without the use of Zr as internal standard. They investigated the stable Sr isotopic composition of fish liver tissues which show a $\delta^{88/86}\text{Sr}$ of $0.207\pm 0.012\%$ (2SD) relative to the SRM 987 standard.

The studies of (OHNO and HIRATA, 2007; OHNO et al., 2008) came up with stable Sr measurements of several standard materials and silicate/carbonate rocks. The Sr isotopic composition of the coral standard JcP-1 was determined with $\delta^{88/86}\text{Sr}=0.2\pm 0.07\%$ and $\delta^{88/86}\text{Sr}=0.19\pm 0.05\%$, respectively. Furthermore, the isotopic composition of two seawater samples was reported in the two studies with $\delta^{88/86}\text{Sr}=0.41\pm 0.08\%$ and $\delta^{88/86}\text{Sr}=0.39\pm 0.07\%$, respectively. Furthermore, the stable Sr isotope

composition of Neoproterozoic cap carbonates was analyzed by (OHNO et al., 2008). Their radiogenic and stable Sr values showed three characteristics: (1) high radiogenic $^{87}\text{Sr}/^{86}\text{Sr}$ at the bottom of the stratigraphic sequence and a subsequent gradual decrease in $^{87}\text{Sr}/^{86}\text{Sr}$, (2) very light $\delta^{88/86}\text{Sr}$ values in the range of $\sim -0.4\text{‰}$ to -0.2‰ at the bottom of the stratigraphic sequence and a subsequent gradual increase, and (3) a clear correlation between the fractionated $^{87}\text{Sr}/^{86}\text{Sr}$ (reported as $\delta^{87}\text{Sr}$, see (OHNO and HIRATA, 2007)) and the $\delta^{88/86}\text{Sr}$ values which reflects mass dependent Sr isotope fractionation. These features were explained by changes in continental weathering and the access of different Sr sources with light isotopic composition. Analyzed silicate/carbonate rock standards did not show stable Sr isotope compositions low enough to be a possible reservoir that is able to reduce the seawater $\delta^{88/86}\text{Sr}$ value in a manner that can explain the observed $\delta^{88/86}\text{Sr}$ values of cap carbonates. Fractionation induced by mass spectrometric measurements was corrected for using the Zr correction technique of (YANG et al., 2008) and the external reproducibility was reported to be 0.06‰ and 0.07‰ (2sd, n=20) for $\delta^{88/86}\text{Sr}$ and $\delta^{87}\text{Sr}$, respectively.

Another study dealing with stable Sr isotope fractionation was carried out by (HALICZ et al., 2008) who investigated the Sr isotope composition of *Porites* sp. and *Acropora* sp. corals from the Gulf of Aqaba and the Red Sea, respectively. The coral samples investigated in this study show average $\delta^{88/86}\text{Sr}$ values of $0.22 \pm 0.07\text{‰}$ (2SD) for *Porites* sp. and $0.21 \pm 0.22\text{‰}$ (2SD) for *Acropora* sp.. These results are in good agreement with $\delta^{88/86}\text{Sr}$ values of *Pavona clavus* reported in the study of (FIETZKE and EISENHAUER, 2006). Seawater samples showed average $\delta^{88/86}\text{Sr}$ values of $0.35 \pm 0.06\text{‰}$ (2SD). Furthermore they determined the Sr isotopic composition of carbonate rocks, the seawater standard IAPSO and Terra Rossa soil. Halicz et al. introduced $\delta^{88/86}\text{Sr}$ as a possible new tracer for processes of chemical weathering and pedogenesis. In their study the bracketing standard technique was applied to correct for instrumental mass fractionation. The external reproducibility in this study was not reported. Reported measurement uncertainty of single samples ranges from $\pm 0.06\text{‰}$ to $\pm 0.22\text{‰}$ (2SD).

In 2010 (DE SOUZA et al., 2010) published stable Sr measurements in a variety of geological and environmental materials including rocks, young soils, water and plants from a small glaciated watershed in the central Swiss Alps. Like the studies introduced previously they applied the bracketing standard technique using MC-ICP-MS. Their data show that plants (*Rhododendron*) preferentially assimilate the lighter Sr isotopes resulting in a significantly lower $\delta^{88/86}\text{Sr}$ compared to the soil they are growing in. They reported the $\delta^{88/86}\text{Sr}$ values of foliar tissues to be lower than in the roots and in the stems and leaves. This observation is contrary to the behavior of Ca isotopes in plants (PAGE et al., 2008; WIEGAND et al., 2005). DeSouza et al., 2010 proposed that the opposite sense of mass fractionation of Sr isotopes compared to Ca isotope fractionation in plants is related to

the processes discriminating between the two elements during allocation to different parts of the plant. Reported errors range between $\pm 0.07\%$ and $\pm 0.12\%$ (2SD).

The determination of stable Sr isotope fractionation is not only used in geochemical terms. This isotope system was recently employed by (KNUDSON et al., 2010) to give answers to specific questions in archeological science. Stable Sr data derived from human teeth and bones had been applied in this study to investigate paleo-diet of archaeological human populations. It was found that stable Sr isotope data can identify the trophic level from which the strontium originated that was found in human teeth. Hence, stable Sr could be utilized as a new proxy for the consumption of local or non-local strontium sources. Some results of these studies are summarized in tab.I.1.

sample	method	$\delta^{88/86}\text{Sr}$ [‰]	error [‰]	study
IAPSO	BS	0.381	± 0.010 (1SEM)	(FIETZKE and EISENHAUER, 2006)
<i>Pavona Clavus</i>	BS	0.240	± 0.036 (1SEM)	(FIETZKE and EISENHAUER, 2006)
Inorganic aragonite	BS	0.0 - 0.2	± 0.025 (1SEM)	(FIETZKE and EISENHAUER, 2006)
IAPSO	DS	0.389	± 0.026 (2SD)	(KRABENHÖFT et al., 2009)
Foraminifera	DS	0.140	± 0.030 (2SD)	(KRABENHÖFT et al., 2010)
<i>Porites</i> sp.	DS	0.205	± 0.017 (2SD)	(KRABENHÖFT et al., 2010)
<i>Acropora</i> sp.	DS	0.18 - 0.21	± 0.022 (2SD)	(KRABENHÖFT et al., 2010)
JCp-1	DS	0.194	± 0.025 (2SD)	(KRABENHÖFT et al., 2009)
River waters	DS	0.24 - 0.42	± 0.040 (2SD)	(KRABENHÖFT et al., 2010)
Hydrothermal fluids	DS	0.270	± 0.030 (2SD)	(KRABENHÖFT et al., 2010)
Coccolithophores	DS	0.270	± 0.032 (2SD)	(KRABENHÖFT et al., 2010)
Halimeda	DS	0.270	± 0.021 (2SD)	(KRABENHÖFT et al., 2010)
<i>Acropora</i> sp.	BS	0.210	± 0.220 (2SD)	(HALICZ et al., 2008)
IAPSO	BS	0.350	± 0.060 (2SD)	(HALICZ et al., 2008)
<i>Porites</i> sp.	BS	0.220	± 0.070 (2SD)	(HALICZ et al., 2008)
Terra rossa soil	BS	-0.180	± 0.150 (2SD)	(HALICZ et al., 2008)
Seawater standard GOA-1	BS	0.310	± 0.140 (2SD)	(HALICZ et al., 2008)
Speleotherm calcite	BS	(-0.140) - (-0.200)	± 0.170 (2SD)	(HALICZ et al., 2008)
JCp-1	BS-Zr	0.190	± 0.050 (2SD)	(OHNO and HIRATA, 2007)
JCp-1	BS-Zr	0.200	± 0.070 (2SD)	(OHNO and HIRATA, 2007)
Silicate rocks	BS-Zr	0.260	± 0.030 (2SD)	(OHNO and HIRATA, 2007)
IAPSO	BS-ZR	0.390	± 0.070 (2SD)	(OHNO and HIRATA, 2007)
Seawater sample	BS-ZR	0.410	± 0.080 (2SD)	(OHNO and HIRATA, 2007)
<i>Lophelia Pertusa</i>	BS	0.06 - 0.18	± 0.050 (2SD)	(RÜGGERBERG et al., 2008)
River water	BS	0.13 - 0.25	± 0.130 (2SD)	(DE SOUZA et al., 2010)
Rhododendron roots	BS	0.140	± 0.030 (2SD)	(DE SOUZA et al., 2010)
Rhododendron stem	BS	0.080	± 0.120 (2SD)	(DE SOUZA et al., 2010)
Rhododendron leaves	BS	-0.080	± 0.120 (2SD)	(DE SOUZA et al., 2010)
Soil	BS	0.370	± 0.090 (2SD)	(DE SOUZA et al., 2010)
Granite	BS	0.150	± 0.120 (2SD)	(DE SOUZA et al., 2010)
Gneiss	BS	0.280	± 0.080 (2SD)	(DE SOUZA et al., 2010)

tab.I.1: Results of stable Sr measurements of selected studies available so far. The errors are given either in 2 standard deviations (2SD) or 1 standard errors of the mean (1SEM) like they were published. (BS=bracketing standard, BS-Zr=bracketing standard with Zirconium as external correction, DS=double spike method).

In fig.I.2 the range of variations in $\delta^{88/86}\text{Sr}$ values of standard materials and natural samples determined in the studies mentioned before is displayed. It is apparent that Sr isotopes are significantly fractionated in different natural materials. The reported errors range from $\sim \pm 0.01\%$ up to $\sim \pm 0.22\%$ (2SD). In all these studies stable Sr data are derived by applying a bracketing standard

method (chapter I.6.2). In order to improve the precision and accuracy of stable Sr isotope analysis, we developed a TIMS double spike method which is the issue of chapter II.

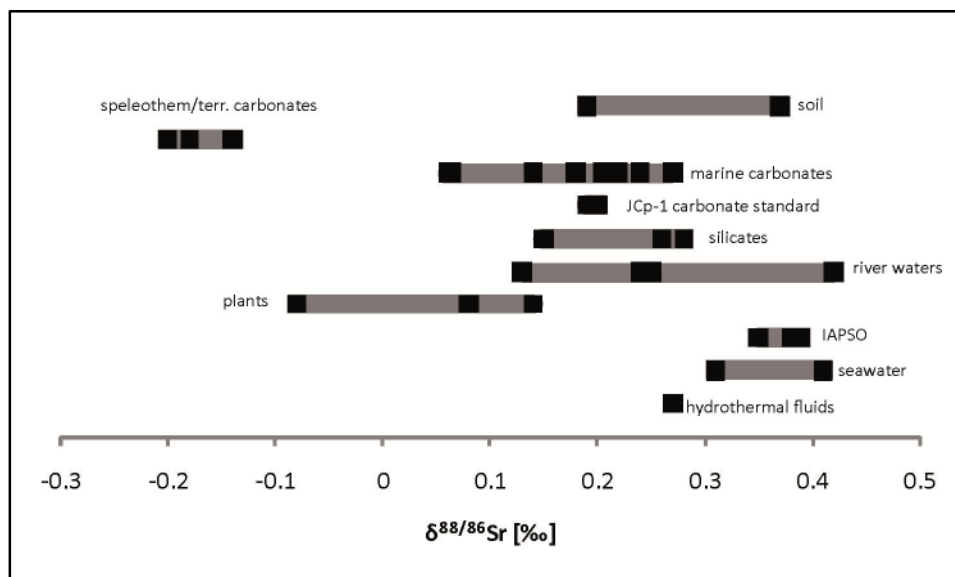


fig.I.2: The range of stable Sr values of different materials measured in the studies summarized in tab.I.1.

I.5 Thermal ionization mass spectrometry

The isotopic composition of alkaline earth elements is generally measured using a Thermal Ionization Mass Spectrometer (TIMS) or Multi Collector Inductively Coupled Mass Spectrometer (MC-ICP-MS) (FIETZKE and EISENHAEUER, 2006; RÜGGERBERG et al., 2008). The main difference between these two types of mass spectrometers is the ion source. While the ionization in TIMS occurs on the hot surface of a metal-filament (e.g. rhenium) a plasma source is used to generate ions in MC-ICP-MS. In our study we choose TIMS for the analysis of the Sr isotopic composition of our samples because the double spike technique combined with TIMS is a well established and robust method for the precise determination of isotopic ratios of different elements (GALER, 1999; HEUSER et al., 2002; JOHNSON and BEARD, 1999; SCHMITT et al., 2009; SIEBERT et al., 2001). Furthermore it is less impacted by isobaric interferences, result in higher precision and a lesser amount of sample material is needed compared to MC-ICP-MS measurements. Isotope analysis where carried out at the IFM-GEOMAR mass spectrometer facility in Kiel using a TRITON TIMS (Thermo Fisher).

Generally mass spectrometers are composed of three primary components: (1) ion source, (2) magnetic analyzer and (3) ion collector. All three parts of the mass spectrometer are evacuated to pressures in the order of 10^{-7} mbar (source) to 10^{-9} mbar (collector). For the analysis of solid samples, the sample is deposited on a Re-filament that is mounted on a sample wheel in the ion source chamber of the TIMS. The filament is heated electrically to a temperature sufficient to ionize the element to be analyzed. The resulting ions are then accelerated by a high voltage electric field (~ 10 kV) and collimated by a series of slits and electrostatic lenses into a focused beam. The ion beam

then passes through a magnetic sector field which deflects the ions into circular paths whose radii are proportional to their mass to charge ratio. For ions with the same charge this results in a lesser deflection for the heavy isotopes compared to the lighter ones. The separated ion beams continue through the analyzer tube to the collector, where they generate a positive electrical charge. The beam entering the collector cup is neutralized by electrons that flow from ground to the collector through a resistor (10^{10} - $10^{12} \Omega$). The voltage difference generated across the resistor is amplified and measured. Comparison of voltages corresponding to individual ion beams then results in the desired isotope ratios.

I.6 Correction methods for instrumental isotope fractionation

A significant limitation of isotopic analysis via mass spectrometric measurements is the large mass fractionation that occurs in the ion source of the instruments. During evaporation from the hot surface of the filament in the TIMS ion source the light isotopes preferably convert into the gas phase. Thus, the molar mass of the remaining sample material on the filament continuously increases and with that, the isotopic composition of the sample will tend to heavier values during the course of the measurement. This phenomenon is visualized in fig.1.3. The $^{88}\text{Sr}/^{86}\text{Sr}$ ratio is determined 126 times (9 blocks of 14 scans) and tends to heavier values during the course of the measurement. This instrumental fractionation exceeds natural isotope fractionation by far which is in the order of several hundred ppm for stable Sr. Therefore, the instrumental-produced mass fractionation has to be corrected for when investigating natural isotope fractionation.

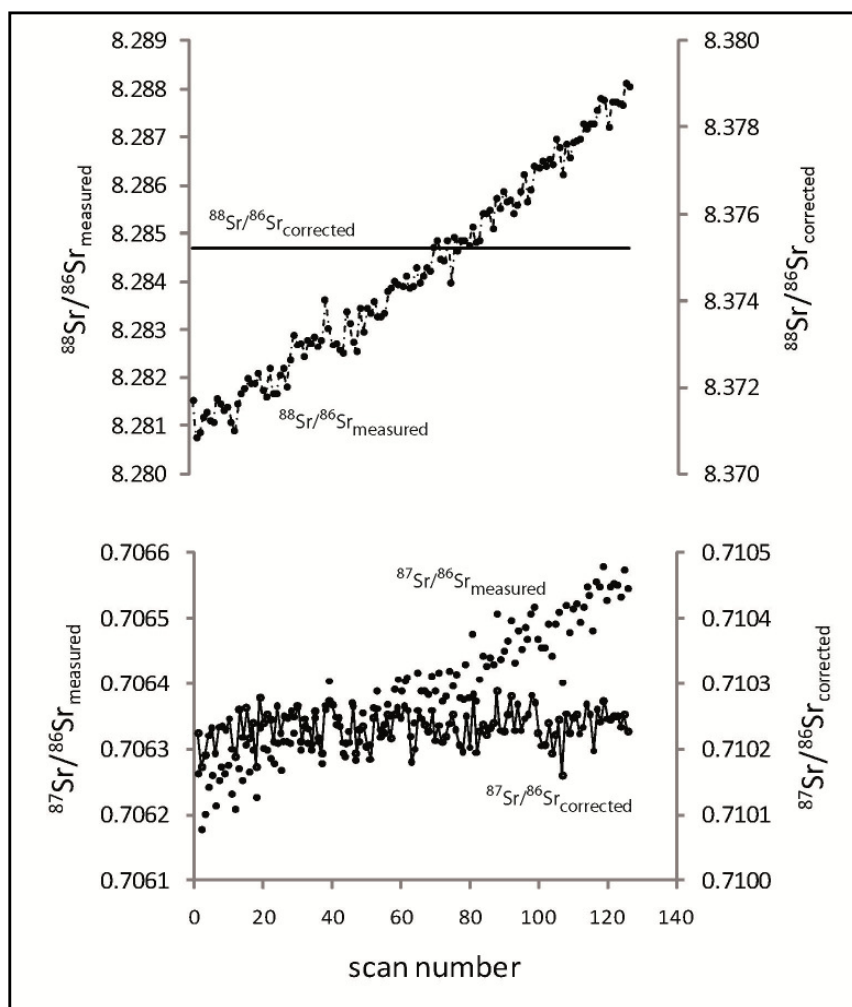


fig.1.3: Principal of mass fractionation correction via internal normalization. The measured $^{87}\text{Sr}/^{86}\text{Sr}$ ratio is normalized to a fixed $^{88}\text{Sr}/^{86}\text{Sr}=8.375209$ ratio (NIER, 1938).

Furthermore, mass dependent Sr isotope fractionation also occurs during chromatographic column separation. Latter has to be carried out in order to separate the matrix, including ^{87}Rb which is interfering with ^{87}Sr during TIMS measurement, from the Sr of the sample. However, the challenge in mass spectrometry is to separate mass dependent isotope fractionation produced in the laboratory and during mass spectrometric measurements from naturally occurring mass dependent isotope fractionation. This is not trivial because the patterns of natural and instrumental mass fractionation are identical. The different ways how to achieve the correction for instrumental mass fractionation are introduced in the following sections.

1.6.1 Internal normalization

A common approach to correct for instrumental mass fractionation is the normalization of the measured isotopic ratios to a fixed reference ratio. This approach termed ‘internal normalization’ is applied when one isotope is varying due to radiogenic in-growth from a parent isotope where natural isotope fractionation is not of interest. This is the case for the conventional radiogenic $^{87}\text{Sr}/^{86}\text{Sr}$ ratio.

Here the measured Sr isotope ratios are normalized to a fixed $^{88}\text{Sr}/^{86}\text{Sr}=8.375209$ ratio (Nier, 1938) to correct for mass dependent fractionation during TIMS measurement. By rearranging the exponential fractionation law (eq.I.1) a β_{norm} can be calculated from the known isotopic masses, the fixed $^{88}\text{Sr}/^{86}\text{Sr}=8.375209$ and the measured (fractionated) $^{88}\text{Sr}/^{86}\text{Sr}$ ratio. The calculated fractionation factor is then used for the correction of the measured $^{87}\text{Sr}/^{86}\text{Sr}$ ratio resulting in $\left(\frac{^{87}\text{Sr}}{^{86}\text{Sr}}\right)_{\text{true}}$.

$$\text{eq.I.9} \quad \beta_{\text{norm}} = \frac{\log\left(\frac{\left(\frac{^{88}\text{Sr}}{^{86}\text{Sr}}\right)_{\text{Nier}}}{\left(\frac{^{88}\text{Sr}}{^{86}\text{Sr}}\right)_{\text{meas}}}\right)}{\log\left[\frac{m_{88}}{m_{86}}\right]} \rightarrow \left(\frac{^{87}\text{Sr}}{^{86}\text{Sr}}\right)_{\text{true}} = \left(\frac{^{87}\text{Sr}}{^{86}\text{Sr}}\right)_{\text{meas}} \left(\frac{m_{87}}{m_{86}}\right)^{\beta_{\text{norm}}}$$

The correction is displayed in fig.I.3. This procedure completely removes any natural mass dependent isotope fractionation that may exist and thus, neglects important additional information. However, this method is very useful for the determination of Sr supply from sources having different $^{87}\text{Sr}/^{86}\text{Sr}$ due to the radiogenic in-growth of ^{87}Sr . The radiogenic Sr isotope ratio $^{87}\text{Sr}/^{86}\text{Sr}$ can be determined with this method with a precision of about 5 ppm. To investigate natural isotope fractionation, one of the methods described in the following has to be applied.

I.6.2 Bracketing standard method

The bracketing standard technique interpolates the mass fractionation of an unknown sample between two runs of a standard material with known isotopic composition to correct for machine drift and mass fractionation during mass spectrometric measurement via MC-ICP-MS.

Dividing the exponential mass fractionation law for the sample by that of the standard measurement preceding the sample analysis results in:

$$\text{eq.I.10} \quad \frac{\left(\frac{^{88}\text{Sr}}{^{86}\text{Sr}}\right)_{\text{true}}^{\text{sample}}}{\left(\frac{^{88}\text{Sr}}{^{86}\text{Sr}}\right)_{\text{true}}^{\text{standard}}} = \frac{\left(\frac{^{88}\text{Sr}}{^{86}\text{Sr}}\right)_{\text{meas}}^{\text{sample}}}{\left(\frac{^{88}\text{Sr}}{^{86}\text{Sr}}\right)_{\text{meas}}^{\text{standard}}} \cdot \left(\frac{m_{88}}{m_{86}}\right)^{\beta_1^{\text{standard}} - \beta^{\text{sample}}}$$

A corresponding equation can also be written for the standard measurement that follows the sample analysis.

$$\frac{\left(\frac{^{88}\text{Sr}}{^{86}\text{Sr}}\right)_{\text{true}}^{\text{sample}}}{\left(\frac{^{88}\text{Sr}}{^{86}\text{Sr}}\right)_{\text{true}}^{\text{standard}}} = \frac{\left(\frac{^{88}\text{Sr}}{^{86}\text{Sr}}\right)_{\text{meas}}^{\text{sample}}}{\left(\frac{^{88}\text{Sr}}{^{86}\text{Sr}}\right)_{\text{meas}}^{\text{standard}}} \cdot \left(\frac{m_{88}}{m_{86}}\right)^{\beta_2^{\text{standard}} - \beta^{\text{sample}}}$$

Assuming that β^{sample} (calculated with eq.I.1) is the mean of the fractionation factors $\beta_1^{\text{standard}}$ and $\beta_2^{\text{standard}}$ derived from standard measurement before and after the sample analysis

$$\text{eq.I.11} \quad \beta^{\text{sample}} = \frac{\beta_1^{\text{standard}} + \beta_2^{\text{standard}}}{2}$$

results in:

$$\text{eq.I.12} \quad \frac{\left(\frac{^{88}\text{Sr}}{^{86}\text{Sr}}\right)_{\text{true}}^{\text{sample}}}{\left(\frac{^{88}\text{Sr}}{^{86}\text{Sr}}\right)_{\text{true}}^{\text{standard}}} = \frac{\left(\frac{^{88}\text{Sr}}{^{86}\text{Sr}}\right)_{\text{meas}}^{\text{sample}}}{1 \left(\frac{^{88}\text{Sr}}{^{86}\text{Sr}}\right)_{\text{meas}}^{\text{standard}}} \cdot \left(\frac{m_{88}}{m_{86}}\right)^{\frac{\beta_2^{\text{standard}} - \beta_1^{\text{standard}}}{2}}$$

and

$$\text{eq.I.13} \quad \frac{\left(\frac{^{88}\text{Sr}}{^{86}\text{Sr}}\right)_{\text{true}}^{\text{sample}}}{\left(\frac{^{88}\text{Sr}}{^{86}\text{Sr}}\right)_{\text{true}}^{\text{standard}}} = \frac{\left(\frac{^{88}\text{Sr}}{^{86}\text{Sr}}\right)_{\text{meas}}^{\text{sample}}}{2 \left(\frac{^{88}\text{Sr}}{^{86}\text{Sr}}\right)_{\text{meas}}^{\text{standard}}} \cdot \left(\frac{m_{88}}{m_{86}}\right)^{\frac{\beta_1^{\text{standard}} - \beta_2^{\text{standard}}}{2}}$$

Multiplication of eq.I.12 and eq.I.13 results in:

$$\text{eq.I.14} \quad \left(\frac{^{88}\text{Sr}}{^{86}\text{Sr}}\right)_{\text{true}}^{\text{sample}} = \left(\frac{^{88}\text{Sr}}{^{86}\text{Sr}}\right)_{\text{true}}^{\text{standard}} \cdot \frac{\left(\frac{^{88}\text{Sr}}{^{86}\text{Sr}}\right)_{\text{meas}}^{\text{sample}}}{\sqrt{1 \left(\frac{^{88}\text{Sr}}{^{86}\text{Sr}}\right)_{\text{meas}}^{\text{standard}} \cdot 2 \left(\frac{^{88}\text{Sr}}{^{86}\text{Sr}}\right)_{\text{meas}}^{\text{standard}}}}$$

This expression reflects the true isotopic composition of the sample. This technique is not applicable to TIMS since each sample is located on a different filament. The conditions in the ion source are highly variable from sample to sample and therefore, mass fractionation during TIMS measurement cannot be accurately corrected for using this technique. When applying this method sample and standard solutions need to have the same concentration of the element of interest. Furthermore, the isotope fractionation occurring during chemical sample treatment cannot be corrected for which is the major disadvantage of the bracketing standard technique. A first application of this method on stable Sr measurements on biogenic and inorganically precipitated aragonite was published by (FIETZKE and EISENHAUER, 2006). They reported a precision of $\pm 0.050\%$ (2SD).

Another method to correct for instrumental mass fractionation during mass spectrometric measurements via bracketing standard was presented by (YANG et al., 2008). They determined the Sr isotopic composition of natural samples also by using MC-ICP-MS. In this technique standard (SRM987) and sample solutions are admixed with zirconium and then used for the correction of instrumental mass fractionation. The certified $^{88}\text{Sr}/^{86}\text{Sr}$ value of the strontium carbonate standard SRM987 ($^{88}\text{Sr}/^{86}\text{Sr}=8.37861$) is used for the correction of $^{90}\text{Zr}/^{91}\text{Zr}$ in the Zr-spiked SRM987 solutions

via internal normalization. Their average is then used to calculate the fractionation correction of the sample. This technique yields a precision of $\sim 0.08\text{‰}$ and thus is not more precise than bracketing standard but much more complex. The method of choice for the investigation of natural Sr isotope fractionation is the double spike technique which is the issue of section I.6.3.

I.6.3 The double spike technique

The double spike technique is a powerful method to correct for instrumental mass fractionation that occurs during mass spectrometric measurements and chemical sample preparation. With this technique it is possible to investigate natural Sr isotope fractionation by the simultaneous determination of the stable Sr isotopic ratio $^{88}\text{Sr}/^{86}\text{Sr}$ and the radiogenic $^{87}\text{Sr}/^{86}\text{Sr}$ ratio without normalizing to a fixed $^{88}\text{Sr}/^{86}\text{Sr}$. The use of this technique was first demonstrated experimentally by (DIETZ et al., 1962) and the theory behind it was then outlined by (DODSON, 1963). The double spike technique was first utilized by (COMPSTON and OVERSPY, 1969) who prepared a $^{207}\text{Pb}/^{204}\text{Pb}$ double spike. They reported substantial improvements in analytical precision by applying this technique to the measurement of different lead standard materials.

The double spike technique has recently received much attention due to its application in non-traditional stable isotope work. Heavy stable isotopes like e.g. Sr have low relative mass differences compared to traditional light isotopes like e.g. C, N or O and hence, they show only small natural isotope fractionation. Several applications for example on Fe e.g. (JOHNSON and BEARD, 1999), Mo e.g. (SIEBERT et al., 2001), Pb e.g. (GALER, 1999), Cd e.g. (SCHMITT et al., 2009) and Ca isotopes e.g. (HEUSER et al., 2002; EISENHAUER et al., 2009) have been presented. Many aspects of this technique have been discussed over the past decades and published literature concerning this topic has been adequately reviewed (GALER, 1999; RUDGE et al., 2009).

The double spike technique is applicable to any element that has four or more isotopes and it has a number of advantages compared to other correction procedures when investigating the natural isotope fractionation. With the double spike technique, standard and sample solutions do not need to have the same Sr concentration (RUDGE et al., 2009). Furthermore, mass dependent fractionation that occurs during ion chromatographic column separation can be accurately corrected for.

When applying the double spike technique, four relative amounts of isotopes are determined. Two of them are adjusted far from their natural abundances by adding the double spike to one fraction of the sample. By the exact knowledge of the double spike isotopic composition, it is possible to calculate the true composition of the sample corrected for mass fractionation that occurs during TIMS measurement and sample preparation. In fig.I.4 the principle of the double spike technique is visualized. In order to explain the underlying principles of the double spike method, the geometry of this technique in the three dimensional isotope-space is introduced in the following.

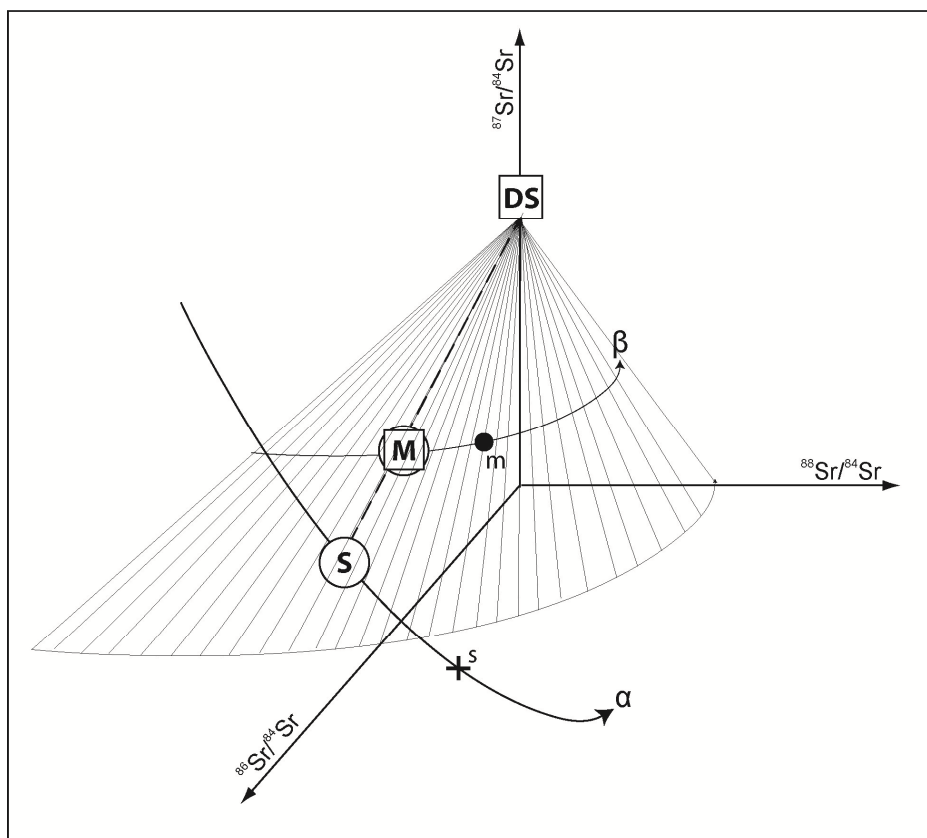


fig.1.4: Schematic sketch of the double spike technique in a three isotope space. 'DS' represents the known isotopic composition of the double spike, 'S' represents the pure sample and 'M' is the mixture of 'DS' and 'S'. 'M' and 'S' fractionate during TIMS measurement along the fractionation lines α and β , respectively. From the known isotopic composition of 'DS' and the measured values of 'm' and 's' it is possible to precisely calculate the isotopic composition of the natural sample. This applies for the geometric as well as for the iterative (this study) approach.

Drawing straight lines through the point representing the double spike (DS) composition and each point of the mass fractionation line of the mixture, results in a surface in the three dimensional isotope-space. One of these lines is representing the mixing line of the DS and the sample (dashed line) which has to be determined from the calculations. Using a common denominator-isotope of all isotope ratios on each axis forming the three dimensional isotope-space ensures linear mixing between the double spike and the sample. The intersection of the surface with the fractionation line of the pure sample represents the true isotopic composition of the sample (RUDGE et al., 2009). The precision of the double spike technique chiefly depends on the exact knowledge of the isotopic composition of the double spike solution which has to be accurately calibrated (see chapter II). Because we assume Sr isotope fractionation to follow the exponential law, we have to solve a set of non-linear equations when calculating the true isotopic composition of the sample. In this study we applied the common isotope dilution equations to calculate $^{84}\text{Sr}_{\text{spike}}/^{84}\text{Sr}_{\text{sample}}$ with the $^{88}\text{Sr}/^{84}\text{Sr}$ ratio and the $^{86}\text{Sr}/^{84}\text{Sr}$ ratio, respectively. To find the true isotopic composition of the sample we used an iterative routine which was adopted from the work of (HEUSER et al., 2002) and modified for Sr analysis (see chapter II and the appendix for detailed information).

Applying the double spike method to stable Sr measurements resulted in an actual long term reproducibility of $\pm 0.025\text{‰}$ (2SD) for the coral standard JCp-1 and $\pm 0.026\text{‰}$ (2SD) for the seawater standard IAPSO (see fig.I.5 and fig.I.6). Method development and double spike calibration are discussed in further detail in chapter II.

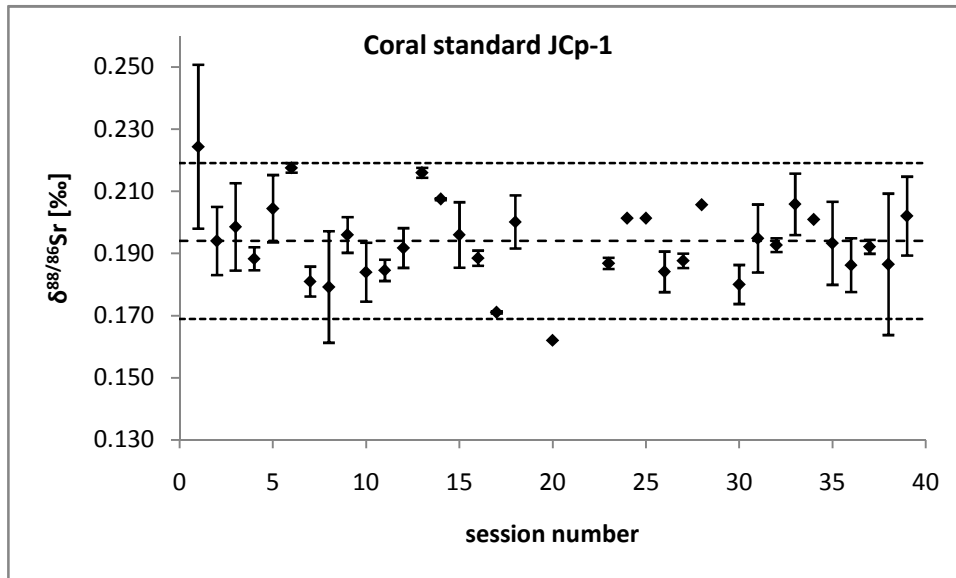


fig.I.5: Long term reproducibility of the coral standard JCp-1. We determined the stable Sr isotope composition with $0.194 \pm 0.025\text{‰}$ (2SD).

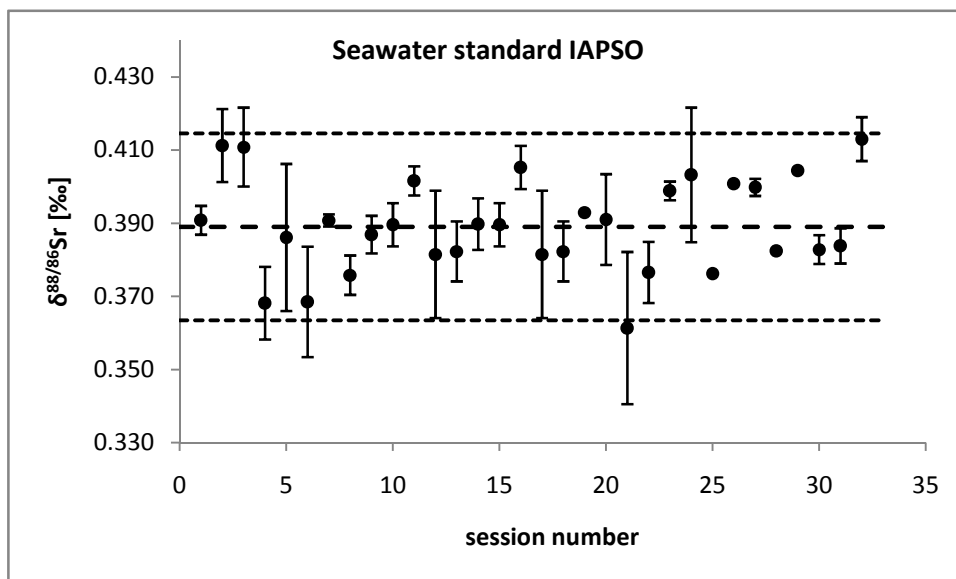


fig.I.6: Long term reproducibility of the seawater standard IAPSO. We determined the stable Sr isotope composition with $0.389 \pm 0.026\text{‰}$ (2SD).

1.7 Thesis outline

This PhD-thesis focuses on the natural Sr isotope fractionation and its precise determination via a TIMS double spike method. The impetus for this work was given by (FIETZKE and EISENHAUER, 2006) who reported significant stable Sr isotope fractionation during CaCO_3 precipitation from seawater. They derived their data via a bracketing standard method and reported an external reproducibility of $\pm 0.05\text{‰}$ (2SD). In order to improve the precision of stable Sr measurements and to apply $\delta^{88/86}\text{Sr}$ to geochemical problems this PhD-project was done. This work is divided into six chapters:

Chapter I. gives a general introduction to stable Sr geochemistry. Furthermore, it provides an overview about the mechanisms driving isotope fractionation in nature and it is outlined how fractionation occurring during mass spectrometric measurements can be corrected for.

The following chapters are presented in the form of manuscripts that have either been published or are ready for submission. They revisit the topics addressed in the general introduction and give examples of the applications of $\delta^{88/86}\text{Sr}$ in the field of isotope bio-geochemistry.

Chapter II. was published as a technical note in the Journal of Analytical Atomic Spectroscopy (KRABBENHÖFT et al., 2009). It represents a detailed description of the development of the Sr double spike method including spike calibration and the evaluation of the spike-corrected Sr isotopic ratios.

Chapter III. was published in Geochimica et Cosmochimica Acta (KRABBENHÖFT et al., 2010). It represents the first application of the Sr double spike technique in order to derive the oceans Sr budget by combining the results of stable and radiogenic Sr isotope measurements of river waters, hydrothermal fluids, marine carbonates and seawater in a three-isotope plot. This approach adds an additional dimension to the radiogenic picture by making the differences in Sr isotopic composition of input and output fluxes apparent. This comparison clearly indicates an isotopic disequilibrium with the combined riverine and hydrothermal input showing a heavier ($\delta^{88/86}\text{Sr} \sim 0.31\text{‰}$) Sr isotopic composition compared to the output represented by marine carbonates ($\delta^{88/86}\text{Sr} \sim 0.21\text{‰}$).

Chapter IV. is focusing on the Sr isotopic composition of scleractinian warm water corals. In this study we analyzed cultured (*Acropora* sp.) and fossil (*Porites* sp.) warm water corals with respect to their Sr isotopic composition. The temperature sensitivity of $\delta^{88/86}\text{Sr}$ was tested and a non-linear relationship was found which is contrary to earlier results published by (FIETZKE and EISENHAUER, 2006; RÜGGERBERG et al., 2008). Furthermore an annual $\delta^{88/86}\text{Sr}$ cycle of a fossil (15 kyr B.P.) *Porites* sp. coral was measured showing a similar seasonal variability like $\delta^{18}\text{O}$ and Sr/Ca values. The average $\delta^{88/86}\text{Sr}$

of the fossil *Porites* sp. coral shows a similar isotopic composition ($\delta^{88/86}\text{Sr}_{\text{mean}}=0.205\pm 0.017\text{‰}$) like recent *Porites* sp. represented in this study by the coral standard JCp-1 ($\delta^{88/86}\text{Sr}_{\text{JCp-1}}=0.194\pm 0.009\text{‰}$). In contrast to Sr/Ca elemental ratios the average $\delta^{88/86}\text{Sr}$ is obviously not affected by enhanced weathering and elevated Sr fluxes from exposed shelves during glacial times.

Chapter V. provides a synthesis of the issues discussed in the frame of this work and gives suggestions of how to proceed in stable Sr isotope research.

Chapter VI. (Appendix) represents a summary of meeting abstracts I was attending during the course of my PhD. Furthermore it provides supporting material for stable Sr isotope researchers like a mathematical derivation of the Sr double spike algorithm and a user manual which describes the data processing from raw numbers to final stable Sr values.

I.8 References

- Abram, N. J., Gagan, M. K., Cole, J. E., Hantoro, W. S., and Mudelsee, M., 2008. Recent intensification of tropical climate variability in the Indian Ocean. *Nature Geoscience* **1**, 849-853.
- Adkins, J.F., Boyle, E.A., Curry, W.B., Lutringer, A., 2003, Stable isotopes in deep-sea corals and a new mechanism for “vital effects” , *Geochimica et Cosmochimica Acta*, Volume **67**, Issue 6, 1129-1143
- Albarède, F., Telouk, P., Blichert-Toft, J., Boyet, M., Agraniér, A., and Nelson, B., 2004. Precise and accurate isotopic measurements using multiple-collector ICPMS. *Geochimica et Cosmochimica Acta* **68**, 2725-2744.
- Amini, M., Eisenhauer, A., Böhm, F., Fietzke, J., Bach, W., Garbe-Schönberg, D., Rosner, M., Bock, B., Lackschewitz, K. S., and Hauff, F., 2008. Calcium isotope ($\delta^{44/40}\text{Ca}$) fractionation along hydrothermal pathways, Logatchev Field (Mid-Atlantic Ridge, 14° 45'N). *Geochimica et Cosmochimica Acta* **72**, 4107-4122.
- Andersson, P. S., Wasserburg, G. J., and Ingri, J., 1992. The sources and transport of Sr and Nd isotopes in the Baltic Sea. *Earth and Planetary Science Letters* **113**, 459-472.
- Basu, A. R., Jacobsen, S. B., Poreda, R. J., Dowling, C. B., and Aggarwal, P. K., 2001. Large groundwater strontium flux to the oceans from the Bengal Basin and the marine strontium isotope record. *Science* **293**, 1470-1473.
- Beck, J. W., Edwards, R. L., Ito, E., Taylor, F. W., Recy, J., Rougerie, F., Joannot, P., and Henin, C., 1992. Sea-surface temperature from coral skeletal strontium calcium ratios. *Science* **257**, 644-647.
- Blum, J. D., 1995. A silicate weathering mechanism linking increases in marine $^{87}\text{Sr}/^{86}\text{Sr}$ with global glaciation. *Letters to Nature* **373**, 415-417.
- Böhm, F., Gussone, N., Eisenhauer, A., Dullo, W. C., Reynaud, S., and Paytan, A., 2006. Calcium isotope fractionation in modern scleractinian corals. *Geochimica et Cosmochimica Acta* **70**, 4452-4462.
- Broecker, W. and Clark, E., 2009. Ratio of coccolith CaCO_3 to foraminifera CaCO_3 in late Holocene deep sea sediments. *Paleoceanography* **24**, 234 p.p., doi:10.1029/2009PA001731.
- Bullen, T. D. and Eisenhauer, A., 2009. Metal stable isotopes In low-temperature systems: A primer. *Elements* **5**, 349-352.
- Burke, W. H., Denison, R. E., Hetherington, E. A., Koepnick, R. B., Nelson, H. F., and Otto, J. B., 1982. Variation of seawater $^{87}\text{Sr}/^{86}\text{Sr}$ throughout Phanerozoic time. *Geology* **10**, 516-519.
- Camoin, G. F., Iryu, Y., McInroy, D. B., and Scientists, a. t. E., 2005. Expedition 310 of the mission-specific drilling platform from and to Papeete, Tahiti, French Polynesia Sites M0005–M0026. *Integrated Ocean Drilling Program Management International, Inc., for the Integrated Ocean Drilling Program*.
- Capo, R. C. and Depaolo, D. J., 1990. Seawater strontium isotopic variations from 2.5 million years ago to the present. *Science* **249**, 51-55.
- Cardinal, D., Hamelin, B., Bard, E., and Pätzold, J., 2001. Sr/Ca, U/Ca and $\delta^{18}\text{O}$ records in recent massive corals from Bermuda: relationships with sea surface temperature. *Chemical Geology* **176**, 213-233.
- Chacko, T., Cole, D. R., and Horita, J., 2001. Equilibrium oxygen, hydrogen and carbon isotope fractionation factors applicable to geologic systems, *Stable Isotope Geochemistry*. Mineralogical Soc America, Washington.
- Chakraborty, S. and Ramesh, R., 1993. Monsoon-induced sea-surface temperature-changes recorded in indian corals. *Terr. Nova* **5**, 545-551.
- Cobb, K. M., Charles, C. D., Cheng, H., and Edwards, R. L., 2003. El Nino/Southern Oscillation and tropical Pacific climate during the last millennium. *Nature* **424**, 271-276.
- Cobb, K., Cole, C., Lough, J., Tudhope, S., 2008, Annually banded corals as climate proxies. “White Paper” for Trieste Meeting 9.-11. June 2008
- Cohen, A. L. and Thorrold, S. R., 2007. Recovery of temperature records from slow-growing corals by fine scale sampling of skeletons. *Geophysical Research Letters* **34**, L17706, doi: 10.1029/2007gl030967.

- Cole, J. E., Fairbanks, R. G., and Shen, G. T., 1993a. Recent variability in the southern oscillation - Isotopic results from a Tarawa atoll coral. *Science* **260**, 1790-1793.
- Cole, J. E., Rind, D., and Fairbanks, R. G., 1993b. Isotopic responses to interannual climate variability simulated by an atmospheric general-circulation model. *Quaternary Science Reviews* **12**, 387-406.
- Compston, W. and Overspy, V. M., 1969. Lead isotopic analysis using a double spike. *Journal of Geophysical Research* **74**, 4338-4348.
- Davis, A. C., Bickle, M. J., and Teagle, D. A. H., 2003. Imbalance in the oceanic strontium budget. *Earth and Planetary Science Letters* **211**, 173-187.
- De La Rocha, C. L. and DePaolo, D. J., 2000. Isotopic evidence for variations in the marine calcium cycle over the Cenozoic. *Science* **289**, 1176-1178.
- De Souza, G. F., Reynolds, B. C., Kiczka, M., and Bourdon, B., 2010. Evidence for mass-dependent isotopic fractionation of strontium in a glaciated granitic watershed. *Geochimica et Cosmochimica Acta* **74**, 2596-2614.
- Delaney, M. L., Linn, L. J., and Davies, P. J., 1996. Trace and minor element ratios in Halimeda aragonite from the Great Barrier Reef. *Coral Reefs* **15**, 181-189.
- Dietz, L. A., Pachucki, C. F., and Land, G. A., 1962. Internal standard technique for precise isotopic abundance measurements in thermal ionization mass spectrometry. *Anal. Chem.* **34**, 709-710.
- Dodson, M. H., 1963. A theoretical study of the use of internal standards for precise isotopic analysis by the surface ionization technique. Part I - General first-order algebraic solutions. *J. Sci. Instrum.* **40**, 289-295.
- Dunbar, R. B., Wellington, G. M., Colgan, M. W., and Glynn, P. W., 1994. Eastern Pacific sea-surface temperature since 1600-AD - The $\delta^{18}\text{O}$ record of climate variability in galapagos corals. *Paleoceanography* **9**, 291-315.
- Eisenhauer, A., Kiskurek, B., and Böhm, F., 2009. Marine Calcification: An Alkaline Earth Metal Isotope Perspective. *Elements* **5**, 365-368.
- Elderfield, H., 1986. Strontium isotope stratigraphy. *Palaeogeography, Palaeoclimatology, Palaeoecology* **57**, 71-90.
- Elderfield, H. and Gieskes, J. M., 1982. Sr isotopes in interstitial waters of marine sediments from deep-sea drilling project cores. *Nature* **300**, 493-497.
- Elderfield, H. and Schultz, A., 1996. Mid-ocean ridge hydrothermal fluxes and the chemical composition of the ocean. *Annu. Rev. Earth Planet. Sci.* **24**, 191-224.
- Fairbanks, R. G. and Dodge, R. E., 1979. Annual periodicity of the skeletal oxygen and carbon stable isotopic composition in the coral *Montastrea Annularis*. *Geochimica et Cosmochimica Acta* **43**, 447-449.
- Fallon, S. J., McCulloch, M. T., van Woerik, R., and Sinclair, D. J., 1999. Corals at their latitudinal limits: laser ablation trace element systematics in Porites from Shirigai Bay, Japan. *Earth and Planetary Science Letters* **172**, 221-238.
- Fantle, M. S. and DePaolo, D. J., 2006. Sr isotopes and pore fluid chemistry in carbonate sediment of the Ontong Java Plateau: Calcite recrystallization rates and evidence for a rapid rise in seawater Mg over the last 10 million years. *Geochimica et Cosmochimica Acta* **70**, 3883-3904.
- Farkaš, J., Buhl, D., Blenkinsop, J., and Veizer, J., 2007. Evolution of the oceanic calcium cycle during the late Mesozoic: Evidence from $\delta^{44/40}\text{Ca}$ of marine skeletal carbonates. *Earth and Planetary Science Letters* **253**, 96-111.
- Faure, G. and Felder, R. P., 1981. Isotopic composition of strontium and sulfur in secondary gypsum crystals, Brown Hills, transantarctic mountains. *Journal of Geochemical Exploration* **14**, 265-270.
- Faure, G. and Mensing, T. M., 2005. Isotopes: Principals and Applications. *John Wiley Sons, Inc., Hoboken, New Jersey*.
- Felis, T., Lohmann, G., Kuhnert, H., Lorenz, S. J., Scholz, D., Patzold, J., Al-Rousan, S. A., and Al-Moghrabi, S. M., 2004. Increased seasonality in Middle East temperatures during the last interglacial period. *Nature* **429**, 164-168.

- Felis, T., Merkel, U., Asami, R., Deschamps, P., Hathorne, E. C., Kölling, M., Bard, E., Cabioch, G., Durand, N., Prange, M., Schulz, M., Cahyarini, S. Y., and Pfeiffer, M., 2010. Pronounced interannual variability in tropical South Pacific temperatures at the end of the last glacial. *submitted*.
- Felis, T., Patzold, J., Loya, Y., Fine, M., Nawar, A. H., and Wefer, G., 2000. A coral oxygen isotope record from the northern Red Sea documenting NAO, ENSO, and North Pacific teleconnections on Middle East climate variability since the year 1750. *Paleoceanography* **15**, 679-694.
- Felis, T., Suzuki, A., Kuhnert, H., Dima, M., Lohmann, G., and Kawahata, H., 2009. Subtropical coral reveals abrupt early-twentieth-century freshening in the western North Pacific Ocean. *Geology* **37**, 527-530.
- Fietzke, J. and Eisenhauer, A., 2006. Determination of temperature-dependent stable strontium isotope ($^{88}\text{Sr}/^{86}\text{Sr}$) fractionation via bracketing standard MC-ICP-MS. *Geochemistry Geophysics Geosystems* **7**, Q08009, doi:10.1029/2006GC001243.
- Fietzke, J., Liebetrau, V., Guenther, D., Gurs, K., Hametner, K., Zumholz, K., Hansteen, T. H., and Eisenhauer, A., 2008. An alternative data acquisition and evaluation strategy for improved isotope ratio precision using LA-MC-ICP-MS applied to stable and Radiogenic strontium isotopes in carbonates. *Journal of Analytical Atomic Spectrometry* **23**, 955-961.
- Gagan, M. K., Ayliffe, L. K., Beck, J. W., Cole, J. E., Druffel, E. R. M., Dunbar, R. B., and Schrag, D. P., 2000. New views of tropical paleoclimates from corals. *Quaternary Science Reviews* **19**, 45-64.
- Gaillardet, J., Dupre, B., and Allègre, C. J., 1999. Geochemistry of large river suspended sediments: Silicate weathering or recycling tracer? *Geochimica et Cosmochimica Acta* **63**, 4037-4051.
- Galer, J. G. S., 1999. Optimal double and triple spiking for high precision lead isotopic measurement. *Chemical Geology* **157**, 255-274.
- Gallup, C. D., Olson, D. M., Edwards, R. L., Gruhn, L. M., Winter, A., and Taylor, F. W., 2006. Sr/Ca-sea surface temperature calibration in the branching caribbean coral *Acropora Palmata*. *Geophysical Research Letters* **33**, L03606, doi:10.1029/2005GL024935.
- Godderis, Y. and Francois, L. M., 1995. The Cenozoic evolution of the strontium and carbon cycles: Relative importance of continental erosion and mantle exchanges. *Chemical Geology* **126**, 169-190.
- Godderis, Y. and Veizer, J., 2000. Tectonic control of chemical and isotopic composition of ancient oceans: The impact of continental growth. *Am. J. Sci.* **300**, 434-461.
- Goldstein, S. J. and Jacobsen, S. B., 1987. The Nd and Sr isotopic systematics of river-water dissolved material: Implications for the sources of Nd and Sr in seawater. *Chemical Geology: Isotope Geoscience section* **66**, 245-272.
- Goldstein, S. J. and Jacobsen, S. B., 1988. Nd and Sr isotopic systematics of river water suspended material: implications for crustal evolution. *Earth Planet. Sci. Lett.* **87**, 249-265.
- Graham, S. T., Famiglietti, J. S., and Maidment, D. R., 1999. Five-minute, 1/2 degrees, and 1 degrees data sets of continental watersheds and river networks for use in regional and global hydrologic and climate system modeling studies. *Water Resources Research* **35**, 583-587.
- Gussone, N., Eisenhauer, A., Heuser, A., Dietzel, M., Bock, B., Böhm, F., Spero, H. J., Lea, D. W., Bijma, J., and Nagler, T. F., 2003. Model for kinetic effects on calcium isotope fractionation ($\delta^{44/40}\text{Ca}$) in inorganic aragonite and cultured planktonic foraminifera. *Geochimica et Cosmochimica Acta* **67**, 1375-1382.
- Haase, K. M., Petersen, S., Koschinsky, A., Seifert, R., Devey, C. W., Keir, R., Lackschewitz, K. S., Melchert, B., Perner, M., Schmale, O., Suling, J., Dubilier, N., Zielinski, F., Fretzdorff, S., Garbe-Schonberg, D., Westernstroer, U., German, C. R., Shank, T. M., Yoerger, D., Giere, O., Kuever, J., Marbler, H., Mawick, J., Mertens, C., Stober, U., Ostertag-Henning, C., Paulick, H., Peters, M., Strauss, H., Sander, S., Stecher, J., Warmuth, M., and Weber, S., 2007. Young volcanism and related hydrothermal activity at 5 degrees S on the slow-spreading southern Mid-Atlantic Ridge. *Geochemistry Geophysics Geosystems* **8**, 17, doi:10.1029/2006GC001509

- Halicz, L., Segal, I., Fruchter, N., Stein, M., and Lazar, B., 2008. Strontium stable isotopes fractionate in the soil environments? *Earth and Planetary Science Letters* **272**, 406-411.
- Halicz, L., Segali, I., Fruchter, N., Lazar, B., and Stein, M., 2007. $^{86}\text{Sr}/^{88}\text{Sr}$ ratio by ICP-MS-MC as a new tracer of terrestrial geochemical processes. *17th Goldschmidt conference 2007*.
- Harrington, G. A. and Herczeg, A. L., 2003. The importance of silicate weathering of a sedimentary aquifer in and Central Australia indicated by very high $^{87}\text{Sr}/^{86}\text{Sr}$ ratios. *Chemical Geology* **199**, 281-292.
- Henderson, G. M., Martel, D. J., Onions, R. K., Shackleton, N. J., 1994. Evolution of seawater $^{87}\text{Sr}/^{86}\text{Sr}$ over the last 400 ka - the absence of glacial interglacial cycles. *Earth and Planetary Science Letters* **128**, 643-651.
- Heuser, A., Eisenhauer, A., Gussone, N., Bock, B., Hansen, B. T., and Nögler, T. F., 2002. Measurement of calcium isotopes ($\delta^{44/40}\text{Ca}$) using a multicollector TIMS technique. *International Journal of Mass Spectrometry* **220**, 385-397.
- Hodell, D. A., Mead, G. A., and Mueller, P. A., 1990. Variation in the strontium isotopic composition of seawater (8 Ma to present) : Implications for chemical weathering rates and dissolved fluxes to the oceans. *Chemical Geology: Isotope Geoscience section* **80**, 291-307.
- Hubbard, D. K., Miller, A. I., and Scaturro, D., 1990. Production and cycling of calcium-carbonate in a shelf-edge reef system (St. Croix, United-States Virgin-Islands) - Applications to the nature of reef systems in the fossil record. *Journal of Sedimentary Petrology* **60**, 335-360.
- Jenkyns, H. C., Jones, C. E., Grocke, D. R., Hesselbo, S. P., and Parkinson, D. N., 2002. Chemostratigraphy of the Jurassic system: applications, limitations and implications for palaeoceanography. *Journal of the Geological Society* **159**, 351-378.
- Johnson, C. M. and Beard, B. L., 1999. Correction of instrumentally produced mass fractionation during isotopic analysis of Fe by thermal ionization mass spectrometry. *International Journal of Mass Spectrometry* **193**, 87-99.
- Johnson, C. M., Beard, B. L., and Albarède, F., 2004. Geochemistry of non-traditional stable isotopes. *Reviews in Mineralogy & Geochemistry* **55**.
- Kendall, C. and McDonnell, 1998, Isotope tracers in catchment hydrology, *Elsevier Science B.V.*, Amsterdam, 51-86
- Kisakürek, B., Eisenhauer, A., Böhm, F., Garbe-Schönberg, D., and Erez, J., 2008. Controls on shell Mg/Ca and Sr/Ca in cultured planktonic foraminifera. *Earth Planet. Sci. Lett* **273**, 260-269.
- Knudson, K. J., Williams, H. M., Buikstra, J. E., Tomczak, P. D., Gordon, G. W., and Anbar, A. D., 2010. Introducing $\delta^{88/86}\text{Sr}$ analysis in archaeology: a demonstration of the utility of strontium isotope fractionation in paleodietary studies. *Journal of Archaeological Science* **37**, 2352-2364.
- Knutson, D. W., Buddemeier, R. W., and Smith, S. V., 1972. Coral chronometers: Seasonal growth bands in reef corals. *Science* **177**, 270-272.
- Krabbenhöft, A., Eisenhauer, A., Böhm, F., Vollstaedt, H., Fietzke, J., Liebetrau, V., Augustin, N., Peucker-Ehrenbrink, B., Müller, M. N., Horn, C., Hansen, B. T., Nolte, N., and Wallmann, K., 2010. Constraining the marine strontium budget with natural strontium isotope fractionations ($^{87}\text{Sr}/^{86}\text{Sr}^*$, $\delta^{88/86}\text{Sr}$) of carbonates, hydrothermal solutions and river waters. *Geochimica et Cosmochimica Acta* **74**, 4097-4109.
- Krabbenhöft, A., Fietzke, J., Eisenhauer, A., Liebetrau, V., Böhm, F., and Vollstaedt, H., 2009. Determination of radiogenic and stable strontium isotope ratios ($^{87}\text{Sr}/^{86}\text{Sr}/\delta^{88/86}\text{Sr}$) by thermal ionization mass spectrometry applying an $^{87}\text{Sr}/^{84}\text{Sr}$ double spike. *Journal of Analytical Atomic Spectrometry* **24**, 1267-1271.
- Krishnaswami, S. and Singh, S. K., 1998. Silicate and carbonate weathering in the drainage basins of the Ganga-Ghaghara-Indus head waters: Contributions to major ion and Sr isotope geochemistry. *Proceedings of the Indian Academy of Sciences-Earth and Planetary Sciences* **107**, 283-291.
- Kuhnert, H., Pätzold, J., Wyrwoll, K. H., and Wefer, G., 2000. Monitoring climate variability over the past 116 years in coral oxygen isotopes from Ningaloo Reef, Western Australia. *International Journal of Earth Sciences* **88**, 725-732.

- Lea, D. W., Pak, D. K., and Spero, H. J., 2000. Climate impact of late quaternary equatorial Pacific sea surface temperature variations. *Science* **289**, 1719-1724.
- Leder, J. J., Swart, P. K., Szmant, A. M., and Dodge, R. E., 1996. The origin of variations in the isotopic record of scleractinian corals: 1. Oxygen. *Geochimica et Cosmochimica Acta* **60**, 2857-2870.
- Lemarchand, D., Wasserburg, G. T., and Papanastassiou, D. A., 2004. Rate-controlled calcium isotope fractionation in synthetic calcite. *Geochimica et Cosmochimica Acta* **68**, 4665-4678.
- Liebetrau, V., Eisenhauer, A., Krabbenhöft, A., Fietzke, J., Böhm, F., Rüggeberg, A., and Guers, K., 2009. New perspectives on the marine Sr-isotope record: $\delta^{88/86}\text{Sr}$, $^{87}\text{Sr}/^{86}\text{Sr}^*$ and $\delta^{44/40}\text{Ca}$ signatures of aragonitic molluscs throughout the last 27 Ma. *Geochimica et Cosmochimica Acta* **73**, A762.
- Lindberg, B. and Mienert, J., 2005. Postglacial carbonate production by cold-water corals on the Norwegian shelf and their role in the global carbonate budget. *Geology* **33**, 537-540.
- Locarnini, R. A., A. V. Mishonov, J. I. Antonov, Boyer, T. P., and Garcia, H. E., 2006. World Ocean Atlas 2005. *NOAA Atlas NESDIS 61*, U.S. Government Printing Office **1**, 182 pp.
- Marriott, C. S., Henderson, G. M., Crompton, R., Staubwasser, M., and Shaw, S., 2004. Effect of mineralogy, salinity, and temperature on Li/Ca and Li isotope composition of calcium carbonate. *Chemical Geology* **212**, 5-15.
- Marshall, A. T. and Clode, P., 2004. Calcification rate and the effect of temperature in a zooxanthellate and an azooxanthellate scleractinian reef coral. *Coral Reefs* **23**, 218-224.
- McArthur, J. M., 1994. Recent trends in strontium isotope stratigraphy. *Terr. Nova* **6**, 331-358.
- McArthur, J. M., Howarth, R. J., and Bailey, T. R., 2001. Strontium isotope stratigraphy: LOWESS Version 3: Best fit to the marine Sr-isotope curve for 0-509 Ma and accompanying look-up table for deriving numerical age. *Journal of Geology* **109**, 155-170.
- McConnaughey, T., 1989. ^{13}C and ^{18}O isotopic disequilibrium in biological carbonates. *Geochimica et Cosmochimica Acta* **53**, 151-162.
- McCrea, J. M., 1950. On the isotopic chemistry of carbonates and a paleotemperature scale. *Journal of chemical physics* **18**, 849-857.
- McCulloch, M. T., Gagan, M. K., Mortimer, G. E., Chivas, A. R., and Isdale, P. J., 1994. A high-resolution Sr/Ca and $\delta^{18}\text{O}$ coral record from the Great-Barrier-Reef, Australia, and the 1982-1983 El-Nino. *Geochimica et Cosmochimica Acta* **58**, 2747-2754.
- McCulloch, M. T., Tudhope, A. W., Esat, T. M., Mortimer, G. E., Chappell, J., Pillans, B., Chivas, A. R., and Omura, A., 1999. Coral record of equatorial sea-surface temperatures during the penultimate deglaciation at Huon Peninsula. *Science* **283**, 202-204.
- Milliman, J. D., 1974. Recent sedimentary carbonates. *Springer-Verlag*.
- Milliman, J. D. and Droxler, A. W., 1996. Neritic and pelagic carbonate sedimentation in the marine environment: Ignorance is not bliss. *Geol. Rundsch.* **85**, 496-504.
- Min, G. R., Edwards, R. L., Taylor, F. W., Recy, J., Gallup, C. D., and Beck, J. W., 1995. Annual cycles of U/Ca in coral skeletons and U/Ca thermometry. *Geochimica et Cosmochimica Acta* **59**, 2025-2042.
- Mitsuguchi, T., Matsumoto, E., Abe, O., Uchida, T., and Isdale, P. J., 1996. Mg/Ca thermometry in coral-skeletons. *Science* **274**, 961-963.
- Nägler, T. F., Eisenhauer, A., Müller, A., Hemleben, C., and Kramers, J., 2000. The $\delta^{44}\text{Ca}$ - temperature calibration on fossil and cultured Globigerinoides sacculifer: New tool for reconstruction of past sea surface temperatures. *Geochemistry Geophysics Geosystems* **1(9)**, 1052, doi:10.1029/2000GC000091.
- Nier, A. O., 1938. The isotopic constitution of strontium, barium, bismuth, thallium and mercury. *Physical Review* **5**, 275-279.
- Nier, A. O., 1940. A mass spectrometer routine for isotope abundance measurements. *Rev. Sci. Instr.* **18**, 398-411.
- O'Neil, J. R., 1986. Theoretical and experimental aspects of isotopic fractionation. *Reviews in Mineralogy and Geochemistry* **16**, 1-40.

- Ohno, T. and Hirata, T., 2007. Simultaneous determination of mass-dependent isotopic fractionation and radiogenic isotope variation of strontium in geochemical samples by multiple collector-ICP-mass spectrometry. *Anal. Sci.* **23**, 1275-1280.
- Ohno, T., Komiya, T., Ueno, Y., Hirata, T., and Maruyama, S., 2008. Determination of $^{88}\text{Sr}/^{86}\text{Sr}$ mass-dependent isotopic and radiogenic isotope variation of $^{87}\text{Sr}/^{86}\text{Sr}$ in the Neoproterozoic Doushantuo Formation. *Gondwana Res.* **14**, 126-133.
- Oliver, L., Harris, N., Bickle, M., Chapman, H., Dise, N., and Horstwood, M., 2003. Silicate weathering rates decoupled from the $^{87}\text{Sr}/^{86}\text{Sr}$ ratio of the dissolved load during Himalayan erosion. *Chemical Geology* **201**, 119-139.
- Page, B. D., Bullen, T. D., and Mitchell, M. J., 2008. Influences of calcium availability and tree species on Ca isotope fractionation in soil and vegetation. *Biogeochemistry* **88**, 1-13.
- Palmer, M. R. and Edmond, J. M., 1989. The Strontium Isotope Budget of the Modern Ocean. *Earth Planet. Sci. Lett.* **92**, 11-26.
- Palmer, M. R. and Edmond, J. M., 1992. Controls over the strontium isotope composition of river water. *Geochimica et Cosmochimica Acta* **56**, 2099-2111.
- Papanastassiou, D. A. and Wasserburg, G. J., 1973. RbSr ages and initial strontium in basalts from Apollo 15. *Earth and Planetary Science Letters* **17**, 324-337.
- Patchett, P. J., 1980a. Sr isotopic fractionation in Allende chondrules: A reflection of solar nebular processes. *Earth and Planetary Science Letters* **50**, 181-188.
- Patchett, P. J., 1980b. Sr isotopic fractionation in Ca-Al inclusions from the Allende meteorite. *Nature* **283**, 438-441.
- Pätzold, J., 1984. Growth rhythms recorded in stable isotopes and density bands in the reef coral *Porites lobata* (Cebu, Philippines). *Coral Reefs* **3**, 87-90.
- Peterman, Z. E., Hedge, C. E., and Tourtelot, H. A., 1970. Isotopic composition of strontium in seawater throughout Phanerozoic time. *Geochimica Cosmochimica Acta* **34**, 105-120.
- Peucker-Ehrenbrink, B. and Miller, M. W., 2004. River Chemistry and Drainage Basin Geology. *Geochimica et Cosmochimica Acta* **68**, A426-A426.
- Peucker-Ehrenbrink, B., Miller, M. W., Arsouze, T., and Jeandel, C., 2010. Continental bedrock and riverine fluxes of strontium and neodymium isotopes to the oceans. *Geochemistry Geophysics Geosystems* **11**, Q03016, 22 pp., doi:10.1029/2009GC002869
- Pfeiffer, M., Timm, O., Dullo, W. C., and Garbe-Schonberg, D., 2006. Paired coral Sr/Ca and $\delta^{18}\text{O}$ records from the Chagos Archipelago: Late twentieth century warming affects rainfall variability in the tropical Indian Ocean. *Geology* **34**, 1069-1072.
- Quade, J., English, N., and DeCelles, P. G., 2003. Silicate versus carbonate weathering in the Himalaya: a comparison of the Arun and Seti River watersheds. *Chemical Geology* **202**, 275-296.
- Reynaud-Vaganay, S., Gattuso, J. P., Cuif, J. P., Jaubert, J., and Juillet-Leclerc, A., 1999. A novel culture technique for scleractinian corals: application to investigate changes in skeletal $\delta^{18}\text{O}$ as a function of temperature. *Marine Ecology-Progress Series* **180**, 121-130.
- Reynaud, S., Ferrier-Pages, C., Boisson, F., Allemand, D., and Fairbanks, R. G., 2004. Effect of light and temperature on calcification and strontium uptake in the scleractinian coral *Acropora verweyi*. *Mar. Ecol.-Prog. Ser.* **279**, 105-112.
- Reynaud, S., Ferrier-Pages, C., Meibom, A., Mostefaoui, S., Mortlock, R., Fairbanks, R., and Allemand, D., 2007. Light and temperature effects on Sr/Ca and Mg/Ca ratios in the scleractinian coral *Acropora* sp. *Geochimica et Cosmochimica Acta* **71**, 354-362.
- Richter, F. M., Rowley, D. B., and DePaolo, D. J., 1992. Sr isotope evolution of seawater: the role of tectonics. *Earth and Planetary Science Letters* **109**, 11-23.
- Rollion-Bard, C., Vigier, N., Meibom, A., Blamart, D., Reynaud, S., Rodolfo-Metalpa, R., Martin, S., and Gattuso, J. P., 2009. Effect of environmental conditions and skeletal ultrastructure on the Li isotopic composition of scleractinian corals. *Earth and Planetary Science Letters* **286**, 63-70.
- Rudge, J. F., Reynolds, B. C., and Bourdon, B., 2009. The double spike toolbox. *Chemical Geology* **265**, 420-431.

- Rüggeberg, A., Fietzke, J., Liebetrau, V., Eisenhauer, A., Dullo, W. C., and Freiwald, A., 2008. Stable strontium isotopes ($\delta^{88/86}\text{Sr}$) in cold-water corals - A new proxy for reconstruction of intermediate ocean water temperatures. *Earth and Planetary Science Letters* **269**, 569-574.
- Russell, W. A., Papanastassiou, D. A., and Tombrello, T. A., 1978. Ca isotope fractionation on the earth and other solar system materials. *Geochimica et Cosmochimica Acta* **42**, 1075-1090.
- Sawaki, Y., Ohno, T., Tahata, M., Komiya, T., Hirata, T., Maruyama, S., Windley, B. F., Han, J., Shu, D. G., and Li, Y., 2010. The Ediacaran radiogenic Sr isotope excursion in the Doushantuo Formation in the Three Gorges area, South China. *Precambrian Research* **176**, 46-64.
- Schauble, E.A., 2004. Applying stable isotope fractionation theory to new systems. *Reviews in Mineralogy and Geochemistry*, v. 55, 1, 65-111, DOI: 10.2138/gsrmg.55.1.65
- Schiebel, R., 2002. Planktic Foraminiferal sedimentation and the marine calcite budget. *Glob. Biogeochem. Cycle* **16**, 21 p.p., doi:10.1029/2001GB001459 .
- Schmitt, A. D., Galer, S. J. G., and Abouchami, W., 2009. High-precision cadmium stable isotope measurements by double spike thermal ionisation mass spectrometry. *Journal of Analytical Atomic Spectrometry* **24**, 1079-1088.
- Shackleton, N. J., 1967. Oxygen isotope analyses and Pleistocene temperature re-assessed. *Nature* **215**, 15-17.
- Shen, C. C., Hastings, D. W., Lee, T. P., Chiu, C. H., Lee, M. Y., Wei, K. Y., and Edwards, R. L., 2001. High precision glacial-interglacial benthic foraminiferal Sr/Ca records from the eastern equatorial Atlantic Ocean and Caribbean Sea. *Earth and Planetary Science Letters* **190**, 197-209.
- Shen, C. C., Lee, T., Chen, C. Y., Wang, C. H., Dai, C. F., and Li, L. A., 1996. The calibration of D[Sr/Ca] versus sea surface temperature relationship for Porites corals. *Geochimica et Cosmochimica Acta* **60**, 3849-3858.
- Siebert, C., Nägler, T. F., and Kramers, J. D., 2001. Determination of molybdenum isotope fractionation by double-spike multicollector inductively coupled plasma mass spectrometry. *Geochemistry Geophysics Geosystems* **2**, art. doi:10.1029/2000GC000124
- Sinclair, D. J., Williams, B., and Risk, M., 2006. A biological origin for climate signals in corals - Trace element "vital effects" are ubiquitous in Scleractinian coral skeletons. *Geophysical Research Letters* **33**, 5 p.p., doi:10.1029/2006GL027183
- Smalley, P. C., Higgins, A. C., Howarth, R. J., Nicholson, H., Jones, C. E., Swinburne, N. H. M., and Bessa, J., 1994. Seawater Sr isotope variations through time - A procedure for constructing a reference curve to date and correlate marine sedimentary-rocks. *Geology* **22**, 431-434.
- Smith, S. V., Buddemeier, R. W., Redalje, R. C., and Houck, J. E., 1979. Strontium-Calcium thermometry in coral skeletons. *Science* **204**, 404-407.
- Stanley, S. M. and Hardie, L. A., 1998. Secular oscillations in the carbonate mineralogy of reef-building and sediment-producing organisms driven by tectonically forced shifts in seawater chemistry. *Palaeogeography Palaeoclimatology Palaeoecology* **144**, 3-19.
- Stoll, H. M. and Schrag, D. P., 1998. Effects of Quaternary sea Level Cycles on Strontium in Seawater. *Geochimica et Cosmochimica Acta* **62**, 1107-1118.
- Stoll, H. M. and Schrag, D. P., 2000. Coccolith Sr/Ca as a new indicator of coccolithophorid calcification and growth rate. *Geochem. Geophys. Geosys.* **1**, 24 p.p., doi:10.1029/1999GC000015.
- Stoll, H. M., Schrag, D. P., and Clemens, S. C., 1999. Are Seawater Sr/Ca Variations Preserved in Quaternary Foraminifera? *Geochimica et Cosmochimica Acta* **63**, 3535-3547.
- Sun, Y., Sun, M., Lee, T., and Nie, B., 2005. Influence of seawater Sr content on coral Sr/Ca and Sr thermometry. *Coral Reefs* **24**, 23-29.
- Swart, P. K., Leder, J. J., Szmant, A. M., and Dodge, R. E., 1996. The origin of variations in the isotopic record of scleractinian corals .2. Carbon. *Geochimica et Cosmochimica Acta* **60**, 2871-2885.
- Tang, J. W., Kohler, S. J., and Dietzel, M., 2008. $\text{Sr}^{2+}/\text{Ca}^{2+}$ and $^{44}\text{Ca}/^{40}\text{Ca}$ fractionation during inorganic calcite formation: I. Sr incorporation. *Geochimica et Cosmochimica Acta* **72**, 3718-3732.
- Taylor, A. S. and Lasaga, A. C., 1999. The role of basalt weathering in the Sr isotope budget of the oceans. *Chemical Geology* **161**, 199-214.

- Thiemens, M. H., 1992. Mass-independent isotopic fractionations and their applications. *Acs Symposium Series* **502**, 138-154.
- Thiemens, M. H., Jackson, T. L., and Brenninkmeijer, C. A. M., 1995. Observation of a mass-independent oxygen isotopic composition in terrestrial stratospheric CO₂, the link to ozone chemistry, and the possible occurrence in the Martian atmosphere. *Geophysical Research Letters* **22**, 255-257.
- Tütken, T., Eisenhauer, A., Wiegand, B., and Hansen, B. T., 2002. Glacial-interglacial cycles in Sr and Nd isotopic composition of Arctic marine sediments: changes in sediment provenance triggered by the Barents Sea ice sheet. *Marine Geology* **182**, 351-372.
- Urey, H., 1947. The thermodynamic properties of isotopic substances. *Journal of the geochemical society*, 562-581.
- Vance, D., Teagle, D. A. H., and Foster, G. L., 2009. Variable Quaternary Chemical Weathering Fluxes and Imbalances in Marine Geochemical Budgets. *Nature* **458**, 493-496.
- Veizer, J., 1989. Strontium isotopes in seawater through time. *Annu. Rev. Earth Planet. Sci.* **17**, 141-167.
- Veizer, J., Ala, D., Azmy, K., Bruckschen, P., Buhl, D., Bruhn, F., Carden, G. A. F., Diener, A., Ebner, S., Godderis, Y., Jasper, T., Korte, C., Pawellek, F., Podlaha, O. G., and Strauss, H., 1999. ⁸⁷Sr/⁸⁶Sr, $\delta^{13}\text{C}$ and $\delta^{18}\text{O}$ evolution of Phanerozoic seawater. *Chemical Geology* **161**, 59-88.
- Veizer, J., Buhl, D., Diener, A., Ebner, S., Podlaha, O. G., Bruckschen, P., Jasper, T., Korte, C., Schaaf, M., Ala, D., and Azmy, K., 1997. Strontium isotope stratigraphy: potential resolution and event correlation. *Palaeogeography Palaeoclimatology Palaeoecology* **132**, 65-77.
- Vigier, N., Rollion-Bard, C., Spezzaferri, S., and Brunet, F., 2007. In situ measurements of Li isotopes in foraminifera. *Geochemistry Geophysics Geosystems* **8**, 679-690.
- Walther, B. D. and Thorrold, S. R., 2006. Water, not food, contributes the majority of strontium and barium deposited in the otoliths of a marine fish. *Marine Ecology-Progress Series* **311**, 125-130.
- Weber, J. N. and Woodhead, P. M., 1972. Temperature dependence of oxygen-18 concentration in reef coral carbonates. *Journal of Geophysical Research* **77**, 463-470.
- Wells, J. W., 1957. Coral Reefs. *Ecological Society America* **67**, 609-631.
- Wickman, F. E., 1948. Isotope ratios: a clue to the age of certain marine sediments. *J. Geol.* **56**, 61-66.
- Wiegand, B. A., Chadwick, O. A., Vitousek, P. M., and Wooden, J. L., 2005. Ca cycling and isotopic fluxes in forested ecosystems in Hawaii. *Geophysical Research Letters* **32**, 4 p.p..
- Yang, L., Peter, C., Panne, U., and Sturgeon, R. E., 2008. Use of Zr for mass bias correction in strontium isotope ratio determinations using MC-ICP-MS. *Journal of Analytical Atomic Spectrometry* **23**, 1269-1274.
- Young, E. D., Galy, A., and Nagahara, H., 2002. Kinetic and equilibrium mass-dependent isotope fractionation laws in nature and their geochemical and cosmochemical significance. *Geochimica et Cosmochimica Acta* **66**, 1095-1104.

Chapter II

MANUSCRIPT I

II. Determination of radiogenic and stable strontium isotope ratios ($^{87}\text{Sr}/^{86}\text{Sr}$, $\delta^{88/86}\text{Sr}$) by thermal ionization mass spectrometry applying an $^{87}\text{Sr}/^{84}\text{Sr}$ double spike

Andre Krabbenhöft,^{ab} Jan Fietzke^a, Anton Eisenhauer^a, Volker Liebetrau^a, Florian Böhm^a and Hauke Vollstaedt^a

^a Wischhofstraße 1-3, D-24148 Kiel, Germany. Tel: +49-(0)431-600-2109;

^b corresponding author (ankrabbenhoeft@ifm-geomar.de)

Published in *Journal of Analytical Atomic Spectrometry* 24 (2009), 1267-1271

II.1 Abstract

Recent findings of natural strontium isotope fractionation have opened a new field of research in non-traditional stable isotope geochemistry. While previous studies were based on data obtained by MC-ICP-MS we here present a novel approach combining thermal ionization mass spectrometry (TIMS) with the use of an $^{87}\text{Sr}/^{84}\text{Sr}$ double spike (DS). Our results for the IAPSO sea water and JCp-1 coral standards, respectively, are in accord with previously published data. Strontium isotope composition of IAPSO sea water standard was determined as $\delta^{88/86}\text{Sr}=0.386(5)\text{‰}$ (δ values relative to the SRM987), $^{87}\text{Sr}/^{86}\text{Sr}^*=0.709312(9)$ $n=10$ and a corresponding conventionally normalized $^{87}\text{Sr}/^{86}\text{Sr}=0.709168(7)$ (all uncertainties 2SEM). For JCp-1 coral standard we obtained $\delta^{88/86}\text{Sr}=0.197(8)\text{‰}$, $^{87}\text{Sr}/^{86}\text{Sr}^*=0.709237(2)$ and $^{87}\text{Sr}/^{86}\text{Sr}=0.709164(5)$ $n=3$. We show that applying this DS-TIMS method the precision is improved by at least a factor of 2 - 3 when compared to MC-ICP-MS.

II.2 Introduction

The Rubidium/Strontium (Rb/Sr) radiogenic isotope system is one of the oldest isotopic applications measured by mass-spectrometry (NIER, 1938; NIER, 1940; PAPANASTASSIOU and WASSERBURG, 1973) and probably the most frequently applied one for absolute and stratigraphic age dating as well as for provenance studies (GOLDSTEIN and JACOBSEN, 1988; TÜTKEN et al., 2002). Thermal ionization mass spectrometry (TIMS) or alternatively multi-collector-inductively-coupled-plasma-mass-spectrometry (MC-ICP-MS) are the common methods in order to determine the radiogenic in-growth and variations of $^{87}\text{Sr}/^{86}\text{Sr}$ from the radioactive beta minus decay of ^{87}Rb to ^{87}Sr via a half-live of about 48 billion years. TIMS and MC-ICP-MS based Sr isotope measurements usually provide an external reproducibility of ~10 to ~15 ppm because during the mass-spectrometer runs any fluctuation of the $^{87}\text{Sr}/^{86}\text{Sr}$ -ratio due to mass and temperature dependent isotope fractionation is normalized and corrected relative to the commonly accepted $^{86}\text{Sr}/^{88}\text{Sr}$ -ratio of 0.1194 (NIER, 1938). Following this

procedure only the radiogenic in-growth of the $^{87}\text{Sr}/^{86}\text{Sr}$ can be determined whereas any other variation due to equilibrium or kinetic isotope fractionation is invisible and cannot be used to constrain additional geochemical information.

Recent studies applying the MC-ICP-MS combined with the bracketing standard method (FIETZKE and EISENHAUER, 2006; HALICZ et al., 2008; OHNO and HIRATA, 2007; RÜGGERBERG et al., 2008) showed that the $^{88}\text{Sr}/^{86}\text{Sr}$ -ratio of seawater ($\delta^{88/86}\text{Sr} \sim -0.381\text{‰}$) significantly deviates from the $^{88}\text{Sr}/^{86}\text{Sr}$ -ratio of SRM987 (per definition $\delta^{88/86}\text{Sr} = 0$). In the same study (FIETZKE and EISENHAUER, 2006) it was also found that $\delta^{88/86}\text{Sr}$ values of marine and artificially precipitated calcium carbonates show a temperature controlled isotopic difference of 0.17 to 0.36‰ between the carbonate precipitates and the bulk solution, with the carbonates isotopically lighter than the seawater. Either one or both major sources for Sr to the ocean (hydrothermal sources and continental weathering) must be fractionated relative to the SRM987.

Although bracketing standard is a suitable method to determine simultaneous natural fractionation of $^{87}\text{Sr}/^{86}\text{Sr}$ and $\delta^{88/86}\text{Sr}$, it can be assumed that TIMS in combination with a double-spike (DS-TIMS) may provide even higher precision and accuracy. So far MC-ICP-MS methods were burdened with the problem of potential fractionation during ion chromatographic Sr separation and the sensitivity for matrix effects during the ICP-MS measurements (FIETZKE and EISENHAUER, 2006; HALICZ et al., 2008; OHNO and HIRATA, 2007; RÜGGERBERG et al., 2008; YANG et al., 2008). Both problems can be overcome by the use of an appropriate double spike.

Sr double spikes have already successfully been used in order to determine Sr isotope values for the early solar system (PATCHETT, 1980a; PATCHETT, 1980b). The application of a Sr double spike follows earlier attempts in the Pb-isotope analytic where double spikes have been used in the sixties of the last century (COMPSTON and OVERSPY, 1969) with recent progress in application induced by the pioneering work of Galer (GALER, 1999). In order to use a DS for Sr isotope analysis at least two isotope measurements have to be performed. One unspiked run (ic-run, isotope composition) and one run with the double spike added to the sample solution (id-run, isotope dilution). Data reduction and the simultaneous calculation of $^{87}\text{Sr}/^{86}\text{Sr}^*$ ($^{87}\text{Sr}/^{86}\text{Sr}^* = \text{fractionated } ^{87}\text{Sr}/^{86}\text{Sr} \text{ ratio from our spike correction algorithm}$) and $\delta^{88/86}\text{Sr}$ can be performed following certain numerical procedures previously designed for Pb (COMPSTON and OVERSPY, 1969) and Ca isotope analysis (HEUSER et al., 2002).

Here we present the application of a $^{87}\text{Sr}/^{84}\text{Sr}$ double spike for the simultaneous determination of $^{87}\text{Sr}/^{86}\text{Sr}^*$ and $\delta^{88/86}\text{Sr}$, respectively. The results of earlier studies could be reproduced with higher external precision (FIETZKE and EISENHAUER, 2006; HALICZ et al., 2008).

II.3 Experimental methods and TIMS measurement

II.3.1 $^{87}\text{Sr}/^{84}\text{Sr}$ -double spike preparation

In order to prepare an $^{87}\text{Sr}/^{84}\text{Sr}$ spike solution we purchased two Sr-carbonates enriched in ^{84}Sr and in ^{87}Sr , respectively, from Oak Ridge National Laboratory, USA with a certified isotopic compositions given in tab.II.1. The abundance of interfering ^{87}Rb was reported to be less than 1 ppm in the ^{84}Sr solution and less than 56 ppm in the ^{87}Sr solution. In order to reach the anticipated $^{87}\text{Sr}/^{84}\text{Sr}$ -ratio of ~ 1 we mixed the two solutions in a way that the mixture consists of 48% of the ^{87}Sr -solution and 52% of the ^{84}Sr -solution, respectively.

With the given abundances of Sr isotopes in the two solutions we calculated theoretical values for $^{86}\text{Sr}/^{84}\text{Sr}$ -, $^{87}\text{Sr}/^{84}\text{Sr}$ - and $^{88}\text{Sr}/^{84}\text{Sr}$ -ratios of the desired $^{87}\text{Sr}/^{84}\text{Sr}$ spike solution. These values were used as start values for the calibration of the spike relative to the SRM987 SrCO_3 standard from the National Institute of Standards and Technology (NIST) as described below.

II.3.2 TIMS multicollector measurement procedure

Sr was extracted from all samples by using standard ion chromatographic procedure (tab.II.2). Prior to the TIMS measurements the solutions were evaporated to dryness and redissolved in 2 μL H_3PO_4 . For TIMS measurements rhenium ribbon single filaments are used in combination with a Ta_2O_5 -activator which stabilizes the signal and enhances the ionization rate. About 2 μL of the Ta_2O_5 -activator solution is first added on the filament and heated to near dryness at a current of about 0.5 A. Then 2 μL of the sample solution containing 250 to 500 ng Strontium were added to the activator solution and heated to dryness at a current of 1 A. Finally we increased the current to a value of 1.6 A and kept it there for about one minute until the sample color turned into a light brown. The last step in this procedure was to heat up the filament until a light red glow was visible. The current was kept at this setting for about 20 to 30 seconds. For the measurements of the SRM987 no column chemistry was necessary because of the negligible amounts of interfering ^{87}Rb in the standard material. Nevertheless aliquots of SRM987 standard material were also separated by the above mentioned ion exchange method showing no significant deviation from the untreated material.

Sr isotope measurements were carried out at the IFM-GEOMAR mass spectrometer facilities in Kiel, Germany, using a TRITON mass spectrometer (ThermoFisher, Bremen, Germany) which operates in positive ionization mode with a 10 kV acceleration voltage and $10^{11} \Omega$ resistors for the Faraday cups. The instrument is equipped with nine moveable Faraday cups as detection system which account for the dispersion of the whole Sr isotope mass range from ~ 84 to 88 amu, respectively.

Mass 85 is measured in order to monitor the interfering ^{87}Rb . Prior to each measurement session a gain calibration of all amplifiers was carried out. Measurement started with a heatup-sequence

(pyrometer controlled) heating up the filament by increasing the current to 2.6 A (ramping velocity of 0.5 A/min). The final current usually corresponds to a temperature of ~1380 °C. The ion beam was then automatically focused (including wheel focus) and peak centering was performed. Then the filament was slowly (0.05 A/min) heated up to ~3.2 A corresponding to a temperature of ~1430 to 1490 °C. When the signal intensity reached 6 V on mass 88, data acquisition was started. 14 scans with 17 seconds integration time and 3 seconds idle time each are summarized to one block. For each sample 9 blocks corresponding to 126 scans were measured. Before each block the baseline (deflected beam) was recorded and the amplifier rotation was performed.

Applying the double spike technique at least two separate runs for one measurement are necessary: one ic-run and one id-run where the $^{86}\text{Sr}/^{84}\text{Sr}$ -, $^{87}\text{Sr}/^{84}\text{Sr}$ - and $^{88}\text{Sr}/^{84}\text{Sr}$ -ratios are determined. To correct for isotope fractionation during TIMS measurement the $^{86}\text{Sr}/^{84}\text{Sr}$ -, $^{87}\text{Sr}/^{84}\text{Sr}$ and the $^{88}\text{Sr}/^{84}\text{Sr}$ -ratios are normalized to the mean of the first block of the $^{87}\text{Sr}/^{84}\text{Sr}$ isotope ratio.

II.3.3 Double spike algorithm

The mean of the measured and normalized $^{86}\text{Sr}/^{84}\text{Sr}$ -, $^{87}\text{Sr}/^{84}\text{Sr}$ - and $^{88}\text{Sr}/^{84}\text{Sr}$ -ratio of the two ic-runs are taken as start values for the spike correction algorithm (fig.II.1).

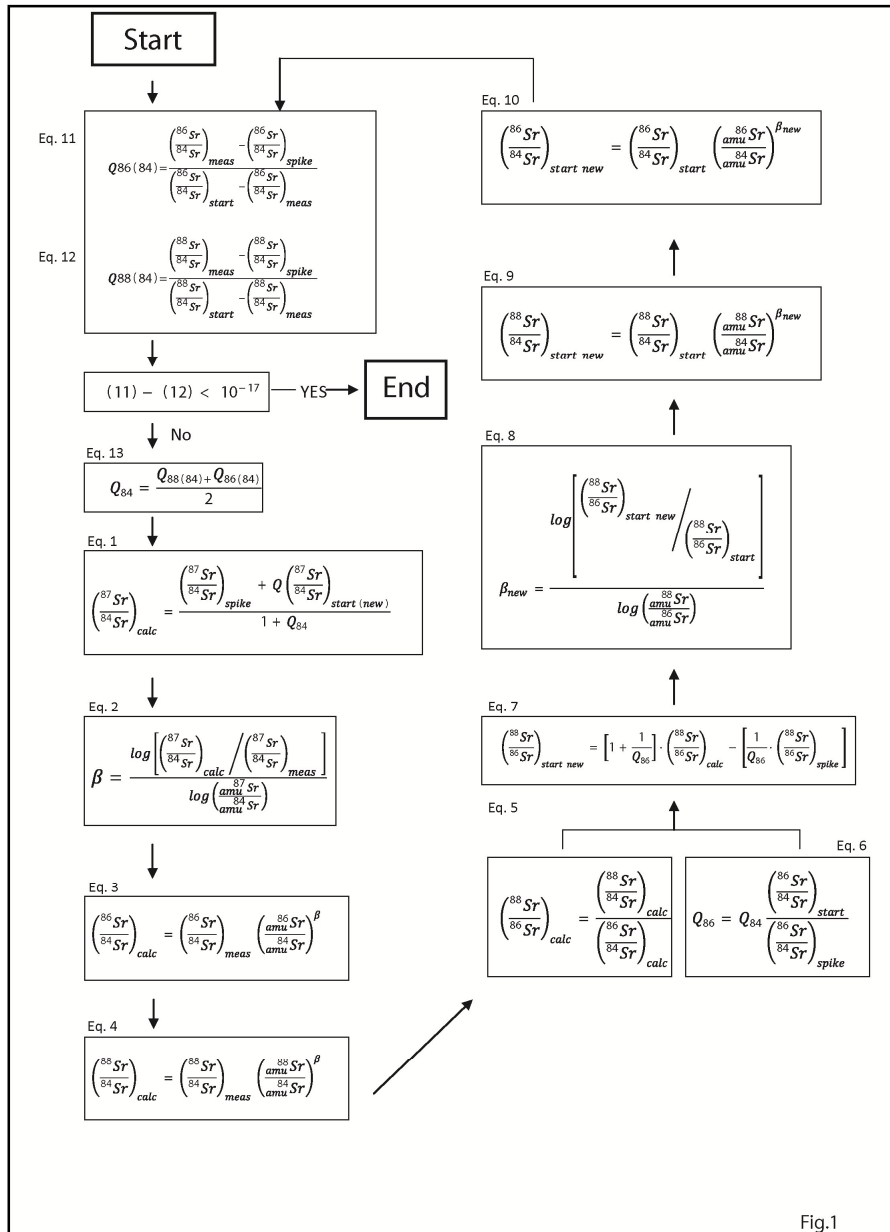


fig.II.1: Flow Chart of the Sr-double spike algorithm applied in order to denormalize measured $^{88}\text{Sr}/^{86}\text{Sr}$ and $^{87}\text{Sr}/^{86}\text{Sr}$ data and to calculate paired $^{87}\text{Sr}/^{86}\text{Sr} \cdot \delta^{88}/^{86}\text{Sr}$ values. Usually about 20 cycles are necessary in order to achieve the desired precision.

The results of the id-runs need to be denormalized and corrected for the added DS. In order to decompose the sample/spike mixture we used an iterative routine closely following the one presented earlier for Ca-isotopes (HEUSER et al., 2002) based on the classical isotope dilution equation and on an similar algorithm presented earlier for Pb isotopes (COMPSTON and OVERSPY, 1969). The

algorithm starts with the calculation of the sample to spike ratio ($Q_{86}(84)=Q_{88}(84)=^{84}\text{Sr}_{\text{sample}}/^{84}\text{Sr}_{\text{spike}}$) from the measured $^{86}\text{Sr}/^{84}\text{Sr}$ ($Q_{86}(84)$) and $^{88}\text{Sr}/^{84}\text{Sr}$ ($Q_{88}(84)$) ratios and their corresponding values of the id- and ic-run (eqs.11 and 12 in fig.II.1). Although the approximation of $^{84}\text{Sr}_{\text{sample}}/^{84}\text{Sr}_{\text{spike}}$ from $Q_{86}(84)$ and $Q_{88}(84)$ are supposed to be identical they differ to a certain extend prior to the denormalization procedure. The $^{87}\text{Sr}/^{84}\text{Sr}_{\text{calc}}$ (eq.1) can be calculated from the $^{87}\text{Sr}/^{84}\text{Sr}$ -ratio of the ic-run and the $^{87}\text{Sr}/^{84}\text{Sr}$ -ratio of the spike as well as from the mean of $Q_{86}(84)$ and $Q_{88}(84)$ in eq.13, respectively. Comparison of $^{87}\text{Sr}/^{84}\text{Sr}_{\text{calc}}$ and $^{87}\text{Sr}/^{84}\text{Sr}_{\text{meas}}$ in eq.2 then allows the calculation of a fractionation factor β which is used to denormalize the $^{86}\text{Sr}/^{84}\text{Sr}$ and $^{88}\text{Sr}/^{84}\text{Sr}$ -ratios in eq.3 and 4, respectively. A first approximate $^{88}\text{Sr}/^{86}\text{Sr}$ -ratio can then be determined by a comparison of $^{88}\text{Sr}/^{84}\text{Sr}_{\text{calc}}$ and $^{86}\text{Sr}/^{84}\text{Sr}_{\text{calc}}$ (eq.5), respectively. From Q_{86} (eq.6) and $^{88}\text{Sr}/^{86}\text{Sr}_{\text{calc}}$ a new $^{88}\text{Sr}/^{86}\text{Sr}$ is determined (eq.7) which is then used for iterative calculation of an improved Sr isotope fractionation factor (β_{new}). This β_{new} allows us to calculate new start values for the algorithm (eq.9 and 10). They again are used to simultaneously calculate $Q_{86}(84)$ and $Q_{88}(84)$. The algorithm usually needs ~ 20 iterative steps in order to meet the stop criteria being the difference of $Q_{86}(84)$ and $Q_{88}(84)$ smaller than $1 \cdot 10^{-17}$. Latter stop criteria guarantees that β_{new} becomes zero.

The $^{88}\text{Sr}/^{86}\text{Sr}$ -ratios are reported in the common δ -notation. The session offset corrected $^{88}\text{Sr}/^{86}\text{Sr}$ -ratios are normalized to the accepted value $^{88}\text{Sr}/^{86}\text{Sr}=8.375209$ and reported in the usual δ -notation (eq.II.1) as defined earlier (FIETZKE and EISENHAUER, 2006).

$$\text{eq.II.1} \quad \delta^{88/86}\text{Sr} = \left(\frac{\left(\frac{^{88}\text{Sr}}{^{86}\text{Sr}} \right)_{\text{sample}}}{\left(\frac{^{88}\text{Sr}}{^{86}\text{Sr}} \right)_{\text{SRM987}}} - 1 \right) \cdot 1000$$

II.4 Results

II.4.1 Spike calibration

In order to perform double spike calibration measurements we used two different Sr standards: (1) NIST SRM987 and (2) the international seawater standard IAPSO. The first one was needed to calibrate the double spike and worked as a general reference standard for all of our measurements. The second standard has a known offset to the SRM987 in its $\delta^{88/86}\text{Sr}$ -value of $\sim 0.381(10)\%$ and serves as an independent control point (FIETZKE and EISENHAUER, 2006). For calibration and spike optimization the SRM987 standard solutions were spiked with different amounts in order to produce solutions with $^{84}\text{Sr}_{\text{spike}}/^{84}\text{Sr}_{\text{sample}}$ ratios in a range from 5 to 30.

The calculated spike isotope ratios using the certified isotope compositions of the enriched solutions (tab.II.1) produced results showing that the $\delta^{88/86}\text{Sr}$ values vary with the $^{84}\text{Sr}_{\text{spike}}/^{84}\text{Sr}_{\text{sample}}$ -ratio (fig.II.2).

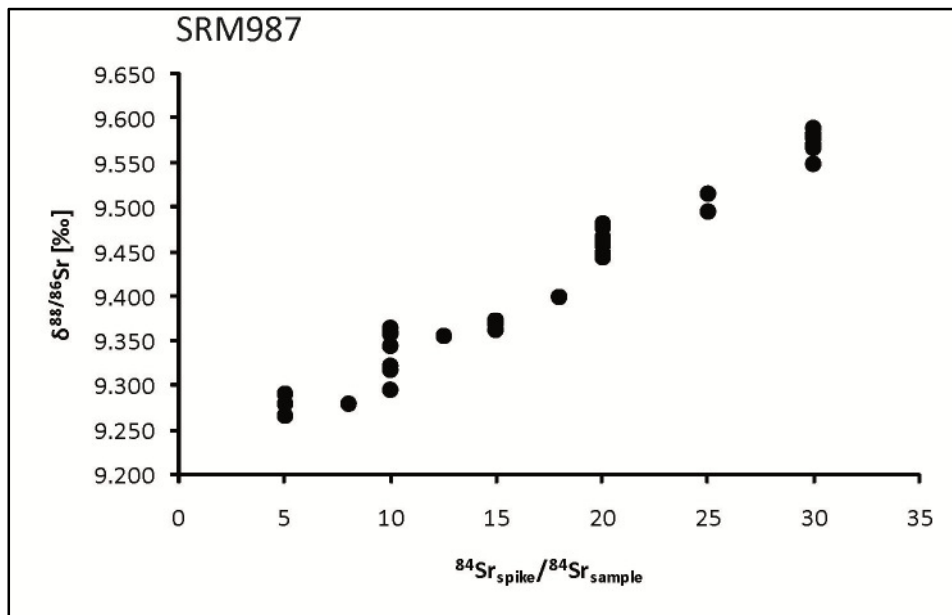


fig.II.2: The SRM987 standard solutions were spiked with different amounts of spike in order to produce solutions with $^{84}\text{Sr}_{\text{sample}}/^{84}\text{Sr}_{\text{spike}}$ ratios in a range from 5 to 30. We observed that the measured $\delta^{88/86}\text{Sr}$ values are positively correlated with the $^{84}\text{Sr}_{\text{spike}}/^{84}\text{Sr}_{\text{sample}}$ -ratio when using the spike isotope ratios for $^{86}\text{Sr}/^{84}\text{Sr}$, $^{87}\text{Sr}/^{84}\text{Sr}$ and $^{88}\text{Sr}/^{84}\text{Sr}$ as calculated from the reported certified values.

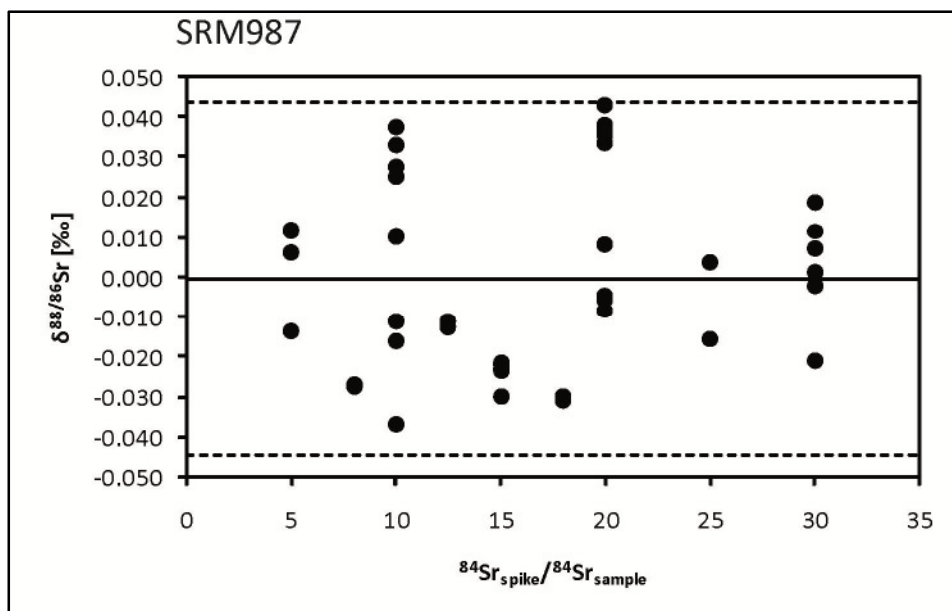


fig.II.3: After optimization of the spike ratios there is no further dependency of the $\delta^{88/86}\text{Sr}$ from the $^{84}\text{Sr}_{\text{spike}}/^{84}\text{Sr}_{\text{sample}}$ -ratio. The black line marks the average value of ~ 0 and the broken line the $\pm 2\text{SD}$ standard deviation from the defined value.

This is a consequence of the deviation of the calculated spike values from the real composition. In order to extract the real composition and for an optimization procedure we generated the least

square sum of all measured $\delta^{88/86}\text{Sr}$ values of SRM987 and minimized it by slightly varying the spike isotope ratios using a least square fit which was performed with the solver function of Microsoft Excel®. After this optimization procedure no further dependency of the $\delta^{88/86}\text{Sr}$ on the $^{84}\text{Sr}_{\text{spike}}/^{84}\text{Sr}_{\text{sample}}$ ratio could be found (fig.II.3). Latter values are then assumed to be the best approximation of the “true” Sr double spike composition as presented in tab.II.3. During the course of the double spike calibration ~40 measurements of SRM987 standard with varying $^{84}\text{Sr}_{\text{spike}}/^{84}\text{Sr}_{\text{sample}}$ ratios have been performed. The typical internal precision of the single measurements was ± 7 ppm (RSD) for the $^{86}\text{Sr}/^{84}\text{Sr}$ -ratio and 9 ppm for the $^{88}\text{Sr}/^{84}\text{Sr}$ -ratio in the ic-runs. We measured ± 11 ppm (RSD) for the $^{86}\text{Sr}/^{84}\text{Sr}$ -ratio and 21 ppm for the $^{88}\text{Sr}/^{84}\text{Sr}$ -ratio in the id-run. The internal precision correlates with the $^{84}\text{Sr}_{\text{spike}}/^{84}\text{Sr}_{\text{sample}}$ -ratio.

II.4.2 Results of standard measurements

Our measurements show that there are significant session-to-session variations in the isotopic ratios of the standard SRM987 measurements (fig.II.4). This behavior is

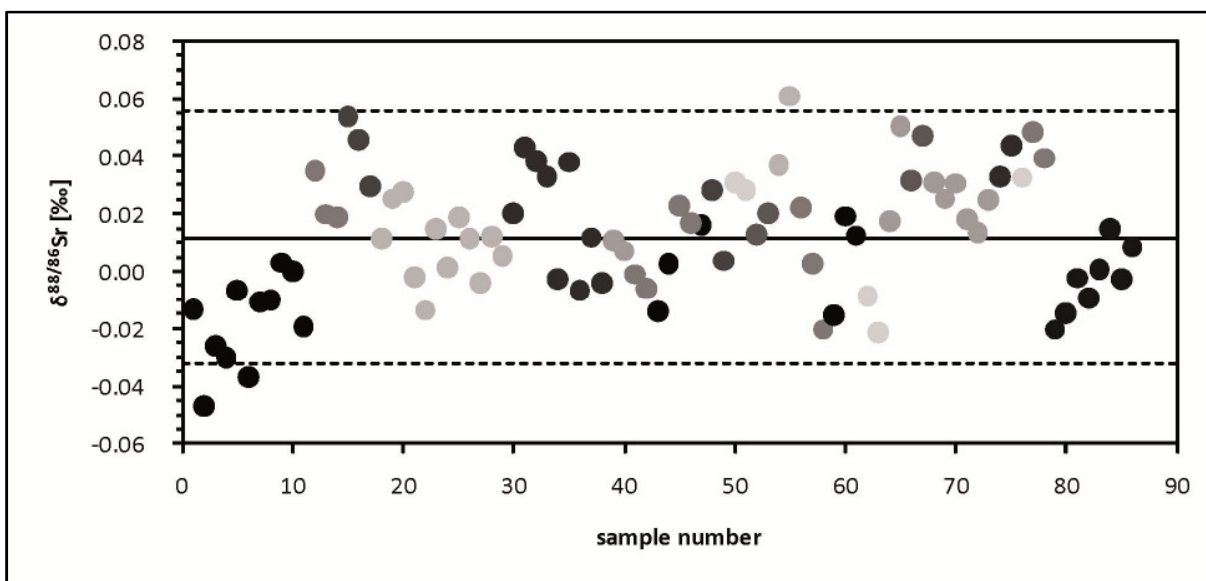


fig.II.4: Long term session-to-session variations for the SRM987 standard result in a $\delta^{88/86}\text{Sr}_{\text{mean}}$ of $\sim 0.012 \pm 0.044$ (2SD). Different color marks different measurement sessions of SRM987. Black line marks the average value and the broken lines mark the 2sd-standard deviation.

also known for other isotope measurements using TIMS. The reasons for this phenomena are not entirely known. Potential sources could be e.g. the Faraday Cup degradation or differing source vacuum conditions due to the use of two distinct cryo traps. In order to account for this observation we calculated the mean of the fractionation corrected isotope $\delta^{88/86}\text{Sr}$ - and $^{87}\text{Sr}/^{86}\text{Sr}^*$ -ratios of SRM987 and determined its offset to the accepted value for $^{88}\text{Sr}/^{86}\text{Sr}=8.375209$ ($\delta^{88/86}\text{Sr}=0$) and $^{87}\text{Sr}/^{86}\text{Sr}=0.710240$, respectively (NIER, 1938). This offset was then used to correct the corresponding values of every single sample and resulted in the session corrected $\delta^{88/86}\text{Sr}$ - and $^{87}\text{Sr}/^{86}\text{Sr}^*$ -values.

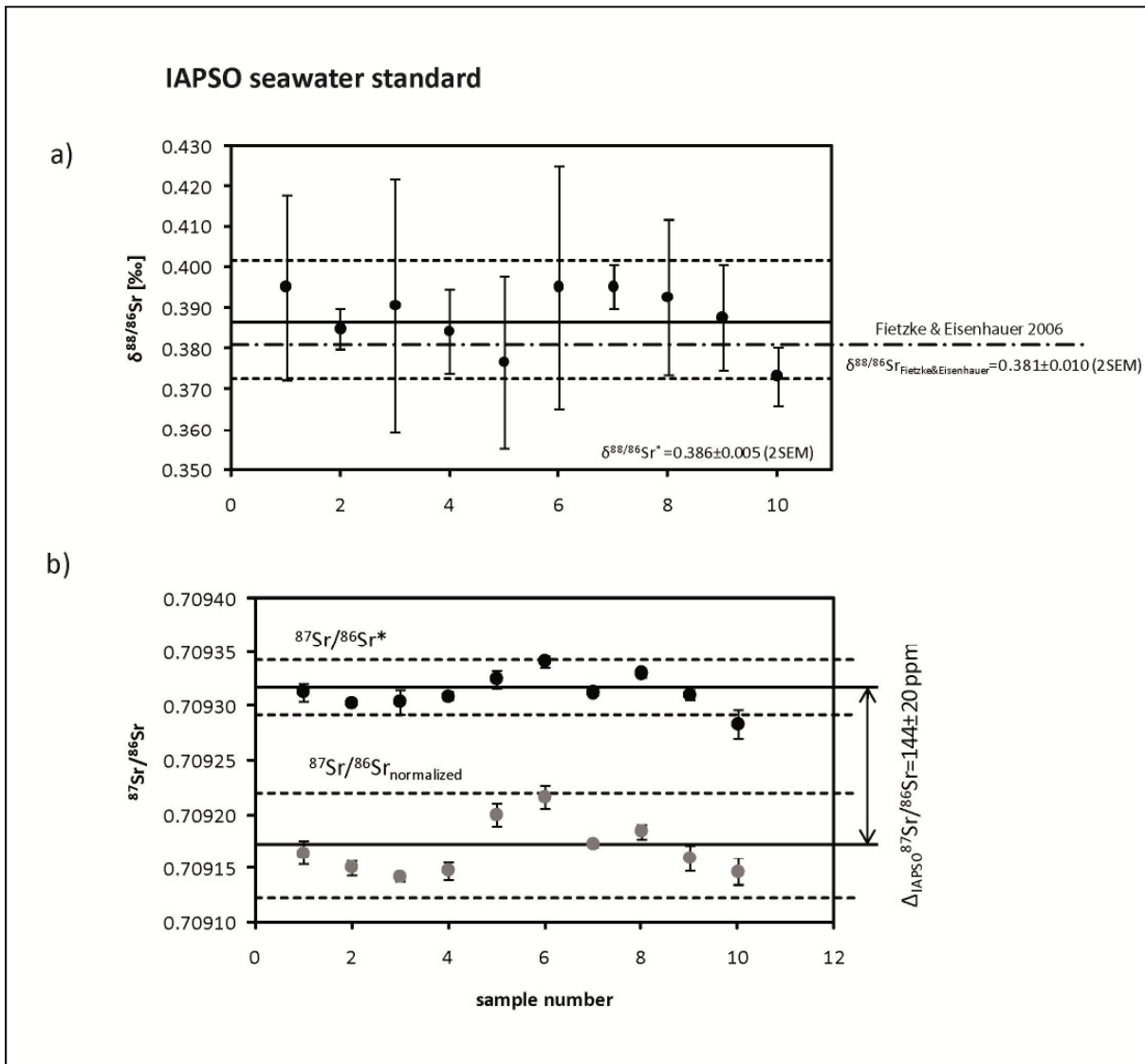


fig.II.5a: Longterm measurements of the IAPSO seawater standard. Every data point represents the mean of up to 5 single measurements of the same solution. The determined value of $\delta^{88/86}\text{Sr}_{\text{mean}} = 0.386 \pm 0.005$ (2SEM) of the measurements (black line) is in agreement with previous data. The error bars are $\pm 2\text{SD}$ (broken lines). fig.II.5b: $^{87}\text{Sr}/^{86}\text{Sr}^*$ (black points) and $^{87}\text{Sr}/^{86}\text{Sr}_{\text{norm}}$ -values (grey points) of the IAPSO seawater standard are significantly different ($^{87}\text{Sr}/^{86}\text{Sr}^* = 0.709312(9)$; $^{87}\text{Sr}/^{86}\text{Sr}_{\text{norm}} = 0.709173(18)$) corresponding to a value of $\sim 144 \pm 20$ ppm.

During the course of this project the $\delta^{88/86}\text{Sr}$ - and $^{87}\text{Sr}/^{86}\text{Sr}^*$ -values of the IAPSO seawater standard (fig.II.5a/b) were found to be 0.386(5)‰ and 0.709312(9) (2SEM, n=10), respectively. The $\delta^{88/86}\text{Sr}$ value for the IAPSO is in general accord with the value determined earlier (FIETZKE and EISENHAUER, 2006). The $^{87}\text{Sr}/^{86}\text{Sr}^*$ value is significantly different from the accepted $^{87}\text{Sr}/^{86}\text{Sr}_{\text{norm}}$ seawater ratio of 0.709168(7). Latter difference of 144 ppm (fig.II.5a/b) is due to the conventional normalization procedure where the measured $^{87}\text{Sr}/^{86}\text{Sr}$ ratio is normalized to a constant $^{88}\text{Sr}/^{86}\text{Sr}$ -ratio of 8.375209 ($\delta^{88/86}\text{Sr} = 0$) neglecting any kind of natural Sr isotope fractionation.

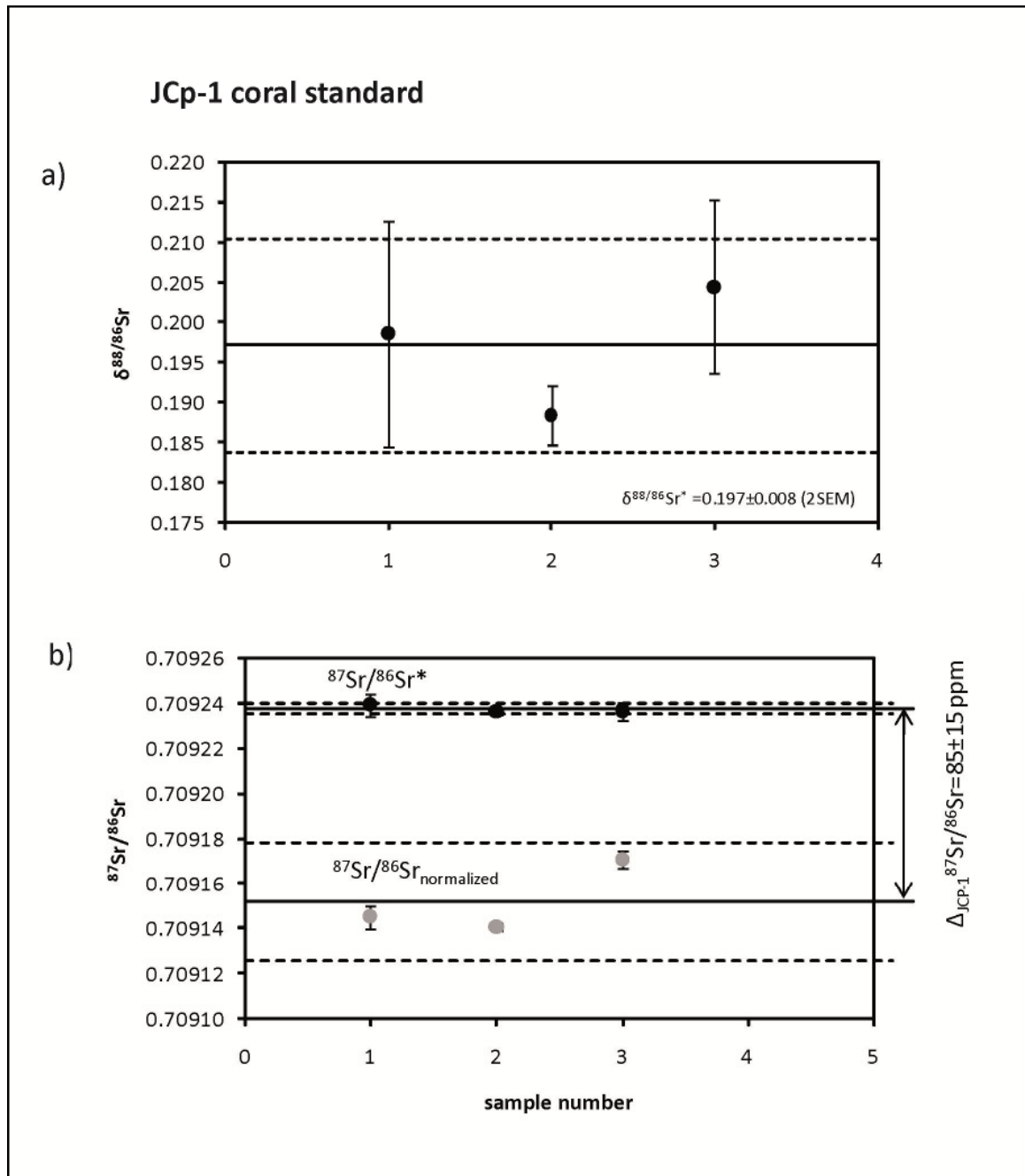


fig.II.6: The $\delta^{88/86}\text{Sr}_{\text{JcP-1-mean}} = 0.197(8)$ (2SEM, black line) of the coral standard JcP-1 measurements. Every data point represents the mean of up to 3 single measurements of the same solution. Note, that the $\delta^{88/86}\text{Sr}_{\text{JcP-1-mean}}$ is isotopically about a factor of 2 lighter than $\delta^{88/86}\text{Sr}_{\text{Seawater}}$. This is due to mass dependent Sr isotope fractionation during CaCO_3 precipitation. The error bars are 2SD (broken lines). fig.II.6b: $^{87}\text{Sr}/^{86}\text{Sr}^*$ - (black points; 0.709237(2)) and $^{87}\text{Sr}/^{86}\text{Sr}_{\text{norm}}$ - values (grey; 0.709164(15)) of coral standard JcP-1 are significantly different. Note that the $^{87}\text{Sr}/^{86}\text{Sr}^*$ of JcP-1 is isotopically lighter than $^{87}\text{Sr}/^{86}\text{Sr}^*$ of seawater by ~ 80 ppm.

Renormalization of our measured $^{87}\text{Sr}/^{86}\text{Sr}^*$ value of 0.709312(9) to a $\delta^{88/86}\text{Sr}$ value of zero results in an average value of $^{87}\text{Sr}/^{86}\text{Sr}_{\text{norm}}$ 0.709166(9) which is in accord with the generally accepted radiogenic $^{87}\text{Sr}/^{86}\text{Sr}$ -ratio for seawater (FANTLE and DEPAOLO, 2006). This is not a contradiction to the above stated value of $^{87}\text{Sr}/^{86}\text{Sr} = 0.709168(7)$ of seawater but a consequence of two different ways of calculating the $^{87}\text{Sr}/^{86}\text{Sr}_{\text{norm}}$ and $^{87}\text{Sr}/^{86}\text{Sr}^*$, respectively. The first value is purely the result of the conventional Sr measurement (ic-run) while the latter uses both measurements (ic-/ id-run) for the

calculation. The values for the modern coral standard JCp-1 are plotted in the same way as for the IAPSO above (fig. II.6a/b).

The measurements show a value of 0.197(8)‰ (2SEM) for $\delta^{88/86}\text{Sr}$ and of 0.709237(2) for the $^{87}\text{Sr}/^{86}\text{Sr}^*$ ratio. There is a significant difference of the $\delta^{88/86}\text{Sr}$ values for JCp-1 and IAPSO in the order of 189 ± 9 ppm. Similar to this observation there is also a significant 75 ± 15 ppm difference between our measured $^{87}\text{Sr}/^{86}\text{Sr}^*$ ratio for JCp-1 and seawater (0.709312(9)). The ~ 80 ppm difference of the JCp-1 carbonate standard to the IAPSO seawater standard in the $^{87}\text{Sr}/^{86}\text{Sr}^*$ and the ~ 2 times larger difference in the $\delta^{88/86}\text{Sr}$ -value indicate mass- and probably temperature dependent Sr isotope fractionation during the precipitation of CaCO_3 from seawater.

This results are in accord with earlier studies (FIETZKE and EISENHAUER, 2006; HALICZ et al., 2008; RÜGGERBERG et al., 2008). Comparison of our data with previous studies show that the here presented DS-TIMS method produces accurate results. The major advantage of our method is the 2 - 3 times better external precision. Additionally the use of a double spike solves the problems inherent in published MC-ICP-MS methods like fractionation during chemical sample pretreatment and matrix related mass bias fluctuations. The analytical blank was determined to 0.3 ng of Sr which was considered to be neglectable.

II.5 Conclusions

With our DS-TIMS method we are able to determine the stable $\delta^{88/86}\text{Sr}$ and the radiogenic $^{87}\text{Sr}/^{86}\text{Sr}^*$ simultaneously. The use of a double spike overcomes the problem of any uncontrolled fractionation during sample pretreatment in particular ion chromatographic separation of Strontium from the sample matrix. The external precision could be improved by a factor of 2 - 3 compared to established MC-ICP-MS methods. Finally this DS-TIMS method is not burdened by mass bias fluctuations known from MC-ICP-MS bracketing standard approaches.

II.6 Tables

	^{84}Sr (%)	^{86}Sr (%)	^{87}Sr (%)	^{88}Sr (%)	Solution
1.	~0.01	0.82(2)	91.26(10)	7.91(10)	^{87}Sr -Solution
2.	99.64(1)	0.14(1)	0.03(1)	0.19(1)	^{84}Sr -Solution

tab.II.1: Original isotope composition of the two Oak Ridge National Laboratory Sr carbonate standards.

step	description
1	Addition of 2 ml 4.5 N HNO_3 to the weighed and grinded sample
2	Splitting the samples into two fractions
3	Addition of the spike solution to one fraction
4	Drying the samples at $\sim 90^\circ\text{C}$
5	Column separation of the spiked and unspiked sample. BIO-RAD 650 μl columns with Eichrom Sr-SPS resin (mesh size 50-100 μm). To perform this separation we filled the columns to one third with the resin followed by a washing procedure
6	Drying the separated samples at $\sim 90^\circ\text{C}$
7	Addition of 200 μl 4.5 N HNO_3 and 50 μl 30 % H_2O_2 and heating the solution in a closed beaker at least 5 hours at $\sim 80^\circ\text{C}$
8	Drying the sample at $\sim 80^\circ\text{C}$
9	Loading the sample with 2 μL H_3PO_4 solution onto Re filaments
10	Measuring the samples

tab.II.2: Sample treatment prior mass spectrometric analysis

$^{86}\text{Sr}/^{84}\text{Sr}$	$^{87}\text{Sr}/^{84}\text{Sr}$	$^{88}\text{Sr}/^{84}\text{Sr}$
0.009898	0.925937	0.083292

tab.II.3: Strontium isotopic composition of the double spike

II.7 Acknowledgements

We wish to thank Ana Kolevica for supporting the lab work of this study. We also thank the two anonymous referees for providing a constructive and kind report. Finally, Torben Stichel is kindly acknowledged for providing the image of “his personal double spike” which was used for the graphical entrance of the article.

II.8 References

- Nier, A. O., 1938. The isotopic constitution of strontium, barium, bismuth, thallium and mercury. *Physical Review* **5**, 275-279.
- Nier, A. O., 1940. A mass spectrometer routine for isotope abundance measurements. *Rev. Sci. Instr.* **18**, 398-411.
- Goldstein, S. J. and Jacobsen, S. B., 1987. The Nd and Sr isotopic systematics of river-water dissolved material: Implications for the sources of Nd and Sr in seawater. *Chemical Geology: Isotope Geoscience section* **66**, 245-272.
- Tütken, T., Eisenhauer, A., Wiegand, B., and Hansen, B. T., 2002. Glacial-interglacial cycles in Sr and Nd isotopic composition of Arctic marine sediments: changes in sediment provenance triggered by the Barents Sea ice sheet. *Marine Geology* **182**, 351-372.
- Fietzke, J. and Eisenhauer, A., 2006. Determination of temperature-dependent stable strontium isotope ($^{88}\text{Sr}/^{86}\text{Sr}$) fractionation via bracketing standard MC-ICP-MS. *Geochemistry Geophysics Geosystems* **7**, Q08009, doi:10.1029/2006GC001243.
- Halicz, L., Segal, I., Fruchter, N., Stein, M., and Lazar, B., 2008. Strontium stable isotopes fractionate in the soil environments? *Earth and Planetary Science Letters* **272**, 406-411.
- Rüggeberg, A., Fietzke, J., Liebetrau, V., Eisenhauer, A., Dullo, W. C., and Freiwald, A., 2008. Stable strontium isotopes ($\delta^{88/86}\text{Sr}$) in cold-water corals - A new proxy for reconstruction of intermediate ocean water temperatures. *Earth and Planetary Science Letters* **269**, 569-574.
- Ohno, T. and Hirata, T., 2007. Simultaneous determination of mass-dependent isotopic fractionation and radiogenic isotope variation of strontium in geochemical samples by multiple collector-ICP-mass spectrometry. *Anal. Sci.* **23**, 1275-1280.
- Yang, L., Peter, C., Panne, U., and Sturgeon, R. E., 2008. Use of Zr for mass bias correction in strontium isotope ratio determinations using MC-ICP-MS. *Journal of Analytical Atomic Spectrometry* **23**, 1269-1274.
- Patchett, P. J., 1980a. Sr isotopic fractionation in Allende chondrules: A reflection of solar nebular processes. *Earth and Planetary Science Letters* **50**, 181-188.
- Patchett, P. J., 1980b. Sr isotopic fractionation in Ca-Al inclusions from the Allende meteorite. *Nature* **283**, 438-441.
- Compston, W. and Overspy, V. M., 1969. Lead isotopic analysis using a double spike. *Journal of Geophysical Research* **74**, 4338-4348.
- Galer, J. G. S., 1999. Optimal double and triple spiking for high precision lead isotopic measurement. *Chemical Geology* **157**, 255-274.
- Heuser, A., Eisenhauer, A., Gussone, N., Bock, B., Hansen, B. T., and Nagler, T. F., 2002. Measurement of calcium isotopes ($\delta^{44/40}\text{Ca}$) using a multicollector TIMS technique. *International Journal of Mass Spectrometry* **220**, 385-397.
- Fantle, M. S. and DePaolo, D. J., 2006. Sr isotopes and pore fluid chemistry in carbonate sediment of the Ontong Java Plateau: Calcite recrystallization rates and evidence for a rapid rise in seawater Mg over the last 10 million years. *Geochimica et Cosmochimica Acta* **70**, 3883-3904.

Chapter III

MANUSCRIPT II

III. Constraining the Marine Strontium Budget with Natural Strontium Isotope Fractionations ($^{87}\text{Sr}/^{86}\text{Sr}^*$, $\delta^{88/86}\text{Sr}$) of Carbonates, Hydrothermal Solutions and River Waters

A. Krabbenhöft*, A. Eisenhauer*, F. Böhm*, H. Vollstaedt*, J. Fietzke*, V. Liebetrau*, N. Augustin*, B. Peucker-Ehrenbrink[#], M. N. Müller^{*1}, C. Horn*, B. T. Hansen^o, N. Nolte^o and K. Wallmann*

*Leibniz-Institut für Meereswissenschaften, IFM-GEOMAR, Wischhofstr. 1-3, 24148 Kiel, Germany

^oGeowissenschaftliches Zentrum der Universität Göttingen (GZG), Abteilung für Isotopengeologie, Goldschmidtstr. 1, 37077 Göttingen, Germany

[#]Woods Hole Oceanographic Institution, Department of Marine Chemistry and Geochemistry, Woods Hole, MA 02543, USA
Corresponding Author: A. Eisenhauer (aeisenhauer@ifm-geomar.de)

Published in *Geochimica et Cosmochimica Acta* 74 (2010), 4097-4109

III.1 Abstract

We present strontium (Sr) isotope ratios that, unlike traditional $^{87}\text{Sr}/^{86}\text{Sr}$ data, are not normalized to a fixed $^{88}\text{Sr}/^{86}\text{Sr}$ ratio of 8.375209 (defined as $\delta^{88/86}\text{Sr}=0$ relative to NIST SRM 987). Instead, we correct for isotope fractionation during mass spectrometry with a ^{87}Sr - ^{84}Sr double spike. This technique yields two independent ratios for $^{87}\text{Sr}/^{86}\text{Sr}$ and $^{88}\text{Sr}/^{86}\text{Sr}$ that are reported as ($^{87}\text{Sr}/^{86}\text{Sr}^*$) and ($\delta^{88/86}\text{Sr}$), respectively. The difference between the traditional radiogenic ($^{87}\text{Sr}/^{86}\text{Sr}$ normalized to $^{88}\text{Sr}/^{86}\text{Sr}=8.375209$) and the new $^{87}\text{Sr}/^{86}\text{Sr}^*$ values reflect natural mass-dependent isotope fractionation. In order to constrain glacial/interglacial changes in the marine Sr budget we compare the isotope composition of modern seawater ($(^{87}\text{Sr}/^{86}\text{Sr}^*, \delta^{88/86}\text{Sr})_{\text{seawater}}$) and modern marine biogenic carbonates ($(^{87}\text{Sr}/^{86}\text{Sr}^*, \delta^{88/86}\text{Sr})_{\text{Carbonates}}$) with the corresponding values of river waters ($(^{87}\text{Sr}/^{86}\text{Sr}^*, \delta^{88/86}\text{Sr})_{\text{River}}$) and hydrothermal solutions ($(^{87}\text{Sr}/^{86}\text{Sr}^*, \delta^{88/86}\text{Sr})_{\text{HydEnd}}$) in a triple isotope plot. The measured ($^{87}\text{Sr}/^{86}\text{Sr}^*, \delta^{88/86}\text{Sr}$)_{River} values of selected rivers that together account for ~18% of the global Sr discharge yield a Sr flux-weighted mean of (0.7114(8), 0.315(8)‰). The average ($^{87}\text{Sr}/^{86}\text{Sr}^*, \delta^{88/86}\text{Sr}$)_{HydEnd} values for hydrothermal solutions from the Atlantic Ocean are (0.7045(5), 0.27(3)‰). In contrast, the ($^{87}\text{Sr}/^{86}\text{Sr}^*, \delta^{88/86}\text{Sr}$)_{Carbonates} values representing the marine Sr output are (0.70926(2), 0.21(2)‰). We estimate the modern Sr isotope composition of the sources at (0.7106(8), 0.310(8)‰). The difference between the estimated ($^{87}\text{Sr}/^{86}\text{Sr}^*, \delta^{88/86}\text{Sr}$)_{input} and ($^{87}\text{Sr}/^{86}\text{Sr}^*, \delta^{88/86}\text{Sr}$)_{output} values reflects isotope disequilibrium with respect to Sr inputs and outputs. In contrast to the modern ocean, isotope equilibrium between inputs and outputs during the last glacial maximum (10-30 kyr before present) can be explained by invoking three times higher Sr inputs from

¹Present address: Laboratoire d'Océanographie de Villefranche-sur-Mer, UMR 7093, Station Zoologique, BP 28, 06234 Villefranche-sur-mer, France.

a uniquely “glacial” source: weathering of shelf carbonates exposed at low sea levels. Our data are also consistent with the “weathering peak” hypothesis that invokes enhanced Sr inputs resulting from weathering of post-glacial exposure of abundant fine-grained material.

III.2 Introduction

The residence time of Sr in seawater of ~ 2.4 Myr is long compared to the mixing time of the oceans of ~ 1.5 kyr. The radiogenic Sr isotope composition ($^{87}\text{Sr}/^{86}\text{Sr}$: ~ 0.709175 ; (VEIZER, 1989) is therefore homogeneous in seawater and in modern marine carbonates (FAURE and FELDER, 1981; MCARTHUR, 1994; MCARTHUR et al., 2001). The modern $^{87}\text{Sr}/^{86}\text{Sr}$ value of seawater is determined by mixing of two isotopically distinct sources: 1) Sr from the weathering of old, rubidium (Rb)-rich continental silicate rocks that have been enriched in ^{87}Sr by the decay of ^{87}Rb ; 2) Sr with low $^{87}\text{Sr}/^{86}\text{Sr}$ values derived from the Earth’s mantle that enters the ocean at mid-ocean ridges and ridge flanks, and from weathering of mantle-derived rocks exposed on the continents (GODDERIS and VEIZER, 2000; PALMER and EDMOND, 1992).

A minor Sr influx from diagenetic alteration and dissolution of sediments on the seafloor has a $^{87}\text{Sr}/^{86}\text{Sr}$ value only slightly lower than modern seawater (ELDERFIELD and GIESKES, 1982). While average riverine $^{87}\text{Sr}/^{86}\text{Sr}$ values are distinctly different from seawater, the large difference in Sr concentration ($[\text{Sr}]_{\text{Rivers}} \sim 1.0 \mu\text{M}$, $[\text{Sr}]_{\text{Seawater}} \sim 90 \mu\text{M}$) ensures that even in marginal seas with high riverine input seawater $^{87}\text{Sr}/^{86}\text{Sr}$ values are close to the global seawater value ($^{87}\text{Sr}/^{86}\text{Sr} = 0.709175$). Exceptions are brackish seas such as the Baltic Sea with salinities below 15 psu (ANDERSSON et al., 1992). The average Sr concentration of river waters that are dominated by silicate weathering input is $\sim 0.2 \mu\text{M}$. The average $^{87}\text{Sr}/^{86}\text{Sr}$ value of young volcanic provinces is ~ 0.705 , but is ~ 0.735 for old crustal terrains (PALMER and EDMOND, 1992). Rivers draining carbonate rocks, in contrast, have much higher Sr concentrations of $\sim 4 \mu\text{M}$ with typical $^{87}\text{Sr}/^{86}\text{Sr}$ values ranging from 0.707 to 0.709 (GAILLARDET et al., 1999). On average, global river water is characterized by Sr concentration of $\sim 1 \mu\text{M}$ and a $^{87}\text{Sr}/^{86}\text{Sr}$ value of ~ 0.7111 (PEUCKER-EHRENBRINK et al., 2010). About one third of this riverine Sr is derived from silicate weathering and about two thirds from weathering of carbonate rocks exposed on the continents (GAILLARDET et al., 1999; PALMER and EDMOND, 1989).

Although the principles of marine Sr geochemistry are well understood, there is an ongoing discussion about the effects of glacial/interglacial changes in continental weathering on the marine Sr budget. Recent findings indicate that $\sim 70\%$ of the silicate weathering flux is affected by non-steady-state processes, possibly creating a ~ 100 kyr periodicity and an imbalance between input and output fluxes during the Quaternary (VANCE et al., 2009). However, the Sr imbalance created by the non-steady state conditions cannot be quantified by radiogenic Sr ratios alone. Marine Sr budgets that are solely based on radiogenic Sr focus on the input fluxes, because marine calcium carbonate

(CaCO₃) and seawater have identical radiogenic Sr isotope values. This approach is a direct consequence of the normalization of measured $^{87}\text{Sr}/^{86}\text{Sr}$ values to a fixed $^{88}\text{Sr}/^{86}\text{Sr}$ ratio of 8.375209 (NIER, 1938) to correct for mass dependent isotope fractionation in nature and during mass-spectrometry, thereby losing the ability to extract information about natural isotope fractionation. In order to overcome this obstacle and investigate combined radiogenic and stable Sr isotope compositions, we determine natural Sr isotope fractionation with a TIMS double spike method (KRABBENHÖFT et al., 2009). First results showed that the $(^{87}\text{Sr}/^{86}\text{Sr}^*, \delta^{88/86}\text{Sr})_{\text{seawater}}$ is homogeneous (LIEBETRAU et al., 2009). We also demonstrated that the stable Sr isotope composition of marine carbonates and corals ($\delta^{88/86}\text{Sr}_{\text{Carbonates}}$) is $\sim 0.2\%$ lighter than seawater. This is caused by the preferential uptake of lighter isotopes during carbonate precipitation (FIETZKE and EISENHAUER, 2006; HALICZ et al., 2008; OHNO et al., 2008). The still limited data base of stable Sr isotope ratios indicates that marine basalts have $\delta^{88/86}\text{Sr}$ values of $\sim 0.25\%$ (HALICZ et al., 2008; OHNO et al., 2008), significantly different from continental igneous rocks and soils that show lighter values in the range of ~ -0.2 to 0.2% .

When natural Sr isotope fractionation is taken into account the Sr isotope composition of marine carbonates and seawater differ. This allows for the simultaneous calculation of input and output fluxes using complete Sr budget equations. This new approach extends the well-established radiogenic Sr isotope systematic to an additional dimension and allows for simultaneous determination of paired $(^{87}\text{Sr}/^{86}\text{Sr}^*, \delta^{88/86}\text{Sr})$ ratios. Here, we present the first results of paired $(^{87}\text{Sr}/^{86}\text{Sr}^*, \delta^{88/86}\text{Sr})$ values for rivers, hydrothermal fluids, marine carbonates and seawater to constrain the contemporary marine Sr budget.

III.3 Materials and methods

III.3.1 River waters

In order to reevaluate the Sr isotope supply via river discharge to the ocean and to constrain the riverine Sr budget for paired ($^{87}\text{Sr}/^{86}\text{Sr}^*$, $\delta^{88/86}\text{Sr}$) ratios, we analyzed a suite of rivers representing ~18% of the global annual riverine Sr flux to the ocean. The Sr isotope values are presented together with complementary information about water discharges, sampling locations and the riverine Sr fluxes (tab.III.1 and fig.III.1).

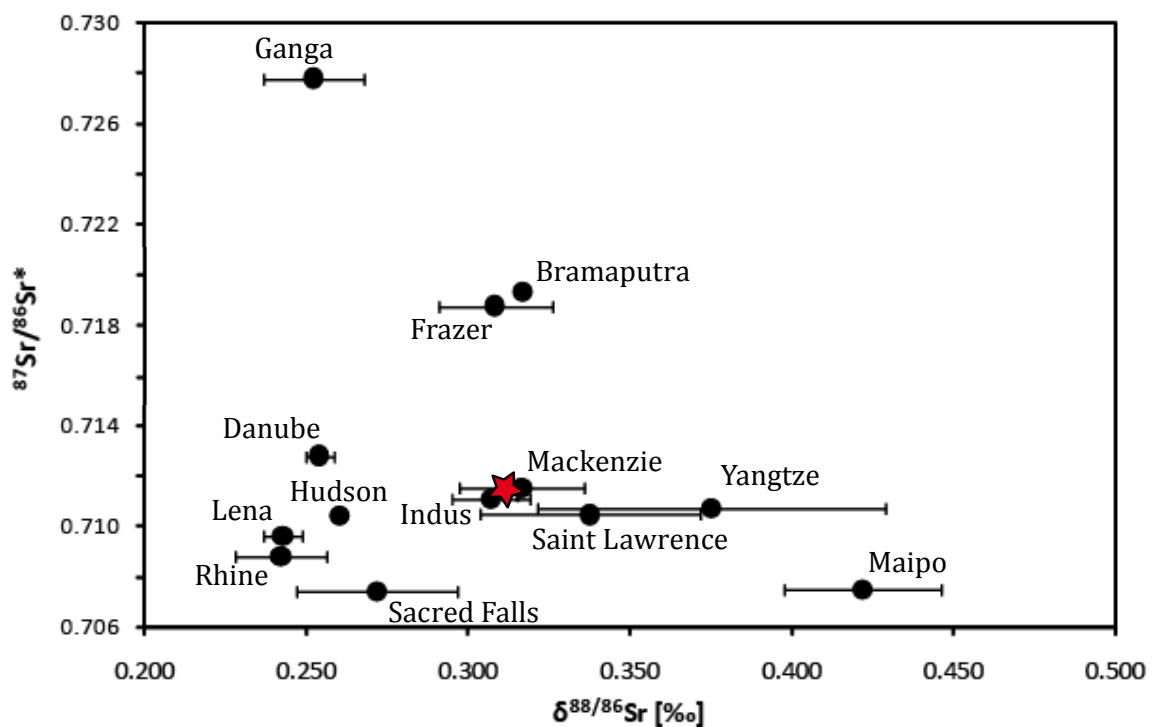


fig.III. 1: Individual ($^{87}\text{Sr}/^{86}\text{Sr}^*$, $\delta^{88/86}\text{Sr}$)_{River}-values corresponding to ~18 % of the global Sr discharge to the ocean are plotted in a triple isotope plot. There is a considerable scatter in both the $^{87}\text{Sr}/^{86}\text{Sr}^*$ and the $\delta^{88/86}\text{Sr}$ values. The Sr flux-weighted global mean of all rivers is marked by the red star.

The analyzed rivers drain various proportions of 9 of the 16 large-scale exorheic drainage regions on Earth (GRAHAM et al., 1999; PEUCKER-EHRENBRINK and MILLER, 2004). We assume that river water samples investigated here are reasonably representative of the 9 large-scale draining regions, because both the average bedrock age (399 Ma) and the relative abundances of sedimentary (70%), volcanic (9%) and intrusive/metamorphic (21%) bedrock are similar to global exorheic bedrock weighted according to water discharge (405 Ma, 73%, 9%, 18%, respectively). The set of rivers investigated here thus does not appear to be significantly biased with respect to the lithological setting and bedrock ages (PEUCKER-EHRENBRINK and MILLER, 2004).

III.3.2 Hydrothermal solutions

Seven hydrothermal vent-fluid samples from the active area at 4°48'S on the Mid-Atlantic Ridge (MAR) have been analyzed for this study (tab.III.2). The 4°48'S hydrothermal system is located on-axis at a water depth of ~3000 m. It is dominated by fresh to slightly altered lava flows and pillows (HAASE et al., 2007). On this plateau at least three high-temperature vent fields (Turtle Pits [TP], Comfortless Cove [CC] and Red Lion [RL]) are located on a flat, 2 km wide, volcanically and tectonically active area (HAASE et al., 2007). The samples analyzed in this study were taken from these high-temperature vent fields using an ROV equipped with a "Multiport Valve-based all-Teflon Fluid Sampling System, (KIPS)" during the RV I'Atalante cruise MARSUED IV in 2007. Comfortless Cove as well as TP are characterized by high fluid temperatures >407°C at 2990 m water depth, close to the critical point of seawater, and show indications of phase separation (HAASE et al., 2007). The RL vent field emits ~370 °C fluids that show no indications of phase separation.

The measured Mg and Sr concentrations of the fluids are positively correlated suggesting that $[Sr]_{HydEnd}$ of the phase-separated Sr sources is lower than seawater. Extrapolating Mg/Sr ratios of the TP and CC fluid samples to a Mg/Sr ratio of zero yields a $[Sr]_{HydEnd}$ of 34(5) μM . Likewise, the $[Sr]_{HydEnd}$ of RL was estimated at ~56(5) μM . Strontium isotope compositions measured in this study are presented in tab.III.2 and in fig.III.2 a and b.

III.3.3 Marine carbonates

The major sink of Sr in the ocean is the formation of aragonitic and calcitic CaCO_3 (MILLIMAN and DROXLER, 1996) where calcium (Ca) is substituted by Sr. In order to quantify the Sr burial flux and its isotope composition we performed Sr isotope measurements on important calcifying marine organisms (tab.III.3). CaCO_3 deposition rates are primarily (~39%) controlled by species living on the shelves and slopes (e.g. mussels, star fish, sea urchins, benthic foraminifera, bryozoans, calcareous algae). Most of the remainder is determined in almost equal proportions by reef corals (20%), coccoliths (16%) and planktic foraminifera (20%). The higher Sr concentrations in aragonite cause larger Sr/Ca ratios than observed in calcite (see tab.III.3). Sr/Ca ratios are well constrained for reef corals, Halimeda, planktic foraminifera and also for many shelf and slope species (e.g. mussels: 1.5 mM, star fish: 2.5 mM, aragonitic algae: 11 mM).

However, the average value for shelf and slope species cannot be constrained well because the relative proportions of calcite and aragonite are not well known. We therefore arbitrarily assume that shelf species are composed of two thirds aragonite (Sr/Ca: ~9 mM) and one third calcite (Sr/Ca: ~1.8 mM), yielding an average shelf carbonate Sr/Ca of ~6.6 mM.

III.3.4 Sample preparation

All solid carbonate samples were weighed in Teflon beakers together with 2 ml H₂O (18.2 MΩ Milli-Q water). Samples were dissolved in 500 µl 4.5 N HNO₃, heated for at least 5 hours and then dried at ~90 °C. In order to remove organic matter 50 µl H₂O₂ and 200 µl 2N HNO₃ were added and samples were heated to ~80°C for at least 5 hours in closed beakers. Subsequently, samples were dried again at ~80°C, dissolved in 2 ml 8 N HNO₃ and split into two fractions that each contained 1000 – 1500 ng Sr, corresponding to a carbonate sample weight of 1 - 2 mg. The Sr double spike was added to one fraction and both fractions were then dried at ~90°C.

Chromatographic column separation was performed using 650 µl BIO-RAD columns filled to one third with Eichrom Sr-SPS resin (grain size 50-100 µm). The resin was washed three times with 4.5 ml H₂O and 4.5 ml 8 N HNO₃. The resin was then conditioned three times with 1 ml 8 N HNO₃ before the sample - dissolved in 1 ml 8 N HNO₃ – was loaded onto the column. In order to remove the sample matrix the resin was washed six times with 1 ml 8 N HNO₃.

The Sr-fraction was eluted into a Teflon beaker in three steps with 1 ml H₂O each. Any resin residue was removed by drying down and then heating samples to 80°C in 50 µl H₂O₂ and 200 µl 2N HNO₃ for at least 5 hours in closed beakers. Finally, samples were dried at ~80°C. About 500 ng Sr was loaded together with 2 µl H₃PO₄ onto a single Re filament after addition of 1.5 µl of Ta₂O₅-activator to stabilize signal intensity.

The sample was then heated on the filament at 0.6 A to near dryness before being dried at 1 A and slowly heated to 1.8 A within 2 minutes. Then, the sample was heated to a dark red glow. After keeping the filament glowing for about 30 seconds the current was turned down and the filament was mounted onto the sample wheel. With the exception of the dissolution step, hydrothermal- and river water samples were treated as described above.

III.3.5 TIMS measurements

The use of a ⁸⁷Sr-⁸⁴Sr double spike enables us to determine natural Sr isotope fractionation after correction for mass-dependent fractionation during TIMS measurements. The details of the ⁸⁷Sr-⁸⁴Sr double spike production, measurement procedure and data reduction are discussed by (KRABBENHÖFT et al., 2009). The Sr isotope measurements were carried out at the IFM-GEOMAR mass spectrometer facility in Kiel and at the "Geowissenschaftliches Zentrum der Universität Göttingen", Germany, using TRITON mass spectrometers (ThermoFisher, Bremen, Germany). The TRITONS were operated in positive ionization mode with a 10 kV acceleration voltage. The instruments are equipped with nine moveable Faraday cups with 10¹¹ Ω resistors that allow for simultaneous detection of all Sr masses. Mass 85 was measured in order to monitor and correct for interfering ⁸⁷Rb assuming an ⁸⁵Rb/⁸⁷Rb ratio of 2.59. Data were acquired at a typical signal intensity of 10 V for mass 88 at an average

filament temperature of $\sim 1450^{\circ}\text{C}$. For each sample 9 blocks with 14 cycles corresponding to 126 single scans were measured. Before each block the baseline was recorded and the amplifier rotation was performed.

The $^{87}\text{Sr}/^{84}\text{Sr}$ double spike technique required two separate analyses of each sample: one ic-analysis (ic=isotope composition; unspiked) and one id-analysis (id=isotope dilution; spiked) with well-known $^{86}\text{Sr}/^{84}\text{Sr}$ -, $^{87}\text{Sr}/^{84}\text{Sr}$ - and $^{88}\text{Sr}/^{84}\text{Sr}$ -ratios of the double spike. The $^{86}\text{Sr}/^{84}\text{Sr}$ - and the $^{88}\text{Sr}/^{84}\text{Sr}$ -ratios are normalized to the mean of the first block of the $^{87}\text{Sr}/^{84}\text{Sr}$ isotope ratio using an exponential fractionation law in an off-line data processing routine. Following this procedure the average internal precision of single $^{86}\text{Sr}/^{84}\text{Sr}$ -ratio measurements is ~ 7 ppm (RSD), and ~ 9 ppm for single $^{88}\text{Sr}/^{84}\text{Sr}$ -ratio determinations in the ic-analyses. We measured ~ 11 ppm (RSD) for the $^{86}\text{Sr}/^{84}\text{Sr}$ -ratio and ~ 21 ppm for the $^{88}\text{Sr}/^{84}\text{Sr}$ -ratio in the id-analyses. Variations in $^{88}\text{Sr}/^{86}\text{Sr}$ are reported in the usual δ -notation: $\delta^{88/86}\text{Sr} [\text{‰}] = \left(\frac{^{88}\text{Sr}/^{86}\text{Sr}_{\text{sample}}}{^{88}\text{Sr}/^{86}\text{Sr}_{\text{SRM987-1}}} - 1 \right) * 1000$. We use the SRM987 standard with an internationally accepted $^{88}\text{Sr}/^{86}\text{Sr}$ value of 8.375209 (NIER, 1938) for normalization. Notations (e.g. $^{87}\text{Sr}/^{86}\text{Sr}_{\text{Norm}}$ and $^{87}\text{Sr}/^{86}\text{Sr}^*$) and additional information about mass-dependent fractionation are summarized in the Appendix.

III.4 Results

III.4.1 Sr isotope composition of the marine input

III.4.1.1 Sr isotope composition of the riverine discharge to the ocean

The $^{87}\text{Sr}/^{86}\text{Sr}_{\text{Norm}}$ and $^{87}\text{Sr}/^{86}\text{Sr}^*$ values of rivers presented in tab.III.1 and fig.III.2 show variations from 0.707321(8) to 0.727705(9) and from 0.707417(9) to 0.727798(6), respectively. The Sr flux-weighted mean river values for $^{87}\text{Sr}/^{86}\text{Sr}_{\text{Norm}}$ and $^{87}\text{Sr}/^{86}\text{Sr}^*$ are 0.7113(4) and 0.7114(8), respectively. The $^{87}\text{Sr}/^{86}\text{Sr}_{\text{Norm}}$ value in particular is in good agreement with the $^{87}\text{Sr}/^{86}\text{Sr}$ value published by (GAILLARDET et al., 1999) and is similar to the values of 0.7101 (GOLDSTEIN and JACOBSEN, 1987) and 0.7119 (PALMER and EDMOND, 1989). The good agreement between our more restricted dataset (18% of the river water flux) and earlier comprehensive analyses (47% of the river water flux) of exoreic rivers (e.g. (PALMER and EDMOND, 1989)) clearly indicates that our sample set is representative of global river runoff.

The $\delta^{88/86}\text{Sr}$ values vary between 0.243(6)‰ for the Lena river and 0.42(2)‰ for the Maipo river. The Sr flux-weighted mean ($^{87}\text{Sr}/^{86}\text{Sr}^*$, $\delta^{88/86}\text{Sr}$) values are (0.7114(8), 0.315(8)‰). The good agreement of the $^{87}\text{Sr}/^{86}\text{Sr}_{\text{Norm}}$ values with the conventional $^{87}\text{Sr}/^{86}\text{Sr}$ values (tab.III.1) clearly indicates that the double spike method can reproduce conventional radiogenic values in addition to yielding new information on the non-radiogenic Sr isotope composition of the samples.

III.4.1.2 Sr isotope composition of the hydrothermal discharge to the ocean

Following the procedure of (AMINI et al., 2008) and assuming that pure hydrothermal solutions are free of Mg, we estimated the $(^{87}\text{Sr}/^{86}\text{Sr}^*, \delta^{88/86}\text{Sr})_{\text{HydEnd}}$ -values at (0.7045(5), 0.27(3)‰) by extrapolating the measured values to a Mg/Sr ratio of zero (tab.III.2, fig.III.2). The $\delta^{88/86}\text{Sr}_{\text{HydEnd}}$ values are isotopically lighter than seawater. This is in good agreement with the reported radiogenic $^{87}\text{Sr}/^{86}\text{Sr}$ - and $\delta^{88/86}\text{Sr}$ -values of basalt of 0.70412(4) and 0.26(3)‰, respectively (OHNO et al., 2008). The latter observation indicates that the isotopic composition of hydrothermal fluids simply reflect the isotopic composition of ocean crust.

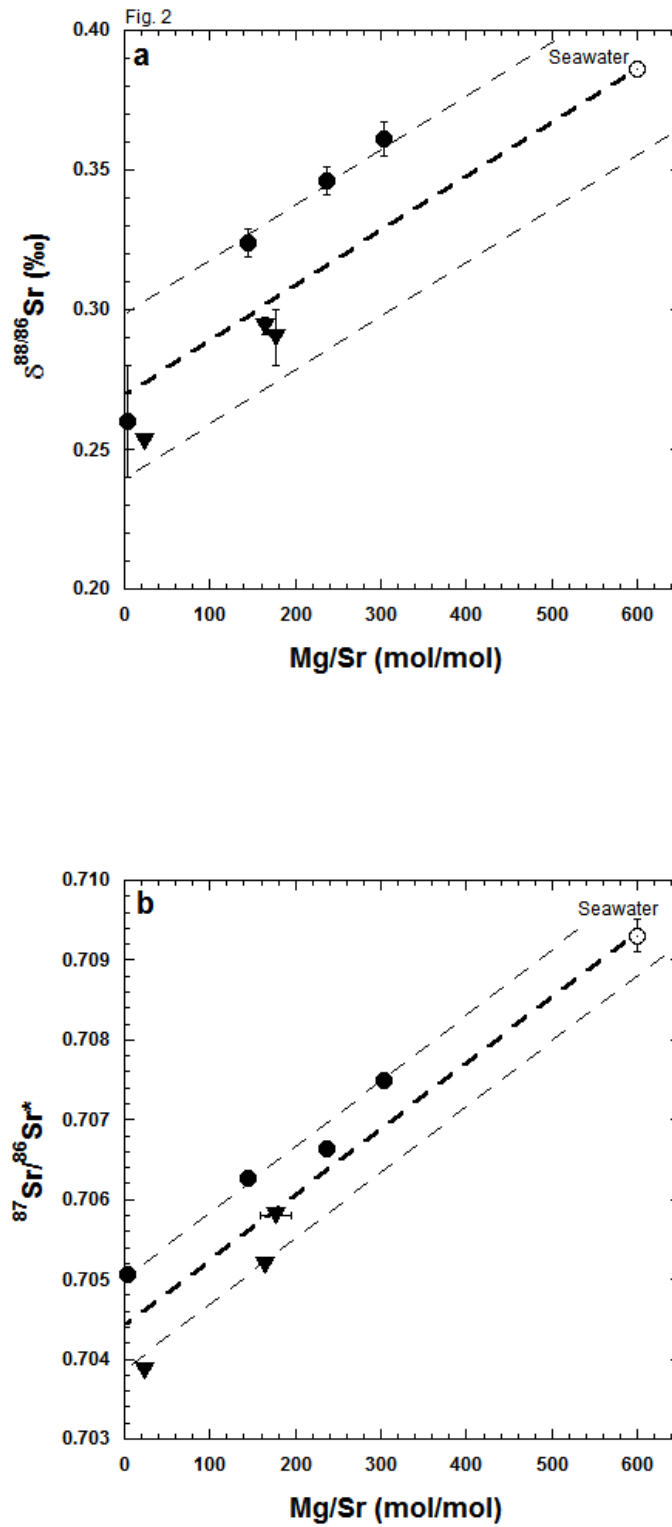


fig.III.2 a/b: ($^{87}\text{Sr}/^{86}\text{Sr}^*$, $\delta^{88/86}\text{Sr}$)-values of hydrothermal fluid samples. Assuming that pure hydrothermal solutions are free of Mg (Mg/Sr=0), hydrothermal $\delta^{88/86}\text{Sr}$ (a) and $^{87}\text{Sr}/^{86}\text{Sr}^*$ (b) end members can be extrapolated (dotted line) from our data. Circles refer to Comfortless Cove (CC) and Turtle Pits (TP), whereas triangles refer to the Red Lion (RL) hydrothermal field at the mid-Atlantic Ridge. Broken lines mark the uncertainties associated with the extrapolated values in (a) and (b).

III.4.1.3 Sr composition of the combined riverine and hydrothermal input to the ocean

The mean ocean input flux and its corresponding isotope compositions can be estimated from the measured and compiled values of the riverine discharge and of the hydrothermal input (tab.III.4; $(^{87}\text{Sr}/^{86}\text{Sr}^*, \delta^{88/86}\text{Sr})_{\text{input}}$: ($\sim 0.7106(8)$, $\sim 0.310(8)\text{‰}$). These composite values are afflicted with larger uncertainties that reflect the assumptions that are described in detail in tab.III.4. The compilation of flux data in tab.III.4 show that the present day Sr supply of $\sim 56 \cdot 10^9$ mol/yr is mainly ($\sim 60\%$) controlled by Sr delivered by riverine discharge to the ocean and to a lesser extent by groundwater ($\sim 29\%$) and hydrothermal ($\sim 4\%$) inputs. Our total flux estimate is in good agreement with the global Sr flux of $\sim 50 \cdot 10^9$ mol/a that (BASU et al., 2001) estimated based on riverine and groundwater inputs alone. They did not include Sr from low temperature alteration of oceanic crust and diagenetic mobilization of Sr from marine sediments. Our estimate is higher than that of (STOLL and SCHRAG, 1998) and (STOLL et al., 1999) of $\sim 40 \cdot 10^9$ mol/yr, because these authors did not take groundwater inputs into account. Addition of our estimate of the groundwater Sr flux ($16.5 \cdot 10^9$ mol/yr) brings both estimates in close agreement.

III.4.2 Isotope composition of the marine Sr output

The primary sink for marine Sr is marine CaCO_3 precipitation. The most simplistic approach to estimate mean global ocean $(^{87}\text{Sr}/^{86}\text{Sr}^*, \delta^{88/86}\text{Sr})_{\text{Carbonate}}$ values is to average $(^{87}\text{Sr}/^{86}\text{Sr}^*, \delta^{88/86}\text{Sr})$ values of the major calcifying species such as tropical corals, green algae (Halimeda), foraminifera and coccoliths (tab.III.3). This approach yields mean global $(^{87}\text{Sr}/^{86}\text{Sr}^*, \delta^{88/86}\text{Sr})_{\text{Carbonate}}$ values of (0.70924(3), 0.22(5)‰), (tab.III.3).

A more refined approach for determining mean global ocean $(^{87}\text{Sr}/^{86}\text{Sr}^*, \delta^{88/86}\text{Sr})_{\text{Carbonate}}$ values is to also consider the individual Sr burial fluxes. These burial fluxes can be estimated from the species-dependent CaCO_3 -burial rates (tab.III.3) and the respective species-dependent Sr/Ca ratios. The mean global $(^{87}\text{Sr}/^{86}\text{Sr}^*, \delta^{88/86}\text{Sr})_{\text{Carbonates}}$ values are determined by the Sr burial flux-weighted means of the major calcifying species and their respective $(^{87}\text{Sr}/^{86}\text{Sr}^*, \delta^{88/86}\text{Sr})$ values. The main disadvantage of this approach is related to the fact that CaCO_3 burial rates are uncertain by at least 50% (MILLIMAN and DROXLER, 1996).

For corals we adopt the $(^{87}\text{Sr}/^{86}\text{Sr}^*, \delta^{88/86}\text{Sr})$ -values of the JcP-1 coral standard (0.70923(1), 0.19(1)‰). Aragonitic azooxanthellate coldwater corals of the species *Lophelia pertusa* that grow between 6 °C and 10 °C show slightly lower $\delta^{88/86}\text{Sr}$ values of 0.06-0.18‰ (RÜGGEBERG et al., 2008). However, coldwater corals contribute only $\sim 1\%$ to the global carbonate sediment budget (LINDBERG and MIENERT, 2005) and are therefore not included in the Sr isotope budget. In contrast, tropical coral reefs contribute $\sim 31\%$ to the ocean's Sr burial flux (tab.III.3). For tropical corals we did not take into

account any temperature sensitivity of the paired ($^{87}\text{Sr}/^{86}\text{Sr}^*$, $\delta^{88/86}\text{Sr}$)-values, as the new double spike technique did not confirm the previously predicted temperature sensitivity of Sr isotope fractionation (FIETZKE and EISENHAUER, 2006).

For this study paired ($^{87}\text{Sr}/^{86}\text{Sr}^*$, $\delta^{88/86}\text{Sr}$)-values of aragonitic *Halimeda* specimen from Tahiti and the Mediterranean Sea yielded average values of 0.70926(3), 0.27(3)‰ (tab.III.3). *Halimeda* mounds contribute ~9% to the ocean's Sr burial flux.

Despite being calcitic, the ($^{87}\text{Sr}/^{86}\text{Sr}^*$, $\delta^{88/86}\text{Sr}$)-values of ~0.70926(3), 0.26(7)‰ from cultured coccoliths are similar to those of the aragonitic species (tab.III.3). Coccoliths contribute ~6% to the global Sr burial flux.

The two species *G. ruber* and *G. sacculifer* are taken to be representative of the Sr isotope composition of calcitic planktic foraminifera. They show identical ($^{87}\text{Sr}/^{86}\text{Sr}^*$, $\delta^{88/86}\text{Sr}$)-values of (0.70920(2), 0.14(1)‰). Note that the paired ($^{87}\text{Sr}/^{86}\text{Sr}^*$, $\delta^{88/86}\text{Sr}$)-values of these foraminifera are considerably lower than those of other species, pointing to a strong physiological control of the trace metal uptake by planktic foraminifera. Planktic foraminifera, like coccoliths, contribute ~5% to the ocean's Sr burial flux.

A significant part of the Sr flux is contributed by non-reef carbonate production on the continental shelf and slope (MILLIMAN and DROXLER, 1996). However, shelf carbonate contributions are rather uncertain due to the unknown partitioning between calcitic and aragonitic species and the lack of knowledge on CaCO_3 production rates of different contributing taxa (tab.III.3). Based on the data compiled in tab.III.3 we approximate the mean ($^{87}\text{Sr}/^{86}\text{Sr}^*$, $\delta^{88/86}\text{Sr}$)-ratios of shelf carbonates at ~(0.70924(1), 0.22(3)‰). We assume that shelf and slope carbonates are two-thirds aragonitic with mean ($^{87}\text{Sr}/^{86}\text{Sr}^*$, $\delta^{88/86}\text{Sr}$) values of reef corals and *Halimeda* (0.70925, 0.23‰), and one-third calcitic with mean ($^{87}\text{Sr}/^{86}\text{Sr}^*$, $\delta^{88/86}\text{Sr}$) values of coccoliths and planktic foraminifera (0.70923, 0.20‰).

Based on data summarized in tab.III.3 we estimate the Sr burial flux-weighted ($^{87}\text{Sr}/^{86}\text{Sr}^*$, $\delta^{88/86}\text{Sr}$)-ratios of the total marine carbonate production at (~0.70926(2), ~0.21(2)‰). The mean global ($^{87}\text{Sr}/^{86}\text{Sr}^*$, $\delta^{88/86}\text{Sr}$)_{Carbonate} values are therefore similar to the values of continental shelf and slope taxa. Furthermore, the flux-weighted average values are within statistical uncertainty identical to those estimated by just averaging the ($^{87}\text{Sr}/^{86}\text{Sr}^*$, $\delta^{88/86}\text{Sr}$) values of the main calcifying species (0.70924(2), 0.22(2)‰; tab.III.3). The close agreement between the two approaches may indicate that the relative contributions of the various burial fluxes are well constrained despite considerable uncertainties in the absolute burial fluxes. Hence, we consider both approaches to be reasonable approximations of the true mean global ($^{87}\text{Sr}/^{86}\text{Sr}^*$, $\delta^{88/86}\text{Sr}$)_{Carbonate} values.

III.5 Discussion

Compilations of the modern input and output data (tab.III.3 and 4) indicate that the Sr outputs ($\sim 174 \cdot 10^9$ mol/yr) are larger than Sr inputs ($\sim 56 \cdot 10^9$ mol/yr), and that the Sr isotope compositions of input and output fluxes are considerably different. Although the estimated difference between input and output values seems to be large, we cannot assign statistical significance because all estimates are afflicted with considerable uncertainties. In order to further examine and better constrain the observed trends, we compare the Sr isotope balance of Sr inputs, outputs and of $[\text{Sr}]_{\text{Seawater}}$ in a triple-isotope-plot. This new approach in Sr isotope geochemistry critically depends on taking Sr isotope fractionation into account.

III.5.1 Sr budget of the global ocean

In fig.III.3 the global means of the $(^{87}\text{Sr}/^{86}\text{Sr}^*, \delta^{88/86}\text{Sr})_{\text{River}}$ - and $(^{87}\text{Sr}/^{86}\text{Sr}^*, \delta^{88/86}\text{Sr})_{\text{HydroEnd}}$ -values define the two end-members of a binary mixing line between the two major sources of Sr in the modern ocean. The calculated combined $(^{87}\text{Sr}/^{86}\text{Sr}^*, \delta^{88/86}\text{Sr})_{\text{Input}}$ -values fall on this binary mixing line and plot relatively close to the Sr isotope composition of average river water, indicating that riverine input is the major Sr source to the present-day ocean ($\sim 60\%$). In contrast, the modern Sr isotope values of $(^{87}\text{Sr}/^{86}\text{Sr}^*, \delta^{88/86}\text{Sr})_{\text{Seawater}}$ and $(^{87}\text{Sr}/^{86}\text{Sr}^*, \delta^{88/86}\text{Sr})_{\text{Carbonates}}$ form a mass-dependent isotope fractionation line. Carbonates are isotopically lighter because they preferentially incorporate the lighter isotopes and leave seawater enriched in the heavy ones.

The intercept of the binary mixing line and the fractionation line $(^{87}\text{Sr}/^{86}\text{Sr}^*, \delta^{88/86}\text{Sr})_{\text{Intercept}}$ (~ 0.70927 , $\sim 0.30\%$) defines the isotope composition of the combined Sr input into the ocean (fig.III.3). These values are significantly different ($\sim 0.0011(8)$, $\sim 0.01(2)\%$) from the calculated $(^{87}\text{Sr}/^{86}\text{Sr}^*, \delta^{88/86}\text{Sr})_{\text{Input}}$ -values, and this difference reflects isotope disequilibrium. There is also a significant difference between the Sr isotopic composition of the $(^{87}\text{Sr}/^{86}\text{Sr}^*, \delta^{88/86}\text{Sr})_{\text{Input}}$ and the Sr output values represented by $(^{87}\text{Sr}/^{86}\text{Sr}^*, \delta^{88/86}\text{Sr})_{\text{Carbonates}}$ of ($\sim 0.0011(8)$, $\sim 0.10(2)\%$). This also indicates disequilibrium between inputs and outputs, because at isotope equilibrium $(^{87}\text{Sr}/^{86}\text{Sr}^*, \delta^{88/86}\text{Sr})_{\text{Input}}$ and $(^{87}\text{Sr}/^{86}\text{Sr}^*, \delta^{88/86}\text{Sr})_{\text{Carbonates}}$ (output) should be identical (see Appendix).

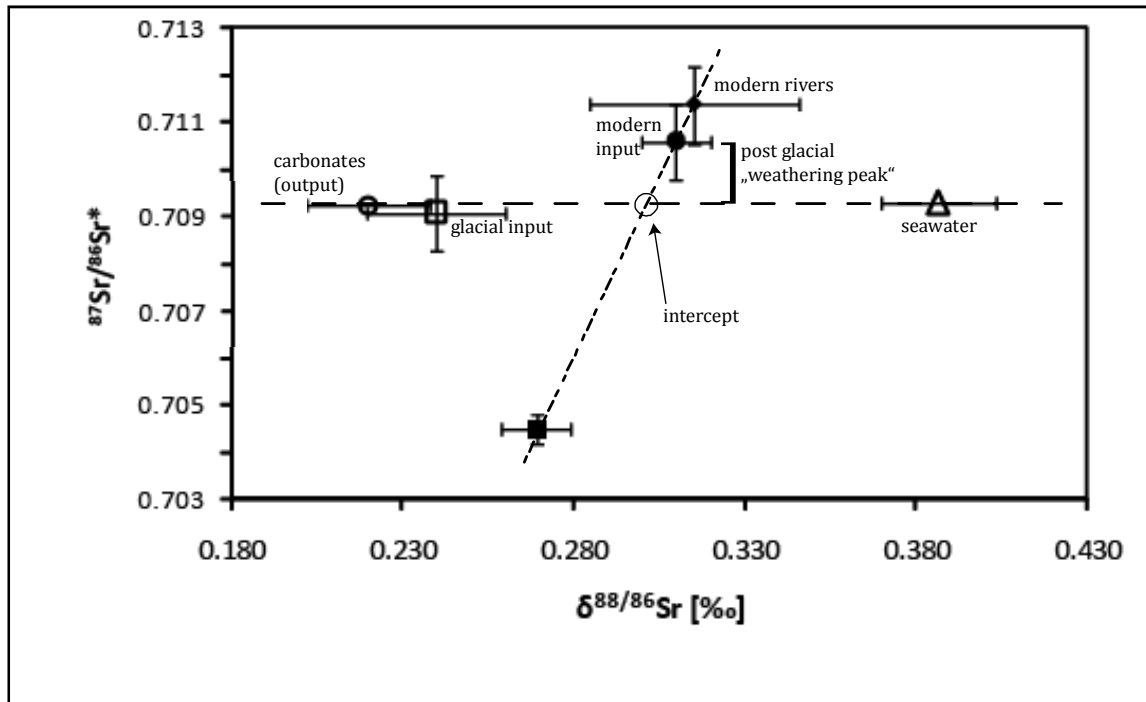


fig.III.3: Triple isotope plot showing the flux-weighted average Sr isotope values of rivers, hydrothermal fluids, marine carbonates and seawater. The $(^{87}\text{Sr}/^{86}\text{Sr}^*, \delta^{88/86}\text{Sr})_{\text{seawater}}$ and the $(^{87}\text{Sr}/^{86}\text{Sr}^*, \delta^{88/86}\text{Sr})_{\text{carbonates}}$ values define a mass-dependent fractionation line, whereas $(^{87}\text{Sr}/^{86}\text{Sr}^*, \delta^{88/86}\text{Sr})_{\text{rivers}}$ and $(^{87}\text{Sr}/^{86}\text{Sr}^*, \delta^{88/86}\text{Sr})_{\text{HydEnd}}$ values define a binary mixing line. The calculated $(^{87}\text{Sr}/^{86}\text{Sr}^*, \delta^{88/86}\text{Sr})_{\text{input}}$ values plots along the binary mixing line but are considerably offset from the isotope composition of marine carbonates. Note that the estimated glacial $(^{87}\text{Sr}/^{86}\text{Sr}^*, \delta^{88/86}\text{Sr})_{\text{input}}$ value is close to that of carbonates, indicating isotope equilibrium. The difference between modern $(^{87}\text{Sr}/^{86}\text{Sr}^*, \delta^{88/86}\text{Sr})_{\text{input}}$ and $(^{87}\text{Sr}/^{86}\text{Sr}^*, \delta^{88/86}\text{Sr})_{\text{intercept}}$ defines the “weathering peak”.

In a first approach taking only $^{87}\text{Sr}/^{86}\text{Sr}^*$ values into account and leaving J_{HydEnd} , J_{OCC} and J_{Dia} (tab.III.4) unchanged we can calculate from our isotope data that the combined J_{River} and J_{GW} input ($\sim 49 \cdot 10^9$ mol/a) is about a factor of three too high to be in agreement with the $^{87}\text{Sr}/^{86}\text{Sr}^*$ output values. This observation is in general accord with earlier statements using traditional $^{87}\text{Sr}/^{86}\text{Sr}$ ratios that the estimated modern riverine flux is relatively accurate within $\sim 30\%$ but is probably not representative of the past, particularly not for elements with residence times in excess of 10^5 years. In this regard, our observation that the modern $(^{87}\text{Sr}/^{86}\text{Sr}^*, \delta^{88/86}\text{Sr})_{\text{input}}$ -value is higher than the $(^{87}\text{Sr}/^{86}\text{Sr}^*, \delta^{88/86}\text{Sr})_{\text{intercept}}$ -value is compatible with earlier statements based on traditional $^{87}\text{Sr}/^{86}\text{Sr}$ values that modern continental weathering rates are 2 - 3 times higher than the long-term mean (VANCE et al., 2009).

This post glacial “weathering peak” (VANCE et al, 2009) is likely caused by weathering of fine-grained material left exposed by the retreating continental ice masses (c.f. (BLUM, 1995), see discussion in chapter III.7). At equilibrium the complete marine Sr budget requires agreement in the $^{87}\text{Sr}/^{86}\text{Sr}^*$ and $\delta^{88/86}\text{Sr}$ values of input and output fluxes. Interestingly, this cannot simply be achieved by reducing individual input fluxes because - within statistical uncertainties - there is no Sr source with a corresponding $\delta^{88/86}\text{Sr}$ value equal to or even lower than the modern $\delta^{88/86}\text{Sr}_{\text{Carbonates}}$ value (see tab.III.4). This major discrepancy indicates that the marine Sr budget cannot be at equilibrium given

the known Sr sources. At least one additional Sr source of sufficient size and with a $\delta^{88/86}\text{Sr}$ value lower than the mean $\delta^{88/86}\text{Sr}_{\text{Carbonates}}$ value is required to achieve equilibrium. The nature of this isotopically light, missing Sr source is discussed below.

Isotope equilibrium can be disturbed by sufficiently large addition or removal of Sr relative to the size of the marine Sr reservoir, provided the isotope composition is significantly different from that of seawater (STOLL and SCHRAG, 1998). The duration of such a perturbation is a function of the residence time, ~ 2.4 Myr in the case of Sr. On time scales much longer than the Sr residence time slight imbalances between input and output fluxes can occur in quasi isotope equilibrium. It is thus very unlikely that the Sr fluxes and isotope compositions of hydrothermal sources are subject to a rapid change, as submarine hydrothermal circulation is controlled by processes in the Earth's mantle characteristic time scales of 10^6 - 10^8 yrs, far in excess of the residence time of Sr in seawater.

A change of the preferred carbonate polymorphism may also lead to changes in Sr concentration of seawater, because Sr/Ca ratios of aragonite are about an order of magnitude higher than those of calcite. Strontium isotope measurements of calcitic foraminifera (tab.III.3) confirm earlier conclusions based on Ca isotopes (FARKAŠ et al., 2007) that fractionation factors for aragonite and calcite differ. A change of the preferred carbonate polymorphism could therefore lead to changes in the isotopic composition of seawater. However, global changes of the preferred marine carbonate polymorphism occur on time scales much longer than the residence time of Sr in seawater (STANLEY and HARDIE, 1998), leaving the system in quasi steady state.

In contrast, continental weathering and related riverine inputs into the ocean may be subject of relatively rapid changes (10 to 100 kyr) when compared to the Sr residence time (~ 2.4 Myr). In addition, glacial/interglacial changes in sea level and the related dynamics of weathering of carbonates exposed on continental shelves may be responsible for substantial and short-term disequilibria between Sr inputs and outputs of the ocean, as proposed earlier by (STOLL and SCHRAG, 1998).

III.6 Sr isotope equilibrium in the ocean during the last glacial

A ~ 120 m drop in glacial sea level (STOLL and SCHRAG, 1998) exposed continental shelves and provided an additional supply of elements from the continents to the ocean. In particular, alkaline earth elements such as Mg, Ca and Sr are mobilized from weathering of carbonate-dominated continental shelves in larger amounts during glacial periods (c.f. (STOLL et al., 1999)). Polymorphism exerts strong controls over Mg and Sr delivery, because calcite is Mg-rich compared to aragonite, whereas aragonite contains about 10 times more Sr than calcite (tab.III.3). During meteoric diagenesis aragonite will eventually recrystallize to calcite and release Sr to the sea. (STOLL and SCHRAG, 1998) and (STOLL et al., 1999) hypothesize that this additional flux caused Sr/Ca of glacial seawater to

increase. In contrast, sea level high-stand during interglacials flooded the shelves that then act as Sr sinks, causing seawater Sr/Ca values to decrease. These glacial/interglacial variations result in an oscillation of the marine Sr/Ca ratio of the order of $\sim\pm 1\%$ relative to the present day value (STOLL and SCHRAG, 1998).

From the numerical integration of the (STOLL and SCHRAG, 1998) data we estimate, for the time interval from 10 to 20 kyr, the average annual Sr flux of $\sim 150 \cdot 10^9$ mol/yr, approximately three times larger than the modern global mean Sr input ($\sim 56 \cdot 10^9$ mol/yr, tab.III.4). The Sr input during the last glacial maximum ($\sim 206 \cdot 10^9$ mol/yr) was therefore dominated by carbonate weathering on the continental shelves rather than by weathering of the continental interiors. Taking shelf carbonate weathering and the above data into account, we estimate glacial ($^{87}\text{Sr}/^{86}\text{Sr}^*$, $\delta^{88/86}\text{Sr}$)_{Input}-values of ($\sim 0.7091(8)$, $\sim 0.24(2)\text{‰}$). These values differ significantly from the present-day ($^{87}\text{Sr}/^{86}\text{Sr}^*$, $\delta^{88/86}\text{Sr}$)_{Input}-values of ($0.7106(8)$, $0.310(8)\text{‰}$). Most importantly, the estimated glacial ($^{87}\text{Sr}/^{86}\text{Sr}^*$, $\delta^{88/86}\text{Sr}$)_{Input}-values are within uncertainty of the modern ($^{87}\text{Sr}/^{86}\text{Sr}^*$, $\delta^{88/86}\text{Sr}$)_{Carbonates}-values of ($0.70926(2)$, $0.21(2)\text{‰}$), indicating isotope equilibrium rather than disequilibrium conditions during the last glacial maximum (fig.III.3)

III.7 Sr budget disequilibrium during glacial/interglacial transitions

The predicted marine Sr equilibrium was probably terminated at the end of the glacial period by the rapid ~ 120 m sea level rise between the glacial low-stand at ~ 20 kyr and the Holocene sea level maximum at ~ 6 kyr. This rise eliminated shelf carbonate weathering as the major source of Sr, leaving riverine, groundwater and hydrothermal inputs as the major, though drastically reduced, Sr fluxes to the modern ocean. Without shelf carbonate weathering, the new post-glacial mean Sr input value is expected to approach the intercept value defined by the binary mixing line and the mass-dependent fractionation line (fig.III.3). However, the post-glacial ($0.7106(8)$, $0.310(8)\text{‰}$)_{Input}-value is significantly more radiogenic in $^{87}\text{Sr}/^{86}\text{Sr}^*$ and tend to be heavier in the $\delta^{88/86}\text{Sr}$ value than the intercept values (~ 0.70927 , $\sim 0.30\text{‰}$). This could indicate that riverine Sr inputs increased during glacial/interglacial transitions while continental shelf input decreased. Enhanced continental weathering may be caused by warmer post-glacial climate, higher atmospheric pCO_2 and enhanced precipitation. The retreating continental glaciers have also exposed finely ground material that provided an extra supply (“weathering peak”, fig.III.3) of isotopically more radiogenic Sr to the ocean (c.f. (BLUM, 1995; VANCE et al., 2009)). This “weathering peak” has not yet disappeared, and the Sr isotope compositions of modern input and output values have not yet reached a new post-glacial equilibrium.

III.8 Conclusion

During glacial periods weathering of continental shelf carbonates complemented inputs from rivers, groundwater and hydrothermal fluids as a fourth source of Sr to seawater. This fourth source dominated Sr fluxes to the ocean during glacial periods. The close agreement of the glacial Sr input values with modern carbonate output values is suggestive of isotope equilibrium during the last glacial maximum. A fundamental change in weathering regime during the glacial/interglacial transition perturbed the glacial Sr equilibrium towards the observed modern disequilibrium. The inferred change in weathering regime was facilitated by the rapid post-glacial sea level rise that flooded the continental shelves, terminated weathering fluxes from shelf carbonates and left riverine, groundwater and hydrothermal Sr fluxes as the major sources to the modern oceans. An additional shift towards heavier and more radiogenic Sr isotope composition may have occurred due to an additional flux of isotopically heavy and radiogenic Sr (“weathering peak”) from the fine-grained, highly reactive detritus that the retreating continental ice shields left behind.

III.9 Tables

Nr.	River	Sample date and location	Water discharge [km ³ /a]	Sr Concen. [μM]****	Sr Flux [mol/a]·10 ⁸	⁸⁷ Sr/ ⁸⁶ Sr	⁸⁷ Sr / ⁸⁶ Sr*	⁸⁷ Sr/Sr ⁸⁶ _{norm}	δ ^{88/86} Sr [‰]
1	Brahmaputra	06/21/06 25.2833°N, 89.6333°E	510 ⁺	6,37	3.25	0.719218(26)	0.719320(3)	0.709205(3)	0.317(1)
2	Danube	05/04/07 48.2261°N, 16.4086°E	207 ⁺	27,58	5.71	0.712723 (7)	0.712808(2)	0.712717(2)	0.254(4)
3	Fraser	08/08/06 49.5633°N, 121.4028°W	112 ⁺	8,53	0.955	0.718662 (1)	0.718764(6)	0.718653(6)	0.31(2)
4	Ganga	08/17/07 24.0553°N, 89.0314°E	493 ⁺	6,59	3.25	0.727702 (9)	0.727798(6)	0.727705(6)	0.25(2)
5	Hudson	07/02/08 42.75°N, 73.68°W	12 ⁺⁺	14,50	0.174	0.710328 (1)	0.710425(1)	0.710332(1)	0.260(1)
6	Indus	02/28/07 25.4422°N, 68.3164°E	90 ⁺	33,33	3.00	0.711003(24)	0.711100(4)	0.710990(4)	0.31(1)
7	Lena	n.a.	525 ⁺	11,01	5.78	0.709536(20)	0.709617(9)	0.709530(8)	0.243(6)
8	Mackenzie	04/07/07 68.4659°N, 134.1283°W	308 ⁺	23,70	7.30	0.711442 (8)	0.711547(7)	0.711434(7)	0.32(2)
9	Maipo	01/29/07 33.6288°N, 70.3548°W	3.6 ⁺⁺⁺	318,47	1.00	n.a.	0.707506(9)	0.707355(9)	0.42(2)
10	Sacred Falls Punaluu, Hawaii	n.a.	n.a.	n.a.	1.00	0.707323 (8)	0.707417(9)	0.707321(2)	0.27(3)
11	Rhine	8/25/07 50.9481°N,6.9714°E	69.4 ⁺	62,25	4.32	0.709377 (9)	0.708799(6)	0.708713(9)	0.24(1)
12	Saint Lawrence	05/18/08 45.8586°N, 73.2397°W	337 ⁺	14,81	4.99	0.710362 (7)	0.71048 (1)	0.710354(7)	0.34(3)
13	Yangtze	2007 30.2872°N, 111.5264°E	900 ⁺⁺	22,31	20.7	0.710587 (7)	0.71072 (2)	0.710587(7)	0.38(5)

tab.III.1: Sr flux and isotope composition of selected rivers. Note: “n.a.”=data not available. Data marked with (+) are from (GAILLARDET et al., 1999), (++) (PALMER and EDMOND, 1989) and (+++) from the United States Geological Survey (<http://www.sage.wisc.edu/riverdata/>). The errors are 2 standard error of the mean (2σ_{mean}). The ⁸⁷Sr/⁸⁶Sr_{norm} value is determined from the δ^{88/86}Sr and the ⁸⁷Sr /⁸⁶Sr* value renormalized to δ^{88/86}Sr=0 (see Appendix). (**): The Sr concentrations have typical uncertainties of ~2%. The Sr flux-weighted global mean (87Sr/86Sr*, δ88/86Sr)River value of (0.7114(8), 0.315(8)‰) was calculated with equation A4 (Appendix).**

Label	Location	Depth [m]	Fluid [%]	T [°C]	Mg/Sr [mol/mol]	$^{87}\text{Sr}/^{86}\text{Sr}^*$	$\delta^{88/86}\text{Sr}[\text{‰}]$
42ROV-3	4°48'S, CC	2990	72	>400	303	0.707488(4)	0.361(6)
42ROV-4	4°48'S, CC	2990	80	>400	236	0.706643(3)	0.346(5)
42ROV-7	4°48'S, CC	2995	88	>400	144	0.706276(2)	0.324(5)
35ROV-8	4°48'S, TP	2990	100	450	3	0.705066(3)	0.26(2)
67ROV-4	4°48'S, RL	3045	80	366	177	0.705808(3)	0.29(1)
67ROV-5	4°48'S, RL	3045	98	366	23	0.703857(1)	0.253(1)
67ROV-6	4°48'S, RL	3045	81	366	164	0.705179(1)	0.294(3)

tab.III.2: Mg/Sr and Sr isotope composition of hydrothermal fluids from MAR, 4°48'S. Note: TP=Turtle Pits, CC=Comfortless Cove; RL=Red Lion. The errors are 2 standard error of the mean ($2\sigma_{\text{mean}}$).

Carbonate Sediment Type	CaCO ₃ Deposition [10 ¹² mol/yr]	CaCO ₃ polymorph	Mean Sr/Ca [mmol/mol]	Sr Burial Flux (10 ⁹ mol/yr)	$^{87}\text{Sr}/^{86}\text{Sr}^*$	$\delta^{88/86}\text{Sr}$ [‰] (SRM987)
	1.	2.	3.	4.	5.	6.
Reef Corals (JcP-1 coral standard)	~6.0 (20%)	Aragonite	~9.0	~54 (31%)	0.70923(1)	0.19(1)‰
<i>Halimeda</i>	~1.5 (5%)	Aragonite	~11	~16 (9%)	0.70926(3)	0.27(3)‰
Coccoliths	~5.0 (16%)	Calcite	2.2	~11 (6%)	0.70926(3)	0.26(7)‰
Planktic Foraminifera	~6.0 (20%)	Calcite	1.4	~8 (5%)	0.70920(2)	0.14(1)‰
Continental shelf and slope taxa (mussels, starfish, etc.)	~13.0 (39%)	Aragonite and calcite	~6.6	~85 (49%)	0.70924(1)	0.22(3)‰
Total Carbonates	~32.0 (100%)	---	n.a.	~174(100%)		
Average					0.70924(2)	0.22(2)‰
Sr burial flux weighted average					0.70926(2)	0.21(2)‰

tab.III.3: Sr burial fluxes and isotopic composition.

Column 1: Reef Corals: The deposition rate of reefs has been estimated at $7.0 \cdot 10^{12}$ mol/yr (MILLIMAN and DROXLER, 1996). Note that the deposition rates in column 1 are afflicted with large statistical uncertainties: reef corals, coccoliths, and planktic foraminifera have uncertainties on the order of $\pm 50\%$, and continental shelf and slope taxa have uncertainties of 50% and >100%, respectively. The CaCO₃ burial rate related to reef coral formation is estimated at $\sim 6.0 \cdot 10^{12}$ mol/yr based on estimates that $\sim 85\%$ of reef CaCO₃ is derived solely from corals (HUBBARD et al., 1990). Mean Sr/Ca values are compiled from published data on *Acropora*, *Diploria*, *Montastrea*, *Montipora*, *Pavona* and *Porites* (COHEN and THORROLD, 2007; GALLUP et al., 2006; SUN et al., 2005). The average ($^{87}\text{Sr}/^{86}\text{Sr}^*$, $\delta^{88/86}\text{Sr}$)-values are adopted from the long-term average value of the JcP-1 coral standard.

Halimeda: Halimeda Sr/Ca ratio is from (DELANEY et al., 1996). ($^{87}\text{Sr}/^{86}\text{Sr}^*$, $\delta^{88/86}\text{Sr}$) values are measured on Halimeda specimens from Tahiti and the Mediterranean Sea.

Coccoliths: CaCO₃ burial rate is from (SCHIEBEL, 2002) and (BROECKER and CLARK, 2009). Mean Sr/Ca ratios are from (STOLL and SCHRAG, 2000). The $\delta^{88/86}\text{Sr}$ value is the average of various measurements on laboratory-cultured *Emiliania huxleyi* and *Coccolithus pelagicus*.

Planktic Foraminifera: The CaCO₃ burial rate is from (SCHIEBEL, 2002). Mean Sr/Ca ratios are from (KISAKÜREK et al., 2008). The ($^{87}\text{Sr}/^{86}\text{Sr}^*$, $\delta^{88/86}\text{Sr}$)-values were determined on *G. ruber* and *G. sacculifer*, separated from core SO 164-03-4 from the central Caribbean Sea (16°32'37"N, 72°12'31"W, 2744 m).

Continental shelf and slope taxa: CaCO₃ sediments on the continental shelves and slopes are produced by a variety of taxa, including species mentioned above. For further discussion we assume shelf species to be two-thirds aragonitic (Sr/Ca ~ 9 mmol/mol) and one-third calcitic (Sr/Ca ~ 1.8 mmol/mol), yielding a Sr/Ca ratio of ~ 6.6 mmol/mol. Note, that despite their importance to the total Sr burial flux, the contribution of the shelf taxa is afflicted with large uncertainty (50 - > 100%).

Column 4 is calculated from the values in columns 1 and 3. The values in brackets in columns 5 and 6 correspond to $2\sigma_{\text{mean}}$ that reflect only Sr isotope error propagation. Burial rate uncertainties are not included in the uncertainties in columns 5 and 6.

Sr Sources		$^{87}\text{Sr}/^{86}\text{Sr}$	$^{87}\text{Sr}/^{86}\text{Sr}_{\text{norm}}$	$^{87}\text{Sr}/^{86}\text{Sr}^*$	$\delta^{88/86}\text{Sr}$ [‰]	Flux [10^9 mol/yr]
River discharge	J_{River}	0.7119(9) ^{1#}	0.7113(4)	0.7114(8)	0.315(8)	$\sim 33.3 \pm 10^1$
Groundwater discharge	J_{GW}	0.7110 ²	n.a.	n.a.	n.a.	$\sim 16.5 \pm 8^2$
Oceanic crust-seawater interaction at mid-ocean ridges	J_{HydEnd}	0.7025 ³	0.70438(3)	0.7045(5)	0.27(3)	$\sim 2.3^3 \pm 1.2^\circ$
Low-temperature interaction on ridge flanks and within the cold oceanic crust	J_{OCC}	0.7025 ³	n.a.	n.a.	n.a.	$\sim 0.8 \pm 0.4^3$
Diagenetic flux from marine sediments	J_{DIA}	0.7084 ¹	n.a.	n.a.	n.a.	$\sim 3.4 \pm 1.7^1$
Sr Flux-weighted average	J_{Input}	~ 0.7109	n.a.	$\sim 0.7106(8)$	$\sim 0.310(8)$	$\sim 56.3 \pm 13$

tab.III.4: Sources of Sr to the ocean.

Note: All ($^{87}\text{Sr}/^{86}\text{Sr}^*$, $\delta^{88/86}\text{Sr}$)-values are from this study. (1) (PALMER and EDMOND, 1989), (2) (BASU et al., 2001), 50% uncertainty is arbitrarily assigned to this value, (3) (DAVIS et al., 2003), 50% uncertainty is arbitrarily assigned to this value. The major Sr inputs to the ocean are river discharge (J_{RW}), groundwater discharge (J_{GW}) and oceanic crust-seawater interaction (J_{OCH}) at mid ocean ridges. All other Sr fluxes generated by low temperatures interactions on ridge flanks, (J_{OCC}), Sr inputs from sedimentary pore waters and from recrystallizing sediments (J_{DIA}) are arbitrarily assigned uncertainties of 50%. “n.a.”: not available. The Sr isotope composition of the input is calculated from the values above. For simplification and due to the lack of data we assume that the ($^{87}\text{Sr}/^{86}\text{Sr}^*$, $\delta^{88/86}\text{Sr}$)-values of J_{GW} are equal to J_{Rivers} and that the ($^{87}\text{Sr}/^{86}\text{Sr}^*$, $\delta^{88/86}\text{Sr}$)-values of J_{OCC} and of J_{DIA} are equal to J_{HydEnd} . #: the statistical uncertainty was estimated from the half difference between the minimum estimate of the global mean value of 0.7101 (GOLDSTEIN and JACOBSEN, 1987) and the maximum estimate by (PALMER and EDMOND, 1989). °: Estimates of the hydrothermal input range from minimum values of $\sim 1.9 \cdot 10^9$ mol/yr (GOLDSTEIN and JACOBSEN, 1987) to $15 \cdot 10^9$ mol/yr (PALMER and EDMOND, 1989). However, the maximum value is estimated based on the assumption of Sr equilibrium, whereas the lower values are based on different independent approaches. Hence, for our discussion we adopted the most recent estimate of (DAVIS et al., 2003) as the best approximation of the global hydrothermal Sr flux. The Sr flux-weighted global mean ($^{87}\text{Sr}/^{86}\text{Sr}^*$, $\delta^{88/86}\text{Sr}$)_{Input} values of (0.7106(8), 0.310(8)‰) were calculated with equation A6 (Appendix).

III.10 Acknowledgements

Financial support was provided by the “Deutsche Forschungsgemeinschaft, DFG, Ei272/29-1 and Ei272/30-1 (TRION)”. We thank A. Kolevica, T. Atwood and C. Miller for laboratory assistance and technical support. The comments and suggestions of two anonymous reviewers and the associate editor Prof. S. Krishnaswami helped to significantly improve this article.

III.11 Appendix

III.11.1 Notation and terminology

$^{87}\text{Sr}/^{86}\text{Sr}$	This is the notation for the traditional radiogenic Sr isotope value. This ratio is measured by plasma or thermal ionization mass spectrometry and normalized to a $^{88}\text{Sr}/^{86}\text{Sr}$ ratio of 8.375209.
$^{87}\text{Sr}/^{86}\text{Sr}^*$	This ratio refers to the $^{87}\text{Sr}/^{86}\text{Sr}$ ratio as measured and normalized to a $^{87}\text{Sr}-^{84}\text{Sr}$ double spike (see KRABBENHÖFT et al., 2009). This ratio was <u>not</u> normalized to a $^{88}\text{Sr}/^{86}\text{Sr}$ ratio of 8.375209.
$\delta^{88/86}\text{Sr}$	This ratio refers to the $^{88}\text{Sr}/^{86}\text{Sr}$ ratio as measured and normalized to an $^{87}\text{Sr}-^{84}\text{Sr}$ double spike (see KRABBENHÖFT et al., 2009). The measured $^{88}\text{Sr}/^{86}\text{Sr}$ ratio is presented in the usual δ -notation in per mill (‰) deviation from the SRM987 standard. Note that a $^{88}\text{Sr}/^{86}\text{Sr}$ ratio of 8.375209 corresponds to a $\delta^{88/86}\text{Sr}$ -value of zero.
$^{87}\text{Sr}/^{86}\text{Sr}_{\text{Norm}}$	This ratio refers to the $^{87}\text{Sr}/^{86}\text{Sr}^*$ ratio which is renormalized to a $^{88}\text{Sr}/^{86}\text{Sr}$ ratio of 8.375209. The subscript “Norm” stands for normalization. The $^{87}\text{Sr}/^{86}\text{Sr}_{\text{Norm}}$ is equivalent to the traditional radiogenic $^{87}\text{Sr}/^{86}\text{Sr}$ ratio. However, in order to provide comparability and to emphasize the double-spike origin of the original value it is marked with the subscript “Norm”.

III.11.2 Sr mass fractionation

$^{87}\text{Sr}/^{86}\text{Sr}^*$ and $^{88}\text{Sr}/^{86}\text{Sr}$ are determined from a double spike measurement following the procedures previously described by (KRABBENHÖFT et al., 2009). The relationship between the traditional radiogenic $^{87}\text{Sr}/^{86}\text{Sr}$ ratio, $^{87}\text{Sr}/^{86}\text{Sr}_{\text{Norm}}$ and $^{87}\text{Sr}/^{86}\text{Sr}^*$ is defined by equation A1:

$$\text{A1: } \frac{\left(\frac{^{87}\text{Sr}}{^{86}\text{Sr}}\right)_{\text{Norm}}}{\left(\frac{^{87}\text{Sr}}{^{86}\text{Sr}}\right)^*} = \left[\frac{\left(\frac{^{88}\text{Sr}}{^{86}\text{Sr}}\right)_{\text{Nier}}}{\left(\frac{^{88}\text{Sr}}{^{86}\text{Sr}}\right)} \right]^{\frac{\ln(m_{87}/m_{86})}{\ln(m_{88}/m_{86})}}$$

The $(^{87}\text{Sr}/^{86}\text{Sr})_{\text{Nier}}$ value has been defined as 8.375209 (Nier, 1938), and corresponds to a $\delta^{88/86}\text{Sr}=0$ relative to NIST SRM 987. The masses of the various Sr isotopes are: $m_{86}=85.909273$, $m_{87}=86.908890$, and $m_{88}=87.905625$. For further details see (Krabbenhöft et al., 2009).

III.11.3 Error notation and propagation

All statistical uncertainties represent 2 standard errors of the mean ($2\sigma_{\text{Mean}}$). We present the statistical uncertainties for $^{87}\text{Sr}/^{86}\text{Sr}$ and $\delta^{88/86}\text{Sr}$ in brackets. The values in the brackets refer to the last digit of the measured values. For example $^{87}\text{Sr}/^{86}\text{Sr}=0.711111(1)$ correspond to 0.711111 ± 0.000001 and $\delta^{88/86}\text{Sr}=0.386(1)$ correspond to $0.386\pm 0.001\%$.

III.11.4 Calculation of flux-weighted mean global river discharge to the ocean

$$\left(\frac{^{87}\text{Sr}}{^{86}\text{Sr}}\right)_{\text{River}} = \frac{\sum^i \left(\frac{^{87}\text{Sr}}{^{86}\text{Sr}}\right)^i \cdot \text{Discharge river } i}{\sum^i (\text{Discharge river } i)}$$

$$\delta^{88/86}\text{Sr}_{\text{River}} = \frac{\sum^i (\delta^{88/86}\text{Sr})^i \cdot \text{Discharge river } i}{\sum^i (\text{Discharge river } i)}$$

III.11.5 Calculation of flux-weighted mean global input to the ocean

$$\left(\frac{^{87}\text{Sr}}{^{86}\text{Sr}}\right)_{\text{Input}} = \frac{\sum^i \left(\frac{^{87}\text{Sr}}{^{86}\text{Sr}}\right)^i \cdot \text{Input } i}{\sum^i (\text{Input } i)}$$

$$\delta^{88/86}\text{Sr}_{\text{River}} = \frac{\sum^i (\delta^{88/86}\text{Sr})^i \cdot \text{Input } i}{\sum^i (\text{Input } i)}$$

III.11.6 Isotope equilibrium

Following the approach of (DE LA ROCHA and DEPAOLO, 2000) the condition of isotope equilibrium with respect to element input and output fluxes to the ocean can be mathematically described for the Sr isotope systems as follows. Note that the equations are given for $\delta^{88/86}\text{Sr}$, but are analogous for $^{87}\text{Sr}/^{86}\text{Sr}^*$:

$$6.1: N_{\text{Sr}} \cdot \frac{\partial \delta^{88/86}\text{Sr}_{\text{Seawater}}}{\partial t} = J_{\text{Input}} \cdot (\delta^{88/86}\text{Sr}_{\text{Input}} - \delta^{88/86}\text{Sr}_{\text{Seawater}}) - J_{\text{Output}} \cdot \Delta_{\text{Output}}$$

In a steady-state ocean where Sr input and output fluxes are equal ($J_{\text{input}}=J_{\text{output}}$) both the Sr isotope composition of seawater and the amount of Sr present in seawater are invariant ($d[\text{Sr}]_{\text{Seawater}}/dt=d(\delta^{88/86}\text{Sr}(t))/dt=0$). Equations A2 and A3 are reduced to A4:

$$6.2: \Delta_{\text{Output}} = \delta^{88/86}\text{Sr}_{\text{Carbonates}} - \delta^{88/86}\text{Sr}_{\text{Seawater}}$$

III.12 References

- Amini, M., Eisenhauer, A., Böhm, F., Fietzke, J., Bach, W., Garbe-Schönberg, D., Rosner, M., Bock, B., Lackschewitz, K. S., and Hauff, F., 2008. Calcium isotope ($\delta^{44/40}\text{Ca}$) fractionation along hydrothermal pathways, Logatchev Field (Mid-Atlantic Ridge, 14° 45'N). *Geochimica et Cosmochimica Acta* **72**, 4107-4122.
- Andersson, P. S., Wasserburg, G. J., and Ingri, J., 1992. The sources and transport of Sr and Nd isotopes in the Baltic Sea. *Earth and Planetary Science Letters* **113**, 459-472.
- Basu, A. R., Jacobsen, S. B., Poreda, R. J., Dowling, C. B., and Aggarwal, P. K., 2001. Large groundwater strontium flux to the oceans from the Bengal Basin and the marine strontium isotope record. *Science* **293**, 1470-1473.
- Blum, J. D., 1995. A silicate weathering mechanism linking increases in marine $^{87}\text{Sr}/^{86}\text{Sr}$ with global glaciation. *Letters to Nature* **373**, 415-417.
- Broecker, W. and Clark, E., 2009. Ratio of coccolith CaCO_3 to foraminifera CaCO_3 in late Holocene deep sea sediments. *Paleoceanography* **24**, doi:10.1029/2009PA001731.
- Cohen, A. L. and Thorrold, S. R., 2007. Recovery of temperature records from slow-growing corals by fine scale sampling of skeletons. *Geophysical Research Letters* **34**, L17706, doi: 10.1029/2007gl030967.
- Davis, A. C., Bickle, M. J., and Teagle, D. A. H., 2003. Imbalance in the oceanic strontium budget. *Earth and Planetary Science Letters* **211**, 173-187.
- De La Rocha, C. L. and DePaolo, D. J., 2000. Isotopic evidence for variations in the marine calcium cycle over the Cenozoic. *Science* **289**, 1176-1178.
- Delaney, M. L., Linn, L. J., and Davies, P. J., 1996. Trace and minor element ratios in Halimeda aragonite from the Great Barrier Reef. *Coral Reefs* **15**, 181-189.
- Elderfield, H. and Gieskes, J. M., 1982. Sr isotopes in interstitial waters of marine sediments from deep-sea drilling project cores. *Nature* **300**, 493-497.
- Farkaš, J., Buhl, D., Blenkinsop, J., and Veizer, J., 2007. Evolution of the oceanic calcium cycle during the late Mesozoic: Evidence from $\delta^{44/40}\text{Ca}$ of marine skeletal carbonates. *Earth and Planetary Science Letters* **253**, 96-111.
- Fietzke, J. and Eisenhauer, A., 2006. Determination of temperature-dependent stable strontium isotope ($^{88}\text{Sr}/^{86}\text{Sr}$) fractionation via bracketing standard MC-ICP-MS. *Geochemistry Geophysics Geosystems* **7**, Q08009, doi:10.1029/2006GC001243.
- Gaillardet, J., Dupre, B., and Allègre, C. J., 1999. Geochemistry of large river suspended sediments: Silicate weathering or recycling tracer? *Geochimica et Cosmochimica Acta* **63**, 4037-4051.
- Gallup, C. D., Olson, D. M., Edwards, R. L., Gruhn, L. M., Winter, A., and Taylor, F. W., 2006. Sr/Ca-sea surface temperature calibration in the branching caribbean coral *Acropora Palmata*. *Geophysical Research Letters* **33**, L03606, doi:10.1029/2005GL024935.
- Godderis, Y. and Veizer, J., 2000. Tectonic control of chemical and isotopic composition of ancient oceans: The impact of continental growth. *Am. J. Sci.* **300**, 434-461.
- Goldstein, S. J. and Jacobsen, S. B., 1987. The Nd and Sr isotopic systematics of river-water dissolved material: Implications for the sources of Nd and Sr in seawater. *Chemical Geology: Isotope Geoscience section* **66**, 245-272.
- Graham, S. T., Famiglietti, J. S., and Maidment, D. R., 1999. Five-minute, 1/2 degrees, and 1 degrees data sets of continental watersheds and river networks for use in regional and global hydrologic and climate system modeling studies. *Water Resources Research* **35**, 583-587.
- Haase, K. M., Petersen, S., Koschinsky, A., Seifert, R., Devey, C. W., Keir, R., Lackschewitz, K. S., Melchert, B., Perner, M., Schmale, O., Suling, J., Dubilier, N., Zielinski, F., Fretzdorff, S., Garbe-Schönberg, D., Westernstroer, U., German, C. R., Shank, T. M., Yoerger, D., Giere, O., Kuever, J., Marbler, H., Mawick, J., Mertens, C., Stober, U., Ostertag-Henning, C., Paulick, H., Peters, M., Strauss, H., Sander, S., Stecher, J., Warmuth, M., and Weber, S., 2007. Young volcanism and related hydrothermal activity at 5 degrees S on the slow-spreading southern Mid-Atlantic Ridge. *Geochemistry Geophysics Geosystems* **8**, 17, doi:10.1029/2006GC001509

- Halicz, L., Segal, I., Fruchter, N., Stein, M., and Lazar, B., 2008. Strontium stable isotopes fractionate in the soil environments? *Earth and Planetary Science Letters* **272**, 406-411.
- Hubbard, D. K., Miller, A. I., and Scaturro, D., 1990. Production and cycling of calcium-carbonate in a shelf-edge reef system (St. Croix, United-States Virgin-Islands) - Applications to the nature of reef systems in the fossil record. *Journal of Sedimentary Petrology* **60**, 335-360.
- Kisakürek, B., Eisenhauer, A., Böhm, F., Garbe-Schönberg, D., and Erez, J., 2008. Controls on shell Mg/Ca and Sr/Ca in cultured planktonic foraminifera. *Earth Planet. Sci. Lett* **273**, 260-269.
- Krabbenhöft, A., Fietzke, J., Eisenhauer, A., Liebetrau, V., Böhm, F., and Vollstaedt, H., 2009. Determination of radiogenic and stable strontium isotope ratios ($^{87}\text{Sr}/^{86}\text{Sr}/\delta^{88/86}\text{Sr}$) by thermal ionization mass spectrometry applying an $^{87}\text{Sr}/^{84}\text{Sr}$ double spike. *Journal of Analytical Atomic Spectrometry* **24**, 1267-1271.
- Liebetrau, V., Eisenhauer, A., Krabbenhöft, A., Fietzke, J., Böhm, F., Rüggeberg, A., and Guers, K., 2009. New perspectives on the marine Sr-isotope record: $\delta^{88/86}\text{Sr}$, $^{87}\text{Sr}/^{86}\text{Sr}^*$ and $\delta^{44/40}\text{Ca}$ signatures of aragonitic molluscs throughout the last 27 Ma. *Geochimica et Cosmochimica Acta* **73**, A762.
- Lindberg, B. and Mienert, J., 2005. Postglacial carbonate production by cold-water corals on the Norwegian shelf and their role in the global carbonate budget. *Geology* **33**, 537-540.
- McArthur, J. M., 1994. Recent trends in strontium isotope stratigraphy. *Terr. Nova* **6**, 331-358.
- McArthur, J. M., Howarth, R. J., and Bailey, T. R., 2001. Strontium isotope stratigraphy: LOWESS Version 3: Best fit to the marine Sr-isotope curve for 0-509 Ma and accompanying look-up table for deriving numerical age. *Journal of Geology* **109**, 155-170.
- Milliman, J. D. and Droxler, A. W., 1996. Neritic and pelagic carbonate sedimentation in the marine environment: Ignorance is not bliss. *Geol. Rundsch.* **85**, 496-504.
- Nier, A. O., 1938. The isotopic constitution of strontium, barium, bismuth, thallium and mercury. *Physical Review* **5**, 275-279.
- Ohno, T., Komiya, T., Ueno, Y., Hirata, T., and Maruyama, S., 2008. Determination of $^{88}\text{Sr}/^{86}\text{Sr}$ mass-dependent isotopic and radiogenic isotope variation of $^{87}\text{Sr}/^{86}\text{Sr}$ in the Neoproterozoic Doushantuo Formation. *Gondwana Res.* **14**, 126-133.
- Palmer, M. R. and Edmond, J. M., 1989. The Strontium Isotope Budget of the Modern Ocean. *Earth Planet. Sci. Lett.* **92**, 11-26.
- Palmer, M. R. and Edmond, J. M., 1992. Controls over the strontium isotope composition of river water. *Geochimica et Cosmochimica Acta* **56**, 2099-2111.
- Peucker-Ehrenbrink, B. and Miller, M. W., 2004. River Chemistry and Drainage Basin Geology. *Geochim. Cosmochim. Acta* **68**, A426-A426.
- Peucker-Ehrenbrink, B., Miller, M. W., Arsouze, T., and Jeandel, C., 2010. Continental bedrock and riverine fluxes of strontium and neodymium isotopes to the oceans. *Geochemistry Geophysics Geosystems* **11**.
- Rüggeberg, A., Fietzke, J., Liebetrau, V., Eisenhauer, A., Dullo, W. C., and Freiwald, A., 2008. Stable strontium isotopes ($\delta^{88/86}\text{Sr}$) in cold-water corals - A new proxy for reconstruction of intermediate ocean water temperatures. *Earth and Planetary Science Letters* **269**, 569-574.
- Schiebel, R., 2002. Planktic Foraminiferal sedimentation and the marine calcite budget. *Glob. Biogeochem. Cycle* **16**, 21.
- Stanley, S. M. and Hardie, L. A., 1998. Secular oscillations in the carbonate mineralogy of reef-building and sediment-producing organisms driven by tectonically forced shifts in seawater chemistry. *Palaeogeography Palaeoclimatology Palaeoecology* **144**, 3-19.
- Stoll, H. M. and Schrag, D. P., 1998. Effects of Quaternary sea level cycles on strontium in seawater. *Geochimica et Cosmochimica Acta* **62**, 1107-1118.
- Stoll, H. M. and Schrag, D. P., 2000. Coccolith Sr/Ca as a new indicator of coccolithophorid calcification and growth rate. *Geochem. Geophys. Geosys.* **1**, 1999GC000015.
- Stoll, H. M., Schrag, D. P., and Clemens, S. C., 1999. Are seawater Sr/Ca variations preserved in quaternary foraminifera? *Geochimica et Cosmochimica Acta* **63**, 3535-3547.
- Sun, Y., Sun, M., Lee, T., and Nie, B., 2005. Influence of seawater Sr content on coral Sr/Ca and Sr thermometry. *Coral Reefs* **24**, 23-29.

- Vance, D., Teagle, D. A. H., and Foster, G. L., 2009. Variable quaternary chemical weathering fluxes and imbalances in marine geochemical budgets. *Nature* **458**, 493-496.
- Veizer, J., 1989. Strontium isotopes in seawater through time. *Annu. Rev. Earth Planet. Sci.* **17**, 141-167.

Chapter IV

MANUSCRIPT III

IV. Strontium Isotope ($\delta^{88/86}\text{Sr}$) Fractionation in Scleractinian Warm Water Corals

A. Krabbenhöft*, A. Eisenhauer*[†], J. Raddatz*, H. Vollstaedt*, V. Liebetrau*, J. Fietzke*, F. Böhm*, T. Felis[&], S. Reynaud[#]

*Leibniz-Institut für Meereswissenschaften, IFM-GEOMAR, Wischhofstr. 1-3, 24148 Kiel, Germany

[#]Centre Scientifique de Monaco, Avenue Saint Martin, 98000, Principality of Monaco

[&]MARUM—Center for Marine Environmental Sciences, University of Bremen, GEO Building, Klagenfurter Str., 28359 Bremen, Germany

[†]Corresponding Author: A. Eisenhauer

IV.1 Abstract

We measured $\delta^{88/86}\text{Sr}$ -, $\delta^{18}\text{O}$ - and Sr/Ca-ratios of a fossil (15 kyr B.P.) *Porites* sp. coral originating from Tahiti (French Polynesia). The elemental as well as the isotopic ratios of the coral show a corresponding seasonal variability. The average $\delta^{88/86}\text{Sr}$ of the fossil *Porites* sp. coral shows a similar isotopic composition ($\delta^{88/86}\text{Sr}_{\text{mean}}=0.205\pm 0.017\text{‰}$) like modern *Porites* sp. represented in this study by the coral standard JCp-1 ($\delta^{88/86}\text{Sr}_{\text{JCp-1}}=0.194\pm 0.009\text{‰}$). In contrast to Sr/Ca elemental ratios the average $\delta^{88/86}\text{Sr}$ is obviously not affected by glacial/interglacial variations of the Sr fluxes from exposed shelves during glacial times. Therefore stable Sr can serve as independent and unbiased parameter for reconstructing paleo-sea-surface-temperatures. Furthermore, the $\delta^{88/86}\text{Sr}$ ratios of *Acropora* sp. samples cultured under controlled temperature conditions were measured and compared with Sr/Ca data published by (REYNAUD et al., 2007). These measurements revealed a nonlinear relationship between temperature and $\delta^{88/86}\text{Sr}$ possibly reflecting processes involved in biomineralization.

IV.2 Introduction

In the last decades significant efforts have been made to identify robust proxies and archives for sea surface temperature (SST). Scleractinian warm water corals, in particular *Porites* spp., incorporate an array of geochemical tracers (e.g. Sr/Ca, Ba/Ca, $\delta^{18}\text{O}$, $\delta^{88/86}\text{Sr}$) recording changes in seawater chemistry and provide information about environmental conditions like SST of the past. Elemental ratios with known temperature dependency are B/Ca (FALLON et al., 1999; SINCLAIR et al., 2006), Mg/Ca (MITSUGUCHI et al., 1996), U/Ca and Sr/Ca (BECK et al., 1992; SMITH et al., 1979). The latter is one of the most promising temperature proxies in corals although it is influenced by several other environmental parameters superimposing the pure temperature signal. Often the measured trace element ratio is different from the thermodynamically expected value which is ascribed to the so called “vital effects” and may be distinctly different between species (WEBER and WOODHEAD, 1972).

Ideally, the Sr/Ca ratio in corals is believed to be controlled predominantly by two factors: (1) the Sr/Ca ratio of ambient seawater and (2) the Sr/Ca temperature dependency of the distribution coefficient between aragonite and seawater (BECK et al., 1992; SMITH et al., 1979). Not only elemental ratios can serve as proxies but also certain isotope ratios measured in the coral skeletons provide information about environmental conditions of the past and coral physiology. In this regard $\delta^{18}\text{O}$ was the first isotope ratio used for SST reconstruction on corals (WEBER and WOODHEAD, 1972). More recent non-traditional stable isotope analysis on scleractinian corals like $\delta^{44/40}\text{Ca}$ were performed by (BÖHM et al., 2006) in order to get insights in the mechanisms driving biological mediated calcification. Furthermore, (FIETZKE and EISENHAUER, 2006; RÜGGERBERG et al., 2008) introduced $\delta^{88/86}\text{Sr}$ as potential paleo-temperature proxie. Latter new non-traditional isotope system may provide additional and independent constraints on past temperature variations and perhaps on coral physiology.

In this regard we focus on the temperature sensitivity of stable Sr isotope fractionation in scleractinian corals during biologically mediated precipitation of calcium carbonate from seawater.

IV.3 Materials

IV.3.1 Cultured warm water coral (*Acropora* sp.)

A single colony of the branching zooxanthellate scleractinian coral, *Acropora* sp. Originating from the Gulf of Aquaba was cultured in the aquarium of the “Centre Scientifique de Monaco, Monaco” (REYNAUD-VAGANAY et al., 1999). “Nubbins” defined as small living coral samples were obtained by cutting terminal portions of branches from the single parent colony and were then glued on glass slides. This technique, first described by (REYNAUD-VAGANAY et al., 1999), offers several advantages like small sample sizes (~1 cm) which makes their manipulation easier and a large number of replicates are available. Experiments can be of relatively short duration due to the rapid horizontal growth on the glass slide. Linear growth varied between 0.04 and 0.13 mm/d and was highest at 27°C (REYNAUD-VAGANAY et al., 1999). Individuals growing at same temperature show no deviation in their linear growth rate. The coral nubbins were distributed in 5 tanks (30 L) heated to 21, 23, 25, 27 and 29 °C and fed once a week with *Artemia salina nauplii* during the course of the experiment. The water temperature of the initial cultured colony was 25°C. From each of the five different temperature experiments two samples were selected for Sr isotope analysis. The tanks were continuously supplied with Mediterranean seawater (salinity=38.5), heated using a temperature controller (EW, PC 902/T) and continuously mixed with a Rena-pump (6 lmin⁻¹). The renewal rate was approximately five times per day. With that, the corals used less than 1% of the Sr in the tanks for calcification. The alteration of the Sr isotopic composition of the solution in the tanks by calcification

can therefore be considered to be negligible. Light was provided by metal halide lamps (Phillips HPIT, 400 W) on a 12:12 h photoperiod, and kept constant ($400 \text{ mol } \gamma/\text{m}^2\cdot\text{s}$) during the course of the experiment. Temperature (accuracy: $\pm 0.05 \text{ }^\circ\text{C}$) was logged at 10 min intervals using a Seamon temperature recorder. Salinity and irradiance were measured using a conductivity meter (Meter LF196), and a 4p quantum sensor (Li-Cor, LI-193SA), respectively. The whole culturing experiment is described in detail in (REYNAUD-VAGANAY et al., 1999).

IV.3.2 Fossil warm water coral (*Porites* sp.)

Annually-banded corals of the genus *Porites* sp. growing in the warm surface waters of the tropical to subtropical Indo-Pacific provide a sub-seasonally resolved archive of past environmental variability (ABRAM et al., 2008; COBB et al., 2003; COLE et al., 1993b; FELIS et al., 2004; FELIS et al., 2009). These warm water corals do not grow in regions where SST during the winter season is significantly below the lower limit of $18 \text{ }^\circ\text{C}$ for coral reef development (WELLS, 1957).

The fossil *Porites* sp. coral examined in this study was recovered off the coast of the island of Tahiti (French Polynesia) in the central tropical South Pacific in the frame of the Integrated Ocean Drilling Program (IODP) Expedition 310 at a depth of 113 m below present sea level (Hole M0024A; $149^\circ 24.2358' \text{ W}$, $17^\circ 29.2918' \text{ S}$, see fig.IV.1), using the mission-specific platform “DP Hunter” (CAMOIN et al., 2005). This massive *Porites* coral (310-M0024A-11R-2W 1-62) is discussed in detail in (FELIS et al., 2010). Briefly, radiography revealed skeletal density banding and a continuous upward growth corresponding to a growth rate of $\sim 2.0 \text{ cm/a}$. Thorough screening for diagenesis indicated that the aragonitic coral skeleton was well-preserved. Uranium-thorium-series dating indicated an age of the coral of about 15 kyr B.P. (FELIS et al., 2010). The monthly resolved records of Sr/Ca and $\delta^{18}\text{O}$ generated from the coral show more than 20 clear annual cycles. For our study one representative annual cycle was selected for $\delta^{88/86}\text{Sr}$ analyses. We took a $\sim 1 \text{ mg}$ split of the sample powder that was used for Sr/Ca and $\delta^{18}\text{O}$ analyses as described in (FELIS et al., 2010). The powder was sampled with sub-monthly resolution resulting in 27 CaCO_3 samples covering a time interval of one year around 15 kyr B.P..

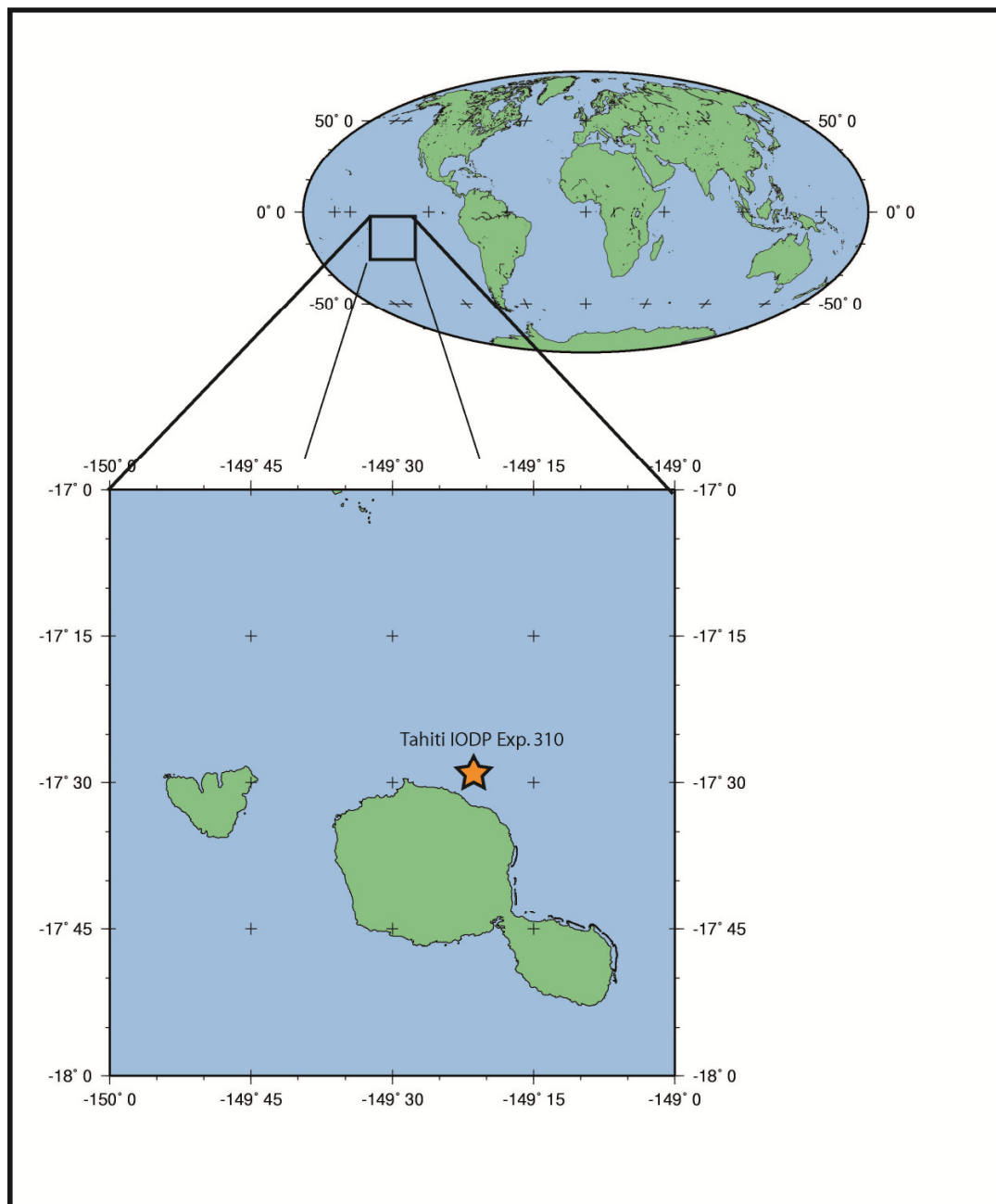


fig.IV.1: Sampling location of fossil warm-water coral *Porites* sp. investigated in this study.

IV.4 Methods

IV.4.1 Sampling, chemical preparation and measurements

Twenty-seven *Porites* sp. coral samples, covering one year of growth (15 kyr B.P.), were obtained by continuous spot-sampling using a 0.7 mm diameter drill bit following well established methods (FELIS et al., 2004; FELIS et al., 2009). *Acropora* sp. samples were not drilled but just broken into small pieces for further processing.

IV.4.2 Stable strontium ($\delta^{88/86}\text{Sr}$) measurements

Chemical sample preparation for $\delta^{88/86}\text{Sr}$ measurements follows earlier published protocols (e.g. KRABBENHÖFT et al., 2009) and is not repeated here. The major difference between earlier $\delta^{88/86}\text{Sr}$ measurements (FIETZKE and EISENHAUER, 2006; RÜGGERBERG et al., 2008) applying the standard-bracketing technique using MC-ICP-MS is that we applied the more precise and accurate Sr double spike technique on a TIMS rather on a MC-ICP-MS as in earlier attempts (FIETZKE and EISENHAUER, 2006; RÜGGERBERG et al., 2008).

IV.4.3 Sr/Ca and $\delta^{18}\text{O}$ measurements

Measurements of Sr/Ca in *Acropora* sp. were carried out by (REYNAUD et al., 2007) and are described in detail therein. Sr/Ca and $\delta^{18}\text{O}$ analyses are described in detail in (FELIS et al., 2010).

IV.5 Results

The results of all Sr isotope measurements are tab.IV.1 and tab.IV.2. All errors are given as 2 standard error of the mean (2SEM) for repeated analyses of the same sample. The long term variability in the $\delta^{88/86}\text{Sr}$ of the JcP-1 carbonate standard is 0.025‰ (2SEM) with an external reproducibility of $\pm 0.025\%$ (2SD).

IV.5.1 Temperature- $\delta^{88/86}\text{Sr}$ relationships of *Acropora* sp.

In order to verify the individual variability in *Acropora* sp. we sub-sampled parts of the coral as shown schematically in fig.IV.2. We focused on analysis of the middle part and the calyx, respectively.

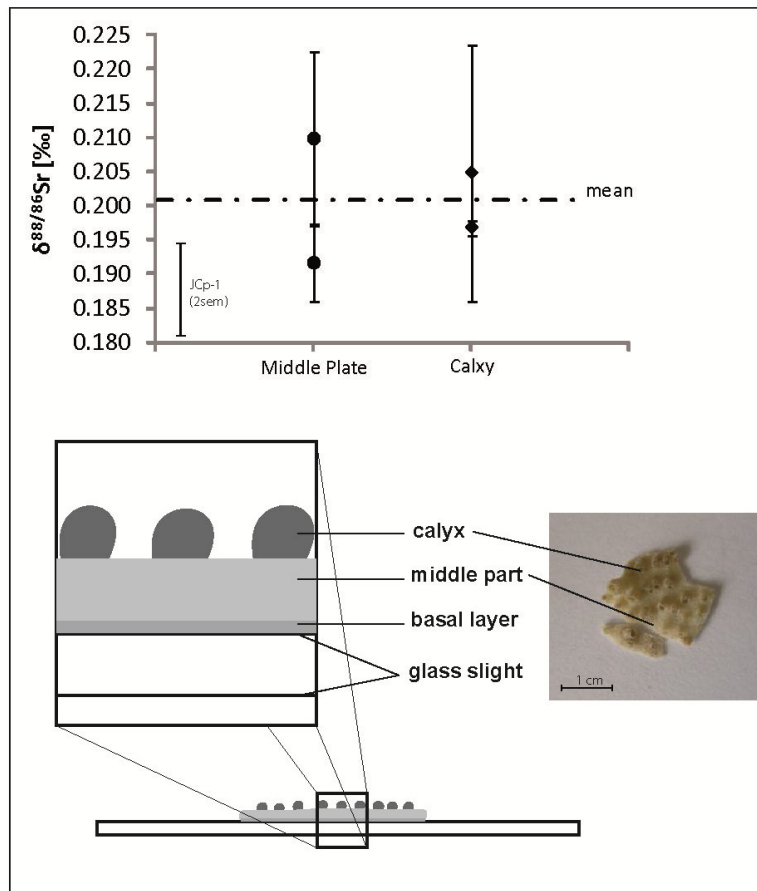


fig.IV.2: Sketch of cultured *Acropora* sp. coral. For the intra-individual heterogeneity test we analyzed the middle part and the calyx separately. *Acropora* sp. shows no evidence for a heterogeneous $\delta^{88/86}\text{Sr}$ distribution in different parts of the coral skeleton.

The whole heterogeneity test procedure was conducted twice on raw substrate aliquots of one individual; by two completely independent lab runs including sub-sampling, cleaning, column chemistry, TIMS measurement and data reduction. The mean value of the stable Sr isotopic composition for the middle part is $\delta^{88/86}\text{Sr}=0.201(13)\text{‰}$. The analysis of the calyx result in similar values $\delta^{88/86}\text{Sr}=0.201(6)\text{‰}$, indicating that the $\delta^{88/86}\text{Sr}$ signal is not varying within a single sample of *Acropora* sp.. The stable Sr isotopic composition of temperature controlled (21, 23, 25, 27 and 29°C) cultured warm water coral *Acropora* sp. (REYNAUD et al., 2004) were analyzed. Except for the 27°C sample we determined the $\delta^{88/86}\text{Sr}$ of all samples twice (in separate sessions) with at least four separate analyses in each run.

The results of the first measurement session were well reproduced in the second run of the samples. We found a mean Sr isotopic composition of $\delta^{88/86}\text{Sr}=0.207(3)\text{‰}$ at a growth temperature of 21°C.

Increasing the water temperature to 25°C results in an increasing fractionation and an isotopic composition of $\delta^{88/86}\text{Sr}=0.186(8)\text{‰}$. A further temperature increase to 29°C results in an isotopic composition of $\delta^{88/86}\text{Sr}=0.200(7)\text{‰}$ which corresponds to the isotope ratio of aragonite *Acropora* sp. precipitated at 21°C. The observed Temperature- $\delta^{88/86}\text{Sr}$ relationship is not compatible to the earlier observations of (FIETZKE and EISENHAUER, 2006) who presented a positive relationship between temperature and $\delta^{88/86}\text{Sr}$.

In contrast our data represent an inverse correlation between temperature and $\delta^{88/86}\text{Sr}$ for the temperature range between 21 and 25°C ($\delta^{88/86}\text{Sr}[\text{‰}]=-0.01\cdot T[\text{°C}]+0.32$), fig.IV.3) or even a non-linear relationship ($\delta^{88/86}\text{Sr}[\text{‰}]=-0.001\cdot(T[\text{°C}])^2-0.040\cdot T[\text{°C}]+0.7$).32) for the entire temperature range investigated. In contrast Sr/Ca ratios of the same coral (REYNAUD et al., 2007) show an inverse but expected dependency on temperature (fig.IV.3, $\delta^{88/86}\text{Sr}[\text{‰}]=-0.047\cdot T[\text{°C}]+10.49$).

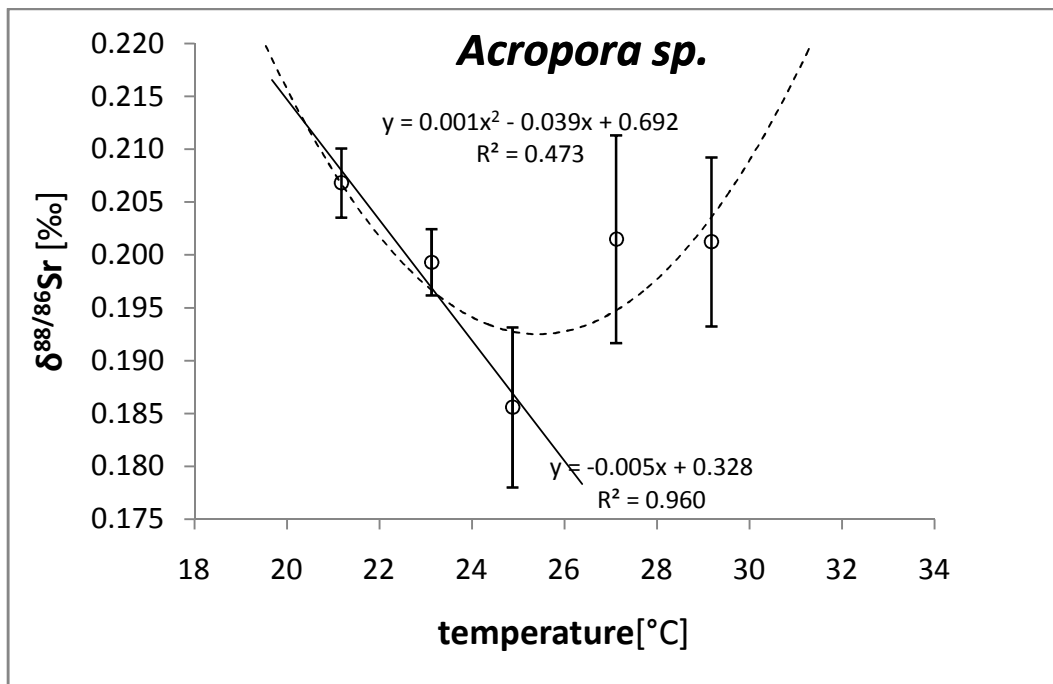


fig.IV.3: Stable Sr (open circles) of *Acropora* sp. plotted against water temperature. Error bars represent 2SEM of measurements of different samples growing at the same temperature. Stable Sr $\delta^{88/86}\text{Sr}$ shows an inverse correlation with temperature in the range between 21 and 25°C ($\delta^{88/86}\text{Sr}[\text{‰}]=-0.01\cdot T[\text{°C}]+0.32$).

IV.5.2 Temperature- $\delta^{88/86}\text{Sr}$ relationships of a fossil *Porites* sp. (Tahiti)

In fig.IV.4 the $\delta^{88/86}\text{Sr}$ values of 27 samples corresponding to one year and a monthly resolution of a fossil Tahiti coral *Porites* sp. are displayed. The Sr isotope composition varies between $\delta^{88/86}\text{Sr}=0.171(17)\text{‰}$ and $\delta^{88/86}\text{Sr}=0.240(22)\text{‰}$. The data show a clear seasonal periodicity throughout the entire record.

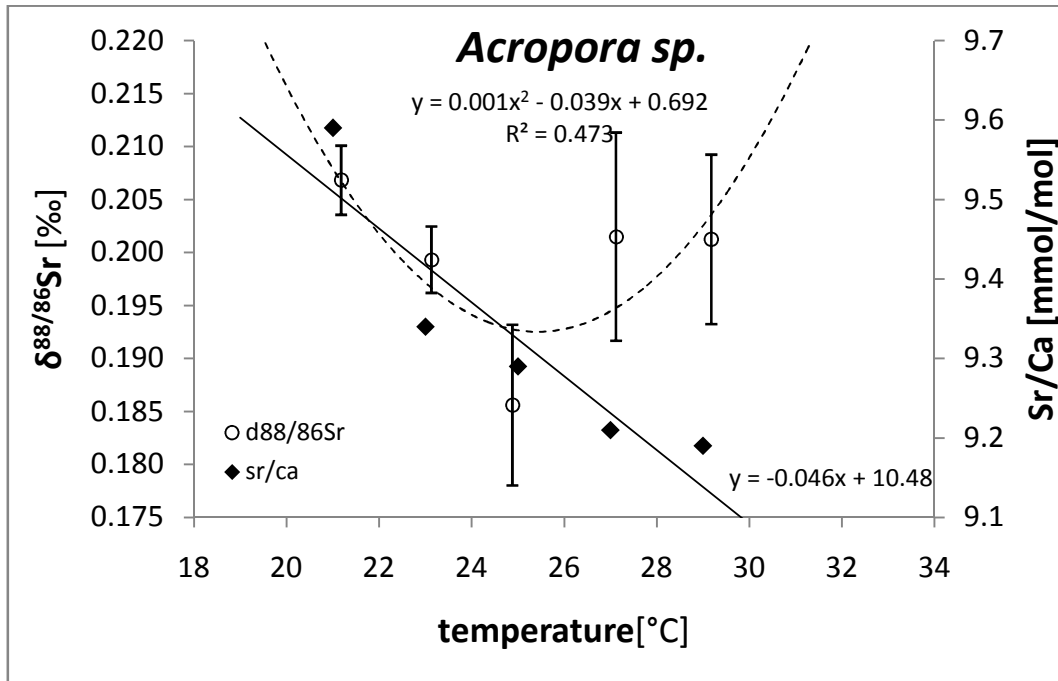


fig.IV.4: Stable Sr (open circles) and Sr/Ca values (diamonds) of *Acropora* sp. plotted against water temperature. Error bars represent 2SEM of measurements of different samples growing at the same temperature. Stable Sr values show an optimum behavior whereas Sr/Ca continuously decreases with increasing temperature.

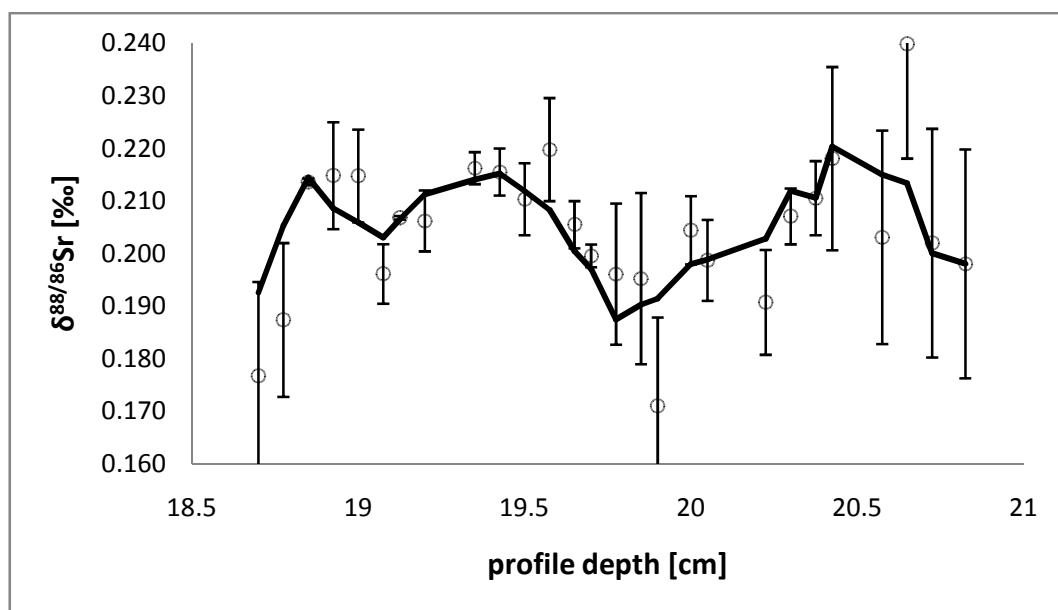


fig.IV.5: Stable Sr data of *Porites* sp. samples from Tahiti. Black circles represent the measured $\delta^{88/86}\text{Sr}$ values of *Porites* sp. samples. The 3-point running mean of our data is represented by the solid black line.

In fig.IV.5 the three point running mean of the $\delta^{88/86}\text{Sr}$ -record is shown together with the corresponding Sr/Ca and $\delta^{18}\text{O}$ record. All three records show a clear periodicity with two relative maxima and one minimum. Although absolute temperatures cannot be retrieved from the Sr/Ca- and $\delta^{18}\text{O}$ -record it is well known that relatively low values in the Sr/Ca and $\delta^{18}\text{O}$ record indicate warmer precipitation temperatures whereas relative higher values indicate lower temperatures. In this regard the Sr/Ca and $\delta^{18}\text{O}$ record provide consistent results indicating that the data minima in the core section between 19 and 20 cm correspond to warmer water temperatures whereas the two data maxima in between 18 to 19 and around 20.5 cm reflect cooler water conditions.

In contrast, based on the observations of (FIETZKE and EISENHAUER, 2006) the $\delta^{88/86}\text{Sr}$ -data minima then correspond to relative cooler water temperatures when compared to the data maxima then reflecting warmer precipitation conditions. However, the application of the (FIETZKE and EISENHAUER, 2006) temperature- $\delta^{88/86}\text{Sr}$ calibration is then in contradiction to the findings from the Sr/Ca- and $\delta^{18}\text{O}$ records. The three records can only be reconciled assuming that the temperature- $\delta^{88/86}\text{Sr}$ relationship for *Porites* is inversely rather than positively correlated to temperature like in *Pavona clavus*. Latter inference indicates a strong species dependency of the temperature- $\delta^{88/86}\text{Sr}$ relationship and will be discussed in more detail in the section below.

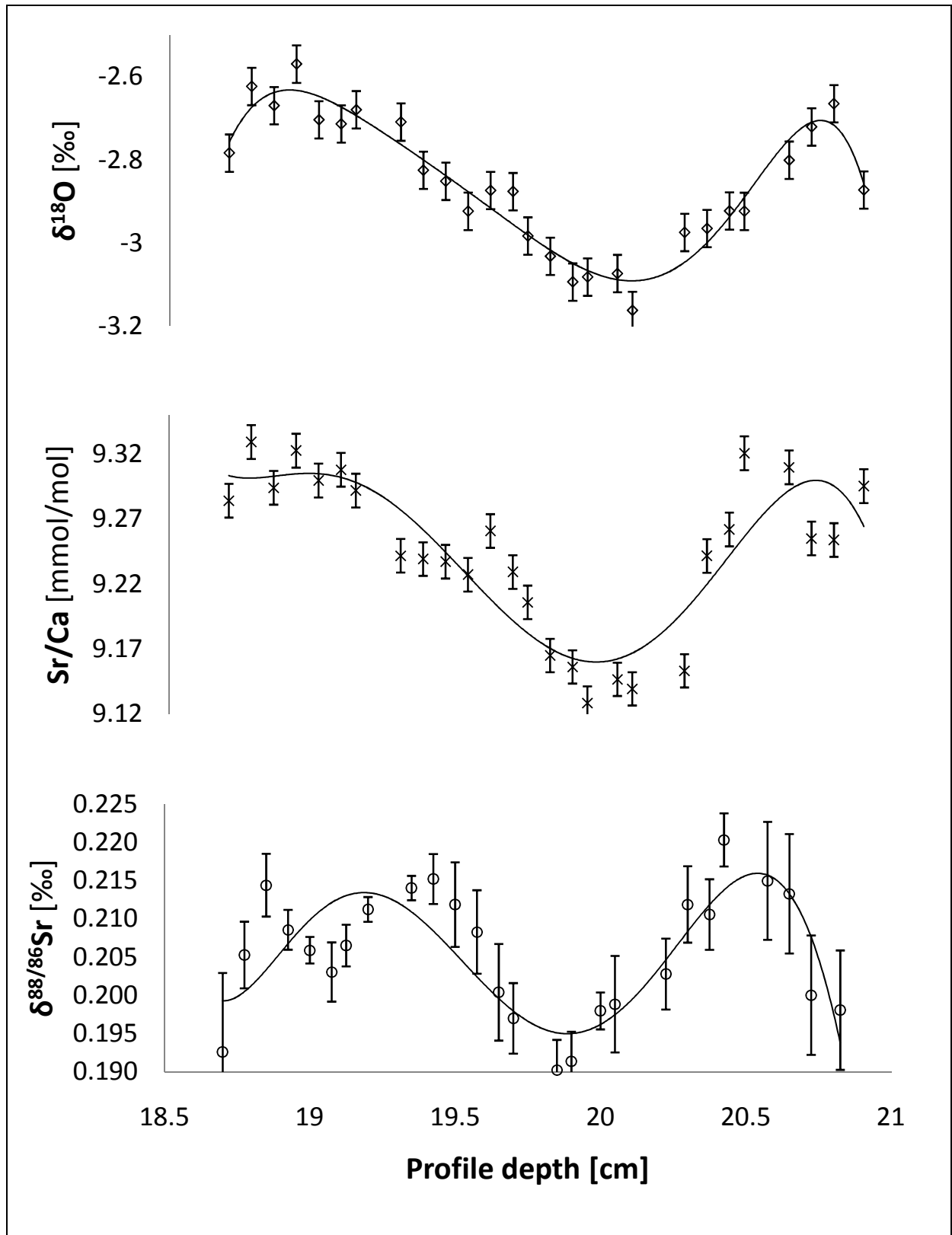


fig.IV.6: Comparison between downcore Sr/Ca (FELIS et al., 2010) elemental ratios, $\delta^{18}\text{O}$ (FELIS et al., 2010) and $\delta^{88/86}\text{Sr}$ values of *Porites* sp. samples from Tahiti. The element ratio as well as the isotopic values show the same pattern. Stable Sr data represent a three point running mean of the original dataset and are fitted by a polynom (black line). Relative standard deviation of the Sr/Ca determinations (*Porites* sp.) was better than 0.2%, which is equivalent to 0.036 mmol/mol (2SD) (FELIS et al., 2010). The analytical error for $\delta^{18}\text{O}$ measurements was better than $\pm 0.14\%$ (2SD) (FELIS et al., 2010).

IV.6 Discussion

IV.6.1 Temperature dependence of $\delta^{88/86}\text{Sr}$ in *Acropora* sp.

We measured the $\delta^{88/86}\text{Sr}$ of five temperature controlled cultured *Acropora* sp. which cover a range of 8°C from 21°C to 29°C (fig.IV.3). The $\delta^{88/86}\text{Sr}$ signal drops in the temperature range from 21 to 25°C (-0.005‰/°C, $r^2=0.92$). Between 25°C and 29°C we observe an increasing $\delta^{88/86}\text{Sr}$ with a slope of 0.003‰/°C ($r^2=0.53$). Compared to the findings of (FIETZKE and EISENHAUER, 2006) we found a much shallower slope in the temperature range they investigated on the warm water species *Pavona Clavus*. Additionally, our data show an inverse correlation between temperature and $\delta^{88/86}\text{Sr}$. Taking the entire temperature range from 21 to 29°C investigated on *Acropora* sp. into account a parabolic function represents the best fit for our actual data set ($\delta^{88/86}\text{Sr}=0.001 \cdot T^2 -0.056 T+0.895$, $r^2=0.81$) showing a minimum at approximately ~25°C.

For *Acropora* sp. the $\delta^{88/86}\text{Sr}$ minimum (fig.IV.3) could be somehow linked to the culturing temperature of the parent colony which was reported to be also ~25°C (REYNAUD et al., 2004). Moreover the mean water temperature of the habitat *Acropora* sp. was sampled from (Gulf of Aqaba) has a mean annual temperature of 25°C. Perhaps the coral physiology is somehow adapted to this environmental condition and the coral is sensible to abrupt temperature variations reflected by changes in the isotopic composition of the coral skeleton. This was also observed by (MARSHALL and CLODE, 2004) who investigated the temperature dependency of calcification rates of *Dendrophyllia* sp. and *Galaxea fascicularis*. They highlighted a similar temperature dependence of zooxanthellate and azooxanthellate corals and suggested that temperature affects some fundamental processes of biological calcification.

Furthermore their data show a maximum calcification rate at 25°C which corresponds to the temperature where we observe maximal Sr isotope fractionation (fig.IV.3). This apparent coincidence implies that calcification rate may be another factor driving $\delta^{88/86}\text{Sr}$ in scleractinian corals.

IV.6.2 Tahiti record IODP Expedition 310 (fossil *Porites* sp.)

The stable Sr data derived from fossil *Porites* sp. covering a period of one year ~15 kyr BP show a clear seasonal periodicity throughout the entire record (fig.IV.4). This periodicity has also been observed by (FELIS et al., 2010) who investigated Sr/Ca elemental ratios and $\delta^{18}\text{O}$ on the same samples. The $\delta^{88/86}\text{Sr}$ shows a significant correlation with Sr/Ca values ($r^2=0.51$, $p=0.00003$) and a weaker but still significant correlation with $\delta^{18}\text{O}$ ($r^2=0.19$, $p=0.024$). The Sr/Ca elemental ratio as well as the isotopic ratio $\delta^{18}\text{O}$ are known to be temperate dependent although their use as temperature proxies is limited due to other environmental parameters superimposing the original signals. Beside temperature, $\delta^{18}\text{O}$ depends on global ice-volume and salinity. Whereas Sr/Ca of coral skeletons is

biased by secondary effects like growth rate, photosynthetic activity of symbionts, the influence of secondary aragonite and other effects. Temperatures reconstructed on the basis of Sr/Ca measurements ($T_{\text{Sr/Ca}}$) on fossil tropical corals suggest a significant cooling of 5°C to 6°C prior 10 kyr B.P. (McCULLOCH et al., 1999).

These estimates are significantly larger compared to temperatures derived from foraminiferal Mg/Ca showing a temperature drop 2°C to 3°C (LEA et al., 2000). This discrepancy can be reconciled by an additional Sr flux originating from exposed shelves during glacial sea level drops (KRABBENHÖFT et al., 2010; STOLL and SCHRAG, 1998). Such an extra supply of Sr to the sea as discussed in detail by (STOLL AND SCHRAG, 1998) accounts for an elevation of $(\text{Sr/Ca})_{\text{seawater}}$ by about 1 to 2%. Other authors suggest even higher changes in seawater Sr/Ca of about 3% (SHEN et al., 2001). According to (KRABBENHÖFT et al., 2010) the Sr isotopic composition of input and output and their fluxes during glacials is similar within uncertainty. Hence, seawater $\delta^{88/86}\text{Sr}$ is not supposed to change during this time periods whereas the Sr input flux is elevated by a factor of 3 (STOLL and SCHRAG, 1998) resulting in an elevation of Sr/Ca seawater by 1-2%. Stable Sr measurements of this study show a similar mean $\delta^{88/86}\text{Sr}$ value of fossil *Porites* sp. (0.205(17)‰) from Tahiti and recent coral aragonite represented by the JCp-1 coral (*Porites*, 0.194(9)‰) standard.

Thus, any temperature reconstruction on these timescales based on stable Sr isotopes ($T_{\delta^{88/86}\text{Sr}}$) are not affected by changes in seawater Sr/Ca. Calculating the absolute temperatures from Sr/Ca ratios after Correge et al. (2006) results in a average temperature of 21.5°C with an amplitude of ~3.3°C within one year. This is far below the recent average seawater temperature (27°C, (LOCARNINI et al., 2006)) of the location *Porites* sp. was sampled and also to cold for post glacial conditions (LEA et al., 2000). Correcting the actually measured Sr/Ca (FELIS et al., 2010) values by taking a shift of 2% in seawater Sr/Ca into account, results in a absolute mean temperature of 24.5°C. Temperatures calculated from the *Acropora* sp. $\delta^{88/86}\text{Sr}$ -temperature calibration result in similar temperatures compared to the corrected Sr/Ca based calculation. However, the annual variability of $T_{\delta^{88/86}\text{Sr}}$ is twice as large as $T_{\text{Sr/Ca}}$ variations throughout the record.

IV.7 Conclusion

The simple linear temperature dependency for *Acropora* sp. found by (FIETZKE and EISENHAUER, 2006; RÜGGERBERG et al., 2008) could not be confirmed in this study. Fossil *Porites* sp. samples (15 kyr B.P.) from Tahiti show annual variability in $\delta^{88/86}\text{Sr}$ with a cyclic variability similar to the one of Sr/Ca and $\delta^{18}\text{O}$, respectively. Based on our preliminary $\delta^{88/86}\text{Sr}$ -temperature calibration temperatures calculated from our $\delta^{88/86}\text{Sr}$ gives absolute values in between 18.7°C to 24.9°C for a fossil coral record off Tahiti representing glacial SST fluctuations 15 kyrs ago but with an seasonal amplitude larger than the corresponding one of $T_{\text{Sr/Ca}}$. In contrast to Sr/Ca elemental ratios we do not observe any shifts in

$\delta^{88/86}\text{Sr}$ of seawater during the LGM. In near future a temperature calibration of $\delta^{88/86}\text{Sr}$ on a recent *Porites* sp. coral has to be performed in order to exclude problems originating from different physiologies of different coral species.

IV.8 Acknowledgements

This work has been made possible thanks to the support from DFG. Additionally we want to thank Ana Kolevica for her inexhaustible Lab-support and Ed Hathorne for his technical advice. Uschi Christiansen is kindly acknowledged for providing x-ray pictures of a recent *Porites* sp. samples. This coral will be used in the near future for a $\delta^{88/86}\text{Sr}$ -temperature calibration which then will be included into our study. Finally we thank Isabelle Taubner and Christian Horn for enduring the discussions in their office during the evolution of the manuscript.

IV.9 References

- Abram, N. J., Gagan, M. K., Cole, J. E., Hantoro, W. S., and Mudelsee, M., 2008. Recent intensification of tropical climate variability in the Indian Ocean. *Nature Geoscience* **1**, 849-853.
- Beck, J. W., Edwards, R. L., Ito, E., Taylor, F. W., Recy, J., Rougerie, F., Joannot, P., and Henin, C., 1992. Sea-Surface Temperature from Coral Skeletal Strontium Calcium Ratios. *Science* **257**, 644-647.
- Böhm, F., Gussone, N., Eisenhauer, A., Dullo, W. C., Reynaud, S., and Paytan, A., 2006. Calcium isotope fractionation in modern scleractinian corals. *Geochimica et Cosmochimica Acta* **70**, 4452-4462.
- Camoin, G. F., Iryu, Y., McInroy, D. B., and Scientists, a. t. E., 2005. Expedition 310 of the mission-specific drilling platform from and to Papeete, Tahiti, French Polynesia Sites M0005–M0026. *Integrated Ocean Drilling Program Management International, Inc., for the Integrated Ocean Drilling Program*.
- Cobb, K. M., Charles, C. D., Cheng, H., and Edwards, R. L., 2003. El Nino/Southern Oscillation and tropical Pacific climate during the last millennium. *Nature* **424**, 271-276.
- Cole, J. E., Rind, D., and Fairbanks, R. G., 1993. Isotopic Responses to Interannual Climate Variability Simulated by an Atmospheric General-Circulation Model. *Quaternary Science Reviews* **12**, 387-406.
- Fallon, S. J., McCulloch, M. T., van Woesik, R., and Sinclair, D. J., 1999. Corals at their latitudinal limits: laser ablation trace element systematics in *Porites* from Shirigai Bay, Japan. *Earth and Planetary Science Letters* **172**, 221-238.
- Felis, T., Lohmann, G., Kuhnert, H., Lorenz, S. J., Scholz, D., Patzold, J., Al-Rousan, S. A., and Al-Moghrabi, S. M., 2004. Increased seasonality in Middle East temperatures during the last interglacial period. *Nature* **429**, 164-168.
- Felis, T., Merkel, U., Asami, R., Deschamps, P., Hathorne, E. C., Kölling, M., Bard, E., Cabioch, G., Durand, N., Prange, M., Schulz, M., Cahyarini, S. Y., and Pfeiffer, M., 2010. Pronounced interannual variability in tropical South Pacific temperatures at the end of the last glacial. *submitted*.
- Felis, T., Suzuki, A., Kuhnert, H., Dima, M., Lohmann, G., and Kawahata, H., 2009. Subtropical coral reveals abrupt early-twentieth-century freshening in the western North Pacific Ocean. *Geology* **37**, 527-530.
- Fietzke, J. and Eisenhauer, A., 2006. Determination of Temperature-Dependent Stable Strontium Isotope ($^{88}\text{Sr}/^{86}\text{Sr}$) Fractionation via Bracketing Standard MC-ICP-MS. *Geochem. Geophys. Geosyst.* **7**, Q08009, doi:10.1029/2006GC001243.
- Krabbenhöft, A., Eisenhauer, A., Böhm, F., Vollstaedt, H., Fietzke, J., Liebetrau, V., Augustin, N., Peucker-Ehrenbrink, B., Müller, M. N., Horn, C., Hansen, B. T., Nolte, N., and Wallmann, K., 2010. Constraining the marine strontium budget with natural strontium isotope fractionations ($^{87}\text{Sr}/^{86}\text{Sr}^*$, $\delta^{88/86}\text{Sr}$) of carbonates, hydrothermal solutions and river waters. *Geochimica et Cosmochimica Acta* **74**, 4097-4109.
- Krabbenhöft, A., Fietzke, J., Eisenhauer, A., Liebetrau, V., Böhm, F., and Vollstaedt, H., 2009. Determination of radiogenic and stable strontium isotope ratios ($^{87}\text{Sr}/^{86}\text{Sr}/\delta^{88/86}\text{Sr}$) by thermal ionization mass spectrometry applying an $^{87}\text{Sr}/^{84}\text{Sr}$ double spike. *Journal of Analytical Atomic Spectrometry* **24**, 1267-1271.
- Lea, D. W., Pak, D. K., and Spero, H. J., 2000. Climate impact of late quaternary equatorial Pacific sea surface temperature variations. *Science* **289**, 1719-1724.
- Locarnini, R. A., A. V. Mishonov, J. I. Antonov, Boyer, T. P., and Garcia, H. E., 2006. World Ocean Atlas 2005. *NOAA Atlas NESDIS 61, U.S. Government Printing Office* **1**, 182 pp.
- Marshall, A. T. and Clode, P., 2004. Calcification rate and the effect of temperature in a zooxanthellate and an azooxanthellate scleractinian reef coral. *Coral Reefs* **23**, 218-224.

- McCulloch, M. T., Tudhope, A. W., Esat, T. M., Mortimer, G. E., Chappell, J., Pillans, B., Chivas, A. R., and Omura, A., 1999. Coral record of equatorial sea-surface temperatures during the penultimate deglaciation at Huon Peninsula. *Science* **283**, 202-204.
- Mitsuguchi, T., Matsumoto, E., Abe, O., Uchida, T., and Isdale, P. J., 1996. Mg/Ca thermometry in coral-skeletons. *Science* **274**, 961-963.
- Reynaud-Vaganay, S., Gattuso, J. P., Cuif, J. P., Jaubert, J., and Juillet-Leclerc, A., 1999. A novel culture technique for scleractinian corals: application to investigate changes in skeletal $\delta^{18}\text{O}$ as a function of temperature. *Marine Ecology-Progress Series* **180**, 121-130.
- Reynaud, S., Ferrier-Pages, C., Boisson, F., Allemand, D., and Fairbanks, R. G., 2004. Effect of light and temperature on calcification and strontium uptake in the scleractinian coral *Acropora verweyi*. *Mar. Ecol.-Prog. Ser.* **279**, 105-112.
- Reynaud, S., Ferrier-Pages, C., Meibom, A., Mostefaoui, S., Mortlock, R., Fairbanks, R., and Allemand, D., 2007. Light and temperature effects on Sr/Ca and Mg/Ca ratios in the scleractinian coral *Acropora* sp. *Geochimica et Cosmochimica Acta* **71**, 354-362.
- Rüggeberg, A., Fietzke, J., Liebetrau, V., Eisenhauer, A., Dullo, W. C., and Freiwald, A., 2008. Stable strontium isotopes ($\delta^{88/86}\text{Sr}$) in cold-water corals - A new proxy for reconstruction of intermediate ocean water temperatures. *Earth and Planetary Science Letters* **269**, 569-574.
- Shen, C. C., Hastings, D. W., Lee, T. P., Chiu, C. H., Lee, M. Y., Wei, K. Y., and Edwards, R. L., 2001. High precision glacial-interglacial benthic foraminiferal Sr/Ca records from the eastern equatorial Atlantic Ocean and Caribbean Sea. *Earth and Planetary Science Letters* **190**, 197-209.
- Sinclair, D. J., Williams, B., and Risk, M., 2006. A biological origin for climate signals in corals - Trace element "vital effects" are ubiquitous in Scleractinian coral skeletons. *Geophysical Research Letters* **33**.
- Smith, S. V., Buddemeier, R. W., Redalje, R. C., and Houck, J. E., 1979. Strontium-Calcium Thermometry in Coral Skeletons. *Science* **204**, 404-407.
- Stoll, H. M. and Schrag, D. P., 1998. Effects of Quaternary sea Level Cycles on Strontium in Seawater. *Geochim. Cosmochim. Acta* **62**, 1107-1118.
- Weber, J. N. and Woodhead, P. M., 1972. Temperature Dependence of Oxygen-18 Concentration in Reef Coral Carbonates. *Journal of Geophysical Research* **77**, 463-670.
- Wells, J. W., 1957. Coral Reefs. *Ecological Society America Memoir* **67**, 609-631.

IV.10 Tables

lab code	T [°C]	$\delta^{88/86}\text{Sr}$ [‰]	2SEM	n	Sr/Ca [mmol/mol]	2SEM
18-ic	23	0.201	0.003	4	0.709279	0.000003
5-ic	21	0.208	0.005	6	0.709238	0.000002
34-ic	25	0.188	0.006	6	0.709231	0.000004
50-ic	29	0.206	0.010	6	0.709307	0.000004
17-ic	23	0.198	0.003	4	0.709337	0.000003
44-ic	27	0.201	0.010	4	0.709284	0.000007
2-ic	21	0.205	0.001	6	0.709243	0.000001
31-ic	25	0.183	0.009	6	0.709221	0.000004
49-ic	29	0.193	0.005	6	0.709229	0.000002

tab.IV.1: $\delta^{88/86}\text{Sr}$ data (*Acropora* sp.). The data are chronologically ordered corresponding to their measurement session.

Lab code	profile depth [cm]	$\delta^{88/86}\text{Sr}$ [‰]	2SEM	n
645-08_1	18.7	0.193	0.006	4
645-08_2		0.161	0.014	4
646-08	18.775	0.187	0.019	6
647-08_1	18.85	0.208	0.006	6
647-08_2		0.219	0.010	1
648-08	18.925	0.215	0.005	6
649-08	19	0.215	0.060	6
650-08	19.075	0.196	0.009	4
651-08	19.125	0.207	0.009	4
653-08_1	19.275	0.213	0.014	4
653-08_2		0.199	0.006	2
654-08	19.35	0.216	0.002	4
655-08	19.425	0.216	0.021	4
656-08	19.5	0.210	0.002	4
657-08_1	19.575	0.212	0.003	6
657-08_2		0.220	0.015	6
658-08_1	19.65	0.203	0.003	6
658-08_2		0.208	0.005	4
659-08_1	19.7	0.204	0.011	4
659-08_2		0.205	0.016	6
659-08_3		0.190	0.005	6
660-08_1	19.775	0.205	0.007	6
660-08_2		0.187	0.003	4
661-08_1	19.85	0.191	0.015	4
661-08_2		0.200	0.003	6
662-08	19.9	0.171	0.001	4
663-08	20	0.204	0.008	4
664-08	20.05	0.199	0.016	4
666-08	20.225	0.191	0.008	6
667-08_1	20.3	0.215	0.019	6
667-08_2		0.199	0.007	4
668-08_1	20.375	0.217	0.005	4
668-08_2		0.204	0.007	6
669-08_1	20.425	0.239	0.041	6
669-08_2		0.197	0.004	3
671-08	20.575	0.203	0.004	4
672-08	20.65	0.240	0.046	6
673-08_1	20.725	0.205	0.010	1
673-08_2		0.199	0.004	4
674-08	20.825	0.198	0.006	8

tab.IV.2: $\delta^{88/86}\text{Sr}$ data (fossil *Porites* sp.)

Chapter V

SUMMARY AND OUTLOOK

V. Summary and outlook

The impetus of this thesis was the pioneering work of (FIETZKE and EISENHAUER, 2006) who investigated natural Sr isotope fractionation by applying the bracketing standard technique on MC-ICP-MS. They reported a significant temperature dependence of Sr isotope fractionation during biologically and inorganically precipitation of CaCO_3 . The bracketing standard technique adequately corrects for instrumental drift and mass fractionation but is not accounting for Sr isotope fractionation that occurs during chemical sample preparation prior mass spectrometric measurement. In order to improve the measurement precision and to overcome the problems of isotope fractionation during chemical sample treatment we developed a Sr double spike method for TIMS. The measurement precision was improved by a factor of at least two when compared to the bracketing standard technique. The whole procedure of the double spike calibration and method development was discussed in chapter II of this thesis.

The new method of Sr isotope measurements enables the simultaneous determination of the radiogenic $^{87}\text{Sr}/^{86}\text{Sr}$ and the stable $^{88}\text{Sr}/^{86}\text{Sr}$ ratio which allows a new view on the oceans Sr budget by divulging differences in the isotopic composition of marine carbonates and seawater were they have been precipitated from. Furthermore, the new $\delta^{88/86}\text{Sr}$ - as an addition to the well established radiogenic Sr system - allows quantitative assertions about the Sr flux of the major sink of the ocean and reveals changes in continental weathering on glacial/interglacial time scales. The recent isotopic disequilibrium of the ocean is visualized in a three-isotope-plot (fig.III.3) where $\delta^{88/86}\text{Sr}$ is plotted against the radiogenic Sr isotope ratio $^{87}\text{Sr}/^{86}\text{Sr}$. This reveals glacial/interglacial variations in continental weathering and the oceans Sr budget and gains the understanding of the global Sr cycle. The application of $\delta^{88/86}\text{Sr}$ to constrain the oceans Sr budget was the issue of chapter III of this thesis. In continuative studies also minor Sr sources like e.g. cold seeps have to be taken into account when constraining the oceans Sr budget. Furthermore, stable Sr database of the river- and hydrothermal discharge has to be expanded in order to get more reliable $\delta^{88/86}\text{Sr}$ values of the Sr input to the ocean.

Chapter IV was dedicated to the investigation of stable Sr isotope fractionation in scleractinian corals. We analyzed cultured and temperature controlled warm water corals (*Acropora* sp.) which revealed a nonlinear behavior of $\delta^{88/86}\text{Sr}$ with changing habitat temperature. This indicates that temperature might not be the only factor controlling $\delta^{88/86}\text{Sr}$ variations in biogenic marine carbonates. The mechanisms driving the Sr isotope fractionation in corals are yet not clearly identified and have to be investigated in more detail in future projects. Skeletal growth rate is a promising candidate for being another parameter influencing the $\delta^{88/86}\text{Sr}$ in corals like it was shown for Ca isotope fractionation in precipitation experiments e.g. (TANG et al., 2008). Moreover, we analyzed the Sr isotopic composition of 27 samples a fossil *Porites* sp. coral covering one annual cycle of CaCO_3 precipitation 15 kyr B.P..

The $\delta^{88/86}\text{Sr}$ values showed a clear periodicity which is similar to the characteristics of $\delta^{18}\text{O}$ and Sr/Ca ratios in the same samples. The similarity of $\delta^{88/86}\text{Sr}$ values derived from recent ($\delta^{88/86}\text{Sr}_{\text{JCP-1}}=0.194(9)$) and fossil ($\delta^{88/86}\text{Sr}_{\text{fossil}}=0.205(7)$) *Porites* sp. samples leads to the suggestion, that seawater $\delta^{88/86}\text{Sr}$ is not affected by changes in seawater Sr/Ca ratio on these timescales which makes $\delta^{88/86}\text{Sr}$ useful as an independent parameter that mirrors changes in SST. Although the temperature effect on Sr isotope fractionation is very small stable Sr could evolve into a new proxy for paleo-climate reconstructions. In the frame of this work it was not possible to make a temperature calibration on recent *Porites* sp. samples. This approach is prepared and will be realized in the near future.

Chapter VI

APPENDIX

VI. Appendix

VI.1 Conference Abstracts

VI.1.1 AGU Fall Meeting 2008

Design and Application of a $^{84}\text{Sr}/^{87}\text{Sr}$ -Double Spike to Determine Natural Strontium Isotope Fractionation in Carbonates and Silicates

A. KRABBENHÖFT^{1*}, A. EISENHAEUER¹, J. FIETZKE¹, F. BÖHM¹, V. LIEBETRAU¹

¹IFM-GEOMAR, Leibniz Institute of Marine Science Wischhofstr. 1-3, D-24148 Kiel, Germany

*correspondence: ankrabbenhoeft@ifm-geomar.de

In order to precisely determine $^{88}\text{Sr}/^{86}\text{Sr}$ and $^{87}\text{Sr}/^{86}\text{Sr}$ -isotope variations in natural samples using TIMS-technique we developed a mixed $^{87}\text{Sr}/^{84}\text{Sr}$ -double spike from two solutions enriched in ^{84}Sr and ^{87}Sr , respectively. After mixing the two solutions the Sr-spike ratios have precisely been determined by calibration to the NBS 987 standard. For the determination of natural $^{88}\text{Sr}/^{86}\text{Sr}$ - and $^{87}\text{Sr}/^{86}\text{Sr}$ -isotope variations in carbonates and silicates two TIMS measurements are required: an unspiked and a spiked run where the Sr-isotope ratios are arbitrarily normalized to a fixed Sr isotope ratio (e.g. mean of the first block). For denormalization and data reduction we adopted the algorithm for Ca isotope measurements (Heuser et al., 2002) presented earlier by Heuser et al. modified for Sr-isotope measurements. It was found that best results can be achieved if the $^{84}\text{Sr}_{\text{spike}}/^{84}\text{Sr}_{\text{sample}}$ ratio is higher than about 12. The algorithm allows the simultaneous calculation of $^{87}\text{Sr}/^{86}\text{Sr}$ and $^{88}\text{Sr}/^{86}\text{Sr}$ ratios. Standard measurements showed a $\delta^{88/86}\text{Sr}$ -value ($\delta^{88/86}\text{Sr} = ((^{88}\text{Sr}/^{86}\text{Sr})_{\text{Sample}} / (^{88}\text{Sr}/^{86}\text{Sr})_{\text{NBS 987}}) - 1) * 1000$) of 0.39 for the IAPSO seawater standard corresponding to an external reproducibility of ± 0.02 (n=12). The IAPSO $\delta^{88/86}\text{Sr}$ -value corresponds to a $^{87}\text{Sr}/^{86}\text{Sr}$ -ratio of 0.709285(6). Both values are in accordance with earlier publications (Fietzke and Eisenhauer, 2006) and theoretical predictions based on the $\delta^{88/86}\text{Sr}$ ratio of seawater and assuming mass-dependent isotope fractionation. Preliminary application of the Sr- double spike to carbonate samples of the Phanerozoic indicate unexpected $\delta^{88/86}\text{Sr}$ variations in the order of about 0.2 to 0.3‰ which indicate varying supply of Sr from isotopically distinctively different sources. Furthermore a direct comparison of double spike TIMS, bracketing standard and laser-ablation MC-ICP-MS (Fietzke et al., 2008) results are in agreement and can be used to discuss limitation and perspectives of future Sr isotope measurements.

Fietzke, J. and Eisenhauer, A., 2006. Determination of temperature-dependent stable strontium isotope ($^{88}\text{Sr}/^{86}\text{Sr}$) fractionation via bracketing standard MC-ICP-MS. *Geochemistry Geophysics Geosystems* **7**, Q08009, doi:10.1029/2006GC001243.

Fietzke, J., Liebetrau, V., Guenther, D., Gurs, K., Hametner, K., Zumholz, K., Hansteen, T. H., and Eisenhauer, A., 2008. An alternative data acquisition and evaluation strategy for improved isotope ratio precision using LA-MC-ICP-MS applied to stable and Radiogenic strontium isotopes in carbonates. *Journal of Analytical Atomic Spectrometry* **23**, 955-961.

Heuser, A., Eisenhauer, A., Gussone, N., Bock, B., Hansen, B. T., and Nagler, T. F., 2002. Measurement of calcium isotopes ($\delta^{44/40}\text{Ca}$) using a multicollector TIMS technique. *International Journal of Mass Spectrometry* **220**, 385-397.

VI.1.2 AGU Fall Meeting 2009

The Marine Strontium Budget Derived from Paired ($^{87}\text{Sr}/^{86}\text{Sr}^* - \delta^{88/86}\text{Sr}$) Values of Marine Carbonates, Hydrothermal Fluids and River Waters

A. KRABBENHOEFT¹, A. EISENHAUER¹, H. VOLLSTAEDT¹, N. AUGUSTIN¹, J. FIETZKE¹, V. LLIEBETRAU¹, B. PEUCKER-EHRENBRINK², N. NOLTE³ AND B.T. HANSEN³

¹IFM-GEOMAR, Leibniz Institute of Marine Science Wischhofstr. 1-3, D-24148 Kiel, Germany

²Woods Hole Oceanographic Institution, Woods Hole, Massachusetts, USA

³Geowissenschaftliches Zentrum der Universität Göttingen (GZG), 37077 Göttingen, Germany

With the normalization to a fixed $^{88}\text{Sr}/^{86}\text{Sr}=8.375209$ ratio to correct for mass dependent fractionation during TIMS measurement any natural Strontium (Sr) isotopic fractionation in $^{88}\text{Sr}/^{86}\text{Sr}$ is ignored and important additional information are lost. A first study performed with a MC-ICP-MS (FIETZKE and EISENHAUER, 2006) showed significant fractionation between the IAPSO seawater standard and the SRM987 carbonate standard in the $\delta^{88/86}\text{Sr}$ value. However, with the application of the Sr double spike TIMS technique (KRABBENHÖFT et al., 2009) we are now entering a new dimension in Sr isotope geochemistry by the simultaneous measurement of paired $^{87}\text{Sr}/^{86}\text{Sr}^* - \delta^{88/86}\text{Sr}$ values of geological samples. The most important advantage of using paired $^{87}\text{Sr}/^{86}\text{Sr}^* - \delta^{88/86}\text{Sr}$ values is that now a complete balance of the oceans Sr budget can be calculated including Sr input and output values. In order to provide a Sr isotope balance for the global ocean we collected paired $^{87}\text{Sr}/^{86}\text{Sr}^* - \delta^{88/86}\text{Sr}$ values of a set of river waters samples, hydrothermal fluids, major marine carbonate producers and seawater. In a 3-isotope-plot the IAPSO seawater standard and the paired $^{87}\text{Sr}/^{86}\text{Sr}^* - \delta^{88/86}\text{Sr}$ values of marine carbonates are connected by a fractionation line, whereas the paired $^{87}\text{Sr}/^{86}\text{Sr}^* - \delta^{88/86}\text{Sr}$ values of river waters and hydrothermal fluids are connected by a binary mixing line. The intercept of these lines provides the isotopic composition of the marine input ($^{87}\text{Sr}/^{86}\text{Sr}^*=0.709314(9) - \delta^{88/86}\text{Sr}=0.284(24)$). The major Sr output corresponds to the Sr incorporated by the major marine calcifiers ($^{87}\text{Sr}/^{86}\text{Sr}^*=0.709312(9) - \delta^{88/86}\text{Sr}=0.240$).

The offset indicates that modern ocean is apparently not in steady state with respect to Sr. Weathering of young carbonates on the shelves during sea level low stands can shift the $\delta^{88/86}\text{Sr}$ of rivers from its recent value of 0.300(24) to 0.23‰ to equilibrate in- and output.

Fietzke, J. and Eisenhauer, A., 2006. Determination of temperature-dependent stable strontium isotope ($^{88}\text{Sr}/^{86}\text{Sr}$) fractionation via bracketing standard MC-ICP-MS. *Geochemistry Geophysics Geosystems* **7**.

Krabbenhöft, A., Fietzke, J., Eisenhauer, A., Liebetrau, V., Böhm, F., and Vollstaedt, H., 2009.

Determination of radiogenic and stable strontium isotope ratios ($^{87}\text{Sr}/^{86}\text{Sr}/\delta^{88/86}\text{Sr}$) by thermal ionization mass spectrometry applying an $^{87}\text{Sr}/^{84}\text{Sr}$ double spike. *Journal of Analytical Atomic Spectrometry* **24**, 1267-1271.

VI.1.3 Goldschmidt Conference 2009

Ocean Sr-budget from paired $\delta^{88/86}\text{Sr}$ and $^{87}\text{Sr}/^{86}\text{Sr}^*$ -ratios

A. KRABBENHOEF¹, A. EISENHAEUER¹, H. VOLLSTAEDT¹, N. AUGUSTIN¹, J. FIETZKE¹, V. LIEBETRAU¹, B. PEUCKER-EHRENBRINK²,
N. NOLTE³ AND B.T. HANSEN³

¹IFM-GEOMAR, Leibniz Institute of Marine Science, Wischhofstr. 1-3, D-24148 Kiel, Germany

²Woods Hole Oceanographic Institution, Woods Hole, Massachusetts, USA

³Geowissenschaftliches Zentrum der Universität Göttingen (GZG), 37077 Göttingen, Germany

The degree of natural $^{88}\text{Sr}/^{86}\text{Sr}$ - and $^{87}\text{Sr}/^{86}\text{Sr}^*$ -isotope fractionation in geological samples using TIMS can be determined with a mixed ^{87}Sr - ^{84}Sr double spike. This allows to correct the $^{88}\text{Sr}/^{86}\text{Sr}$ - and $^{87}\text{Sr}/^{86}\text{Sr}^*$ -isotope-ratios for mass dependent fractionation. Measurements of the seawater standard IAPSO ($\delta^{88/86}\text{Sr}=0.386(5)$, $^{87}\text{Sr}/^{86}\text{Sr}=0.709312(9)$ $2\sigma_{\text{mean}}$, $n=10$) and the JcP-1coral standard ($\delta^{88/86}\text{Sr}=0.197(8)$, $^{87}\text{Sr}/^{86}\text{Sr}=0.709237(2)$) are in accordance with earlier publications (FIETZKE and EISENHAEUER, 2006; OHNO and HIRATA, 2007). A further advantage of this technique is that the Sr isotope ratios can be determined with higher precision than with the classical technique normalizing $^{87}\text{Sr}/^{86}\text{Sr}$ values to a fix $^{88}\text{Sr}/^{86}\text{Sr}$ ratio of 8.375209 ($\delta^{88/86}\text{Sr}=0$). The new possibility of simultaneous determination of paired $^{88}\text{Sr}/^{86}\text{Sr}$ - $^{87}\text{Sr}/^{86}\text{Sr}^*$ ratios allow a two-dimensional view of the Sr isotope system in three-isotope diagrams which allow to better constrain the present and past Sr budget of the ocean. In order to constrain the present Sr budget of the ocean we measured $\delta^{88/86}\text{Sr}$ and $^{87}\text{Sr}/^{86}\text{Sr}^*$ -ratios of a set of river water samples and hydrothermal fluids being the major Sr sources. The Sr isotope values of the JcP-1 coral standard were taken to represent the CaCO_3 flux to the ocean floor being the major sink. Model calculation showed that the modern ocean is not in steady state rather the Sr sources supply roughly double the amount of Sr to the ocean than is removed by the sinks.

Fietzke, J. and Eisenhauer, A., 2006. Determination of temperature-dependent stable strontium isotope ($^{88}\text{Sr}/^{86}\text{Sr}$) fractionation via bracketing standard MC-ICP-MS. *Geochemistry Geophysics Geosystems* **7**.

Ohno, T. and Hirata, T., 2007. Simultaneous determination of mass-dependent isotopic fractionation and radiogenic isotope variation of strontium in geochemical samples by multiple collector-ICP-mass spectrometry. *Anal. Sci.* **23**, 1275-1280.

VI.1.4 Geologische Vereinigung Annual Meeting 2009

The Marine Strontium Budget Derived from Paired ($^{87}\text{Sr}/^{86}\text{Sr}^*$ - $\delta^{88/86}\text{Sr}$) Values of Marine Carbonates, Hydrothermal Fluids and River Waters

A. KRABBENHOEFT¹, A. EISENHAUER¹, H. VOLLSTAEDT¹, N. AUGUSTIN¹, J. FIETZKE¹, V. LLIEBETRAU¹, B. PEUCKER-EHRENBRINK², N. NOLTE³ AND B.T. HANSEN³

¹IFM-GEOMAR, Leibniz Institute of Marine Science Wischhofstr. 1-3, D-24148 Kiel, Germany

²Oceanographic Institution, Woods Hole, Massachusetts, USA

³Geowissenschaftliches Zentrum der Universität Göttingen (GZG), 37077 Göttingen, Germany

With the normalization to a fixed $^{88}\text{Sr}/^{86}\text{Sr}=8.375209$ ratio to correct for mass dependent fractionation during TIMS measurement any natural Strontium (Sr) isotopic fractionation in $^{88}\text{Sr}/^{86}\text{Sr}$ is ignored and important additional information are lost. A first study performed with a MC-ICP-MS (FIETZKE and EISENHAUER, 2006) showed significant fractionation between the IAPSO seawater standard and the SRM987 carbonate standard in the $\delta^{88/86}\text{Sr}$ value. However, with the application of the Sr double spike TIMS technique (KRABBENHÖFT et al., 2009) we are now entering a new dimension in Sr isotope geochemistry by the simultaneous measurement of paired $^{87}\text{Sr}/^{86}\text{Sr}^*$ - $\delta^{88/86}\text{Sr}$ values of geological samples. The most important advantage of using paired $^{87}\text{Sr}/^{86}\text{Sr}^*$ - $\delta^{88/86}\text{Sr}$ values is that now a complete balance of the oceans Sr budget can be calculated including Sr input and output values. In order to provide a Sr isotope balance for the global ocean we collected paired $^{87}\text{Sr}/^{86}\text{Sr}^*$ - $\delta^{88/86}\text{Sr}$ values of a set of river waters samples, hydrothermal fluids, major marine carbonate producers and seawater. In a 3-isotope-plot the IAPSO seawater standard and the the paired $^{87}\text{Sr}/^{86}\text{Sr}^*$ - $\delta^{88/86}\text{Sr}$ values of marine carbonates are connected by a fractionation line, whereas the paired $^{87}\text{Sr}/^{86}\text{Sr}^*$ - $\delta^{88/86}\text{Sr}$ values of river waters and hydrothermal fluids are connected by a binary mixing line. The intercept of these lines provides the isotopic composition of the marine input ($^{87}\text{Sr}/^{86}\text{Sr}^*=0.709314(9)$ - $\delta^{88/86}\text{Sr}=0.284(24)$). The major Sr output δ corresponds to the Sr incorporated by the major marine calcifiers ($^{87}\text{Sr}/^{86}\text{Sr}^*=0.709312(9)$ - $\delta^{88/86}\text{Sr}=0.240$). The offset indicates that modern ocean is apparently not in steady state with respect to Sr. Weathering of young carbonates on the shelves during sea level low stands can shift the $\delta^{88/86}\text{Sr}$ of rivers from its recent value of 0.300(24) to 0.23‰ to equilibrate in- and output.

Fietzke, J. and Eisenhauer, A., 2006. Determination of temperature-dependent stable strontium isotope ($^{88}\text{Sr}/^{86}\text{Sr}$) fractionation via bracketing standard MC-ICP-MS. *Geochemistry Geophysics Geosystems* **7**.

Krabbenhöft, A., Fietzke, J., Eisenhauer, A., Liebetrau, V., Böhm, F., and Vollstaedt, H., 2009.

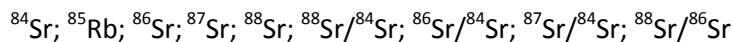
Determination of radiogenic and stable strontium isotope ratios ($^{87}\text{Sr}/^{86}\text{Sr}$ / $\delta^{88/86}\text{Sr}$) by thermal ionization mass spectrometry applying an $^{87}\text{Sr}/^{84}\text{Sr}$ double spike. *Journal of Analytical Atomic Spectrometry* **24**, 1267-1271.

VI.2 Data export and evaluation manual

To ensure a comfortable data processing an EXCEL[®] spread sheet for data reduction was developed. The aim was to simplify Sr data reduction and to shorten the time needed for evaluation of raw data. Emphasis was put to clarity to prevent input errors. Furthermore, a number of criteria have been established in order to access the data quality. The actual version of the spread sheet is available at U:\FB2\MG\akolevica\QS-Sr-stabil\aktuelles Makro.

VI.2.1 Data export from TIMS

The following values have to be exported from the TIMS machine:



Here you have to make sure that:

- The “Header” of the files is exported (Export configuration, fig.VI.1)
- Invalid values are not marked (Export configuration, fig.VI.1)
- Choose only (D_i) in the “View Control” menu (red circle, fig.VI.1)

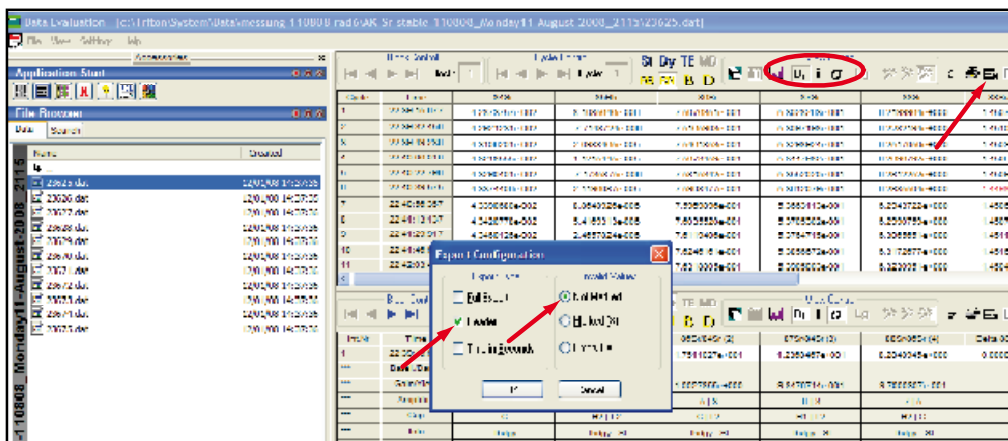


fig.VI.1: Data evaluation software

Choose a file on the left hand side and then click “Ex” on the top right side. The *.dat file is then exported to a *.exp file which can be used for further data processing.

VI.2.2 Data reduction with the EXCEL® spread sheet

VI.2.2.1 Overview

1	2	3	4	5	6	7	8	9	10	11					
100 05:14:20:676	8.65E-01	-1.95E-06	7.48E-01	1.27E+00	6.20E+00	7.17E+00	8.65E-01	1.47E+00	8.29E+00	-0.017027	1.470012	7.151974	0.364538	1.470012	7.161
101 05:14:37:558	8.66E-01	1.54E-06	7.49E-01	1.27E+00	6.21E+00	7.17E+00	8.65E-01	1.47E+00	8.29E+00	-0.016020	1.470012	7.151765	0.364595	1.470012	7.161
102 05:14:54:236	8.67E-01	-1.46E-05	7.50E-01	1.28E+00	6.21E+00	7.17E+00	8.65E-01	1.47E+00	8.29E+00	-0.018827	1.470012	7.151393	0.364526	1.470012	7.161

fig.VI.2: Worksheets within the EXCEL® spreadsheet for stable Strontium data reduction.

Here a brief overview over the worksheets (fig.VI.2) within the stable Strontium evaluation spread sheet is given. Detailed information to every single worksheet is given below:

1. **"1"- "21"**: Here the TIMS raw data sets are imported to the EXCEL spread sheet.
2. **"précis"**: Here the samples are labeled according to their properties (ic-, id-, standard, sample, blank) to ensure correct evaluation.
3. **"linear"**: Here a simple linear fractionation law is used for spike correction (not relevant for users).
4. **"algo"**: Here a more appropriate exponential fractionation law is used for spike correction (not relevant for users).
5. **"plots"**: Here the development of the $^{88}\text{Sr}/^{84}\text{Sr}$ isotope ratio during the course of the measurement is plotted (Quality control).
6. **"SRM987"**: Here the results for the standard measurements are summarized.
7. **"samples"**: Here the results for the samples are summarized.
8. **"3-iso-plot"**: Here the $^{88}\text{Sr}/^{84}\text{Sr}$ is plotted against the $^{86}\text{Sr}/^{84}\text{Sr}$ for each sample (Quality control).
9. **"Blank and Concentration"**: Here the spike/sample ratio and the amount of Strontium in each sample is calculated (Quality control).
10. **"QS"**: Here results from linear and exponential evaluation are compared. (Quality control)
11. **"update"**: Here the latest updates of the spread sheet are reported.

VI.2.3 Data import to Excel®

VI.2.3.1 Worksheet “1” – “21”

This procedure starts in worksheet 1 (left hand side of the red rectangle in fig.VI.2) and is schematically displayed in fig.VI.3.

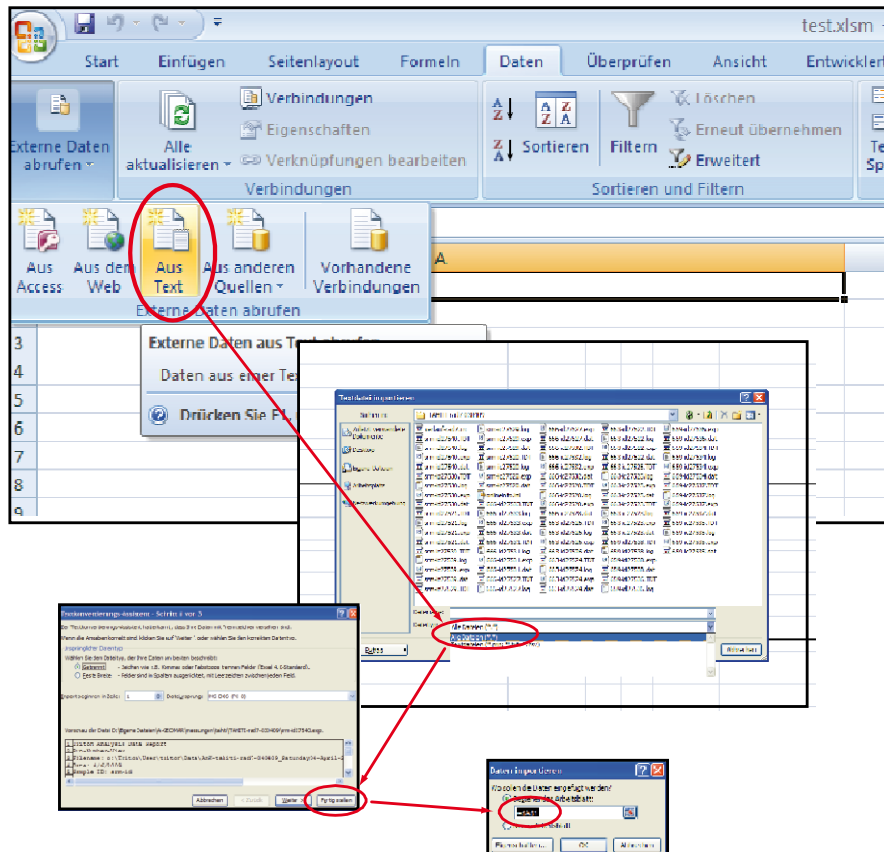


fig.VI.3: Data import in Excel®

Import the *.exp- files in the displayed way. This procedure has to be repeated for the 21 export-files of the analyzed samples in worksheet 1 – 21 (fig.VI.3). Make sure that data is imported to cell A1 of every worksheet.

In worksheet 1, three free parameters are marked in green (fig.VI.4).

L	M	N	O
	Isotopenmassen:		
	Sr-m-84:	83.913428	
	Sr-m-86:	85.909273	
	Sr-m-87:	86.908890	
	Sr-m-88:	87.905625	
	Isotope min signal:	0.000010	
	Motfb 87/84:	1.470012	
	Signifikanz T-Test:	0.010000	
	Rb corr.-factor	2.593245	
	$^{88}\text{Sr}/^{86}\text{Sr}$	8.375209	
	$^{87}\text{Sr}/^{86}\text{Sr}$	0.71024	
			no Rb c
	beta	87/84 true	88/84 true 86/

fig.VI.4: Free parameters in worksheet 1-21. The default settings turned out to be reasonable.

- **Isotope min signal:** Represents a lower limit for the output voltage of ^{84}Sr . This value depends on the method chosen for Strontium measurement and is reasonable for maximum voltage of 10 Volts on ^{88}Sr .
- **Signifikanz T-Test:** Here the Rb confidence level of the Rubidium measurement can be adjusted. It is testing if the signal on mass 85 is significant above zero. A value of 0.01 means a confidence level of 99%. When the signal on mass 85 turns out to be significant the ^{87}Sr value will be corrected.
- **Rb-corr. Factor:** This value represents the isotopic ratio $^{85}\text{Rb}/^{87}\text{Sr}$ and hence is not really a free parameter.

Only these parameters can be changed in worksheet 1. They are taken over to worksheet 2-21 automatically. These worksheets include the traditional radiogenic evaluation (with and without rubidium correction). Invalid values are eliminated by a two sigma test.

VI.2.3.2 Worksheet “précis”

This worksheet represents a summary of the measured isotopic ratios of all analyzed samples. The columns F-H ($_{\text{Motfb}}\text{Sr}^{88/84}$, $_{\text{Motfb}}\text{Sr}^{87/84}$, $_{\text{Motfb}}\text{Sr}^{86/84}$ (Motfb = mean of the first block)) should be filled with numbers. If not, there might be an error occurred during data import (imported in cell A1? Just imported header + 126 measurements?).

In order to make sure that isotope values are assigned correctly to the algorithm, samples have to be labeled in the following way (fig.VI.5):

	SRM987	Sample 1	Sample 2	Sample x	Blank
IC measurement #1	srm-ic-1	1-ic-1	2-ic-1	x-ic-1	
IC measurement #2	srm-ic-2	1-ic-2	2-ic-2	x-ic-2	
ID measurement #1	srm-id-1	1-id-1	2-id-1	x-id-1	Blk-1
ID measurement #y	srm-id-y	1-id-y	2-id-y	x-id-y	Blk-y

fig.VI.5: Labeling of samples

	A	B	C	D	E	F	G	H
	wheel position	sample	session	sample id	comment	MotbSr ^{88/84}	MotbSr ^{87/84}	MotbSr ^{86/84}
2	1	Sample ID: srm987ic	Analysis date: 5/15/2010	srm-ic-1		144.930080	12.357464	17.493821
3	2	Sample ID: srm987id	Analysis date: 5/15/2010	srm-id-1		7.249729	1.478116	0.874281
4	3	Sample ID: srm987ic	Analysis date: 5/16/2010	srm-ic-2		145.139434	12.370951	17.506691
5	4	Sample ID: srm987id	Analysis date: 5/16/2010	srm-id-2		7.243635	1.477188	0.873913
6	5	Sample ID: srm987id	Analysis date: 5/16/2010	srm-id-3		7.243518	1.477170	0.873905
7	6	Sample ID: 141-ic	Analysis date: 5/15/2010	1-ic-1		145.461034	12.368321	17.507790
8	7	Sample ID: 141-id	Analysis date: 5/15/2010	1-id-1		2.778339	1.128518	0.333915
9	8	Sample ID: 141-ic	Analysis date: 5/15/2010	1-ic-2		145.503429	12.370724	17.509484
10	9	Sample ID: 141-id	Analysis date: 5/15/2010	1-id-2		2.769738	1.125883	0.333396
11	10	Sample ID: 142-ic	Analysis date: 5/15/2010	2-ic-1		144.835380	12.321502	17.442854
12	11	Sample ID: 142-id	Analysis date: 5/15/2010	2-id-1		1.968380	1.064902	0.236535
13	12	Sample ID: 142-ic	Analysis date: 5/15/2010	2-ic-2		145.568949	12.368330	17.486711
14	13	Sample ID: 142-id	Analysis date: 5/16/2010	2-id-2		1.967009	1.064416	0.236442
15	14	Sample ID: 143-ic	Analysis date: 5/16/2010	3-ic-1		145.994527	12.400101	17.530749
16	15	Sample ID: 143-id	Analysis date: 5/16/2010	3-id-1		1.967562	1.061681	0.237008
17	16	Sample ID: 143-ic	Analysis date: 5/16/2010	3-ic-2		145.679353	12.379895	17.510928
18	17	Sample ID: 143-id	Analysis date: 5/16/2010	3-id-2		1.968496	1.062065	0.237063
19	18	Sample ID: 144-ic	Analysis date: 5/16/2010	4-ic-1		146.158136	12.408506	17.531714
20	19	Sample ID: 144-id	Analysis date: 5/16/2010	4-id-1		1.644556	1.037588	0.197889
21	20	Sample ID: 144-ic	Analysis date: 5/16/2010	4-ic-2		145.695155	12.378624	17.503102
22	21	Sample ID: 144-id	Analysis date: 5/16/2010	4-id-2		1.652604	1.041408	0.198373

fig.VI.6: Labeling of samples in "précis" worksheet.

VI.2.4 Data evaluation

After all turret positions are imported and labeled a summary of isotope ratios are given in the worksheets "srm987" (for standard) and "samples" (for all sample measurements". Here the mean values of all measured samples are given with their corresponding errors.

VI.2.5 Standard measurement

A summary of isotope ratios of the standard SRM987 is given in the worksheet "srm987". Please note that all ratios are not normalized (mean $\delta^{88/86}\text{Sr}_{\text{SRM987}}$ is NOT zero). Every measurement of the standard should be recorded in a srm987 long term table, located at U:\FB2\MG\akolevica\QS-Sr-stabil\ Langzeit-Standards.

VI.2.5.1 Sample measurement

A summary of isotope ratios of the samples is given in the worksheet "samples". All isotope ratios are corrected for SRM987 offset to $^{88}\text{Sr}/^{86}\text{Sr}=8.375209$ and $^{87}\text{Sr}/^{86}\text{Sr}=0.710240$. SRM987 offsets are found in columns R+S. All important isotope ratios ($\delta^{88/86}\text{Sr}$, $^{87}\text{Sr}/^{86}\text{Sr}_{\text{corr}}$, $^{87}\text{Sr}/^{86}\text{Sr}_{\text{norm-corr}}$ and $^{87}\text{Sr}/^{86}\text{Sr}^*_{\text{corr}}$) are marked with red color in the labeling.

VI.2.5.2 Blank measurement

If a blank measurement was performed the $^{88}\text{Sr}/^{84}\text{Sr}_{\text{corr}}$ and $^{86}\text{Sr}/^{84}\text{Sr}_{\text{corr}}$ ratios are shown in worksheet "Blank & Concentration" in the cells G3 and G4, respectively (fig.VI.7). If cell I3 is filled with the net weight of spike added to the blank ($\mu\text{l spike}=\text{mg}$), the amount of spike is calculated in J3 and K3.

1	Blank									
2	Lab. No.:	Sample	Comment	Operator	Date	$^{88}\text{Sr}/^{84}\text{Sr}_{\text{corr}}$	$^{86}\text{Sr}/^{84}\text{Sr}_{\text{corr}}$	net weight spike [mg]	amount Sr_{blank} [ng]	over ^{86}Sr
3		Sample ID: BLK		Operator: HV	Analysis date: 11/8/2010	0.13257178	0.01584935	1	0.19	0.19
4		x		Operator: HV	Analysis date: 11/8/2010	#DIV/0!	#DIV/0!			
5		x		Operator: HV	Analysis date: 11/8/2010	#DIV/0!	#DIV/0!			

fig.VI.7: Calculation of blank amount in worksheet "Blank & Concentration"

VI.2.6 Error detection "cookbook"

If a sample shows strange isotopic composition (Attention: some natural samples CAN have "strange" isotopic composition without there is a problem with the measurement) you have to check for indications of a bad measurement run. Therefore we give a "receipt" to find eventual errors that may occurred during measurement or sample preparation. When there is a value you wouldn't expect you have to search for the error that may occurred:

- Check the plots of the single samples in the worksheet "plots". Ideally, the signal should show a continuous increase. If $^{88}\text{Sr}/^{84}\text{Sr}$ ratios show large variations during different measurement blocks it might be useful to delete some measurement blocks in the corresponding worksheet of the sample ("1" – "21").
- Check if signal intensity on ^{88}Sr is stable and high enough (should be above 3 V when method intensity aim was 10 V) in worksheets "1" – "21". If signal intensity is considerable low and produces exceptional isotope ratios (possibly due to consumed sample on the filament) these measurement blocks should be deleted.
- In the worksheet "3-iso-plot" a $^{86}\text{Sr}/^{84}\text{Sr}$ vs. $^{88}\text{Sr}/^{84}\text{Sr}$ for all single IC- and ID-measurements are shown. All IC measurements should fall onto a linear mass fractionation line (more

precisely it is an exponential curve, but the extract on the diagram is nearly linear). If deviations from this line are observed, a contamination is likely. In similarity, ID measurements should fall onto a linear line, although they are more separated due to different spike/sample ratios. If a sample is contaminated delete the label on “*précis*” worksheet.

- d) Check $^{87}\text{Sr}/^{86}\text{Sr}$ values of the IC runs of the sample in “*précis*” worksheet column “T”. Compare these values to expected values (i.e. $^{87}\text{Sr}/^{86}\text{Sr}=0.709175$ for recent marine carbonates or seawater samples or ~ 0.704 for basalts). If one of the IC runs show unexceptional values you might delete this measurement in worksheet “*précis*” by deleting the corresponding label (chapter VI.2.3.2).
- e) Look for ^{84}Sr Spike/Sample ratios on worksheet “Blank & Concentration”. Fill in the amount of spike added to the ID part of the sample (mg spike= μl spike). Aimed ratio is 20. However samples should fall within a reasonable range of 10-50.
- f) In the worksheet “QS” you’ll find a plot, showing the difference of $^{88}\text{Sr}/^{86}\text{Sr}$ ID-ratios calculated from exponential law and linear law (y-axis), respectively. They are plotted against absolute IC $^{88}\text{Sr}/^{86}\text{Sr}$ from calculated exponential law (x-axis; this gives the “location of fractionation”). Furthermore an empirical function is plotted within the diagram (derived from evaluation of ~ 200 measurements). If huge deviations from empirical function are observed, mass fractionation during measurement was NOT exponential. Therefore calculated $^{88}\text{Sr}/^{86}\text{Sr}$ might not be accurate.

VI.2.7 Further information

a) Worksheet “linear”

In this worksheet the spike correction algorithm uses a linear fractionation law. This is valuable when the sample is not fractionated to a large extend during TIMS measurement.

b) Worksheet “algo”

Here the exponential law is used for the spike correction algorithm. When the isotopic composition of one sample seems strange or is far away from reasonable values you can check in the “algo”-sheet whether an ic- or id- measurement has gone wrong. If some values show an indication for bad measurement or contamination the mark of this sample in “*précis*” has to be deleted (see worksheet “*précis*”). The result of this single measurement is then not taken into account for further proceedings.

c) Worksheet “SRM987”

Here a compilation of all measures NIST SRM987 standards in your session is given. The results given here are not session offset corrected in order to monitor long term machine drifts.

d) Worksheet “samples”

Here the results of all measured samples are summarized.

e) Worksheet “Blank and Concentration”

In this worksheet the amount of Sr in your sample is calculated. Therefore the amount of spike [mg] per filament has to be written in column “I”. Then the Sr amount is calculated through the $^{88}\text{Sr}/^{84}\text{Sr}$ and the $^{86}\text{Sr}/^{84}\text{Sr}$ ratio in column “K” and “L”. These two calculations should result in approximately the same values. Additionally the $^{84}\text{Sr}_{\text{spike}}/^{84}\text{Sr}_{\text{sample}}$ ratio is calculated which should be around 20.

f) Worksheet “update”

Here the latest changes on the Sr evaluation sheet are documented.

g) Worksheet “Blank and Concentration”

In this worksheet the amount of Sr in your sample is calculated. Therefore the amount of spike [mg] per filament has to be written in column “I”. Then the Sr amount is calculated through the $^{88}\text{Sr}/^{84}\text{Sr}$ and the $^{86}\text{Sr}/^{84}\text{Sr}$ ratio in column “K” and “L”. These two calculations should result in approximately the same values. Additionally the $^{84}\text{Sr}_{\text{spike}}/^{84}\text{Sr}_{\text{sample}}$ ratio is calculated which should be around 20.

h) Worksheet “update”

Here the latest changes on the Sr evaluation sheet are documented.

VI.3 The Sr double spike data reduction algorithm

For a deeper understanding of the double spike algorithm a derivation of the equations used for the double spike correction is given in the following. The algorithm starts with the simple isotope dilution equations. The mixture of a spike and a sample can be expressed for each single isotope as:

$$\text{eq.VI.1} \quad N_{\text{mix meas}}^A = N_{\text{sample ic}}^A + N_{\text{spike}}^A$$

and

$$\text{eq.VI.2} \quad N_{\text{mix meas}}^B = N_{\text{sample ic}}^B + N_{\text{spike}}^B$$

where N are the amounts of isotope A and B, respectively. Dividing these two equations results in:

$$\text{eq.VI.3} \quad \left(\frac{N^A}{N^B}\right)_{\text{mix meas}} = \frac{N_{\text{sample ic}}^A + N_{\text{spike}}^A}{N_{\text{sample ic}}^B + N_{\text{spike}}^B}$$

Substitution of $N_{\text{sample ic}}^A$ and N_{spike}^A with:

$$\text{eq.VI.4} \quad N_{\text{sample ic}}^A = N_{\text{sample ic}}^B \cdot \left(\frac{N_{\text{sample ic}}^A}{N_{\text{sample ic}}^B}\right) = N_{\text{sample ic}}^B \cdot \left(\frac{N^A}{N^B}\right)_{\text{sample ic}}$$

$$\text{eq.VI.5} \quad N_{\text{spike}}^A = N_{\text{spike}}^B \cdot \left(\frac{N_{\text{spike}}^A}{N_{\text{spike}}^B}\right) = N_{\text{spike}}^B \cdot \left(\frac{N^A}{N^B}\right)_{\text{spike}}$$

results in:

$$\text{eq.VI.6} \quad \left(\frac{N^A}{N^B}\right)_{\text{mix meas}} = \frac{N_{\text{sample ic}}^B \cdot \left(\frac{N^A}{N^B}\right)_{\text{sample ic}} + N_{\text{spike}}^B \cdot \left(\frac{N^A}{N^B}\right)_{\text{spike}}}{N_{\text{sample ic}}^B + N_{\text{spike}}^B}$$

Rearranging eq.VI.6

$$\left(\frac{N^A}{N^B}\right)_{\text{mix meas}} \cdot (N_{\text{sample ic}}^B + N_{\text{spike}}^B) = N_{\text{sample ic}}^B \cdot \left(\frac{N^A}{N^B}\right)_{\text{sample ic}} + N_{\text{spike}}^B \cdot \left(\frac{N^A}{N^B}\right)_{\text{spike}}$$

$$\left(\frac{N^A}{N^B}\right)_{\text{mix meas}} \cdot N_{\text{sample ic}}^B + \left(\frac{N^A}{N^B}\right)_{\text{mix meas}} \cdot N_{\text{spike}}^B = N_{\text{sample ic}}^B \cdot \left(\frac{N^A}{N^B}\right)_{\text{sample ic}} + N_{\text{spike}}^B \cdot \left(\frac{N^A}{N^B}\right)_{\text{spike}}$$

$$N_{\text{sample ic}}^B \cdot \left(\left(\frac{N^A}{N^B}\right)_{\text{mix meas}} - \left(\frac{N^A}{N^B}\right)_{\text{sample ic}} \right) = N_{\text{spike}}^B \cdot \left(\left(\frac{N^A}{N^B}\right)_{\text{spike}} - \left(\frac{N^A}{N^B}\right)_{\text{mix meas}} \right)$$

$$\frac{N_{\text{sample ic}}^B}{N_{\text{spike}}^B} = \frac{\left(\frac{N^A}{N^B}\right)_{\text{mix meas}} - \left(\frac{N^A}{N^B}\right)_{\text{sample ic}}}{\left(\frac{N^A}{N^B}\right)_{\text{spike}} - \left(\frac{N^A}{N^B}\right)_{\text{mix meas}}}$$

with B=⁸⁴Sr and A=⁸⁸Sr, ⁸⁷Sr, ⁸⁶Sr this results in the equation 11 and 12 of the algorithm for the spike correction (fig.II.1, chapter II.3.3):

$$\text{eq.VI.7} \quad \frac{N_{\text{sample ic}}^{84}}{N_{\text{spike}}^{84}} = \frac{\left(\frac{N^{88}}{N^{84}}\right)_{\text{mix meas}} - \left(\frac{N^{88}}{N^{84}}\right)_{\text{sample ic}}}{\left(\frac{N^{88}}{N^{84}}\right)_{\text{spike}} - \left(\frac{N^{88}}{N^{84}}\right)_{\text{mix meas}}} = Q_{84(88)}$$

$$\text{eq.VI.8} \quad \frac{N_{\text{sample ic}}^{84}}{N_{\text{spike}}^{84}} = \frac{\left(\frac{N^{86}}{N^{84}}\right)_{\text{mix meas}} - \left(\frac{N^{86}}{N^{84}}\right)_{\text{sample ic}}}{\left(\frac{N^{86}}{N^{84}}\right)_{\text{spike}} - \left(\frac{N^{86}}{N^{84}}\right)_{\text{mix meas}}} = Q_{84(86)}$$

From the isotope dilution equations a $Q_{84 \text{ mean}}$ can be calculated:

$$Q_{84 \text{ mean}} = \frac{Q_{84(88)} + Q_{84(86)}}{2}$$

By rearranging $Q_{84(87)}$

$$\text{eq.VI.9} \quad \frac{N_{\text{sample ic}}^{84}}{N_{\text{spike}}^{84}} = \frac{\left(\frac{N^{87}}{N^{84}}\right)_{\text{mix meas}} - \left(\frac{N^{87}}{N^{84}}\right)_{\text{sample ic}}}{\left(\frac{N^{87}}{N^{84}}\right)_{\text{spike}} - \left(\frac{N^{87}}{N^{84}}\right)_{\text{mix meas}}} = Q_{84(87)}$$

a $^{87}\text{Sr}/^{84}\text{Sr}$ composition of the spike/sample MIX can be calculated:

$$\begin{aligned} \frac{N_{\text{sample ic}}^{84}}{N_{\text{spike}}^{84}} \cdot \left(\left(\frac{N^{87}}{N^{84}}\right)_{\text{spike}} - \left(\frac{N^{87}}{N^{84}}\right)_{\text{mix meas}} \right) &= \left(\frac{N^{87}}{N^{84}}\right)_{\text{mix meas}} - \left(\frac{N^{87}}{N^{84}}\right)_{\text{sample ic}} \\ \frac{N_{\text{sample ic}}^{84}}{N_{\text{spike}}^{84}} \cdot \left(\frac{N^{87}}{N^{84}}\right)_{\text{spike}} - \frac{N_{\text{sample ic}}^{84}}{N_{\text{spike}}^{84}} \cdot \left(\frac{N^{87}}{N^{84}}\right)_{\text{mix meas}} &= \left(\frac{N^{87}}{N^{84}}\right)_{\text{mix meas}} - \left(\frac{N^{87}}{N^{84}}\right)_{\text{sample ic}} \\ \frac{N_{\text{sample ic}}^{84}}{N_{\text{spike}}^{84}} \cdot \left(\frac{N^{87}}{N^{84}}\right)_{\text{spike}} + \left(\frac{N^{87}}{N^{84}}\right)_{\text{sample ic}} &= \left(\frac{N^{87}}{N^{84}}\right)_{\text{mix meas}} + \frac{N_{\text{sample ic}}^{84}}{N_{\text{spike}}^{84}} \cdot \left(\frac{N^{87}}{N^{84}}\right)_{\text{mix meas}} \\ \frac{N_{\text{sample ic}}^{84}}{N_{\text{spike}}^{84}} \cdot \left(\frac{N^{87}}{N^{84}}\right)_{\text{spike}} + \left(\frac{N^{87}}{N^{84}}\right)_{\text{sample ic}} &= \left(\frac{N^{87}}{N^{84}}\right)_{\text{mix meas}} \cdot \left(1 + \frac{N_{\text{sample ic}}^{84}}{N_{\text{spike}}^{84}}\right) \end{aligned}$$

With

$$Q_{87} = \frac{\left(\frac{N^{87}}{N^{84}}\right)_{\text{mix meas}} - \left(\frac{N^{87}}{N^{84}}\right)_{\text{sample ic}}}{\left(\frac{N^{87}}{N^{84}}\right)_{\text{spike}} - \left(\frac{N^{87}}{N^{84}}\right)_{\text{mix meas}}}$$

It turns into:

$$Q_{87} \cdot \left(\frac{N^{87}}{N^{84}}\right)_{\text{spike}} + \left(\frac{N^{87}}{N^{84}}\right)_{\text{sample ic}} = \left(\frac{N^{87}}{N^{84}}\right)_{\text{mix meas}} \cdot (1 + Q_{87})$$

And finally it turns into equation 1 of the algorithm which is used to calculate a $^{87}\text{Sr}/^{84}\text{Sr}$ ratio of the spike and sample mixture:

$$\text{eq.VI.10} \quad \left(\frac{N^{87}}{N^{84}}\right)_{\text{mix CALC}} = \frac{Q_{87} \cdot \left(\frac{N^{87}}{N^{84}}\right)_{\text{spike}} + \left(\frac{N^{87}}{N^{84}}\right)_{\text{sample ic}}}{(1+Q_{87})}$$

On the basis of that it is possible to calculate a fractionation factor β by using the exponential fractionation law:

$$\text{eq.VI.11} \quad \left(\frac{N^{87}}{N^{84}}\right)_{\text{mix CALC}} = \left(\frac{N^{87}}{N^{84}}\right)_{\text{mix meas}} \cdot \left(\frac{mSr^{87}}{mSr^{84}}\right)^\beta$$

$$\text{eq.VI.12} \quad \beta = \frac{\log\left(\frac{\left(\frac{N^{87}}{N^{84}}\right)_{\text{mix CALC}}}{\left(\frac{N^{87}}{N^{84}}\right)_{\text{mix meas}}}\right)}{\log\left(\frac{mSr^{87}}{mSr^{84}}\right)}$$

This corresponds to equation 2 in the algorithm. This β can then be used to calculate the isotopic composition of the mixture (eq. 3 and eq.4 of the algorithm):

$$\text{eq.VI.13} \quad \left(\frac{N^{88}}{N^{84}}\right)_{\text{mix CALC}} = \left(\frac{N^{88}}{N^{84}}\right)_{\text{mix meas}} \cdot \left(\frac{mSr^{88}}{mSr^{84}}\right)^\beta$$

$$\text{eq.VI.14} \quad \left(\frac{N^{86}}{N^{84}}\right)_{\text{mix CALC}} = \left(\frac{N^{86}}{N^{84}}\right)_{\text{mix meas}} \cdot \left(\frac{mSr^{86}}{mSr^{84}}\right)^\beta$$

Expanding the fraction $\frac{N_{\text{sample ic}}^{86}}{N_{\text{spike}}^{86}}$ results in eq.6 of the algorithm:

$$\frac{N_{\text{sample ic}}^{86}}{N_{\text{spike}}^{86}} = \frac{N_{\text{sample ic}}^{84} \cdot \left(\frac{N^{86}}{N^{84}}\right)_{\text{sample ic}}}{N_{\text{sample ic}}^{84} \cdot \left(\frac{N^{86}}{N^{84}}\right)_{\text{spike}}} = Q_{84 \text{ mean}} \cdot \frac{\left(\frac{N^{86}}{N^{84}}\right)_{\text{sample ic}}}{\left(\frac{N^{86}}{N^{84}}\right)_{\text{spike}}}$$

This allows the calculation of the $^{88}\text{Sr}/^{86}\text{Sr}$ ratio of the sample by rearranging the isotope dilution equation (eq.7 in the algorithm flow chart):

$$\frac{N_{\text{sample ic}}^{88}}{N_{\text{spike}}^{88}} = \frac{\left(\frac{N^{86}}{N^{88}}\right)_{\text{mix meas}} - \left(\frac{N^{86}}{N^{88}}\right)_{\text{sample ic}}}{\left(\frac{N^{86}}{N^{88}}\right)_{\text{spike}} - \left(\frac{N^{86}}{N^{88}}\right)_{\text{mix meas}}} = Q_{86(88)}$$

$$\frac{N_{\text{sample ic}}^{88}}{N_{\text{spike}}^{88}} \cdot \left(\frac{N^{86}}{N^{88}}\right)_{\text{spike}} - \frac{N_{\text{sample ic}}^{88}}{N_{\text{spike}}^{88}} \cdot \left(\frac{N^{86}}{N^{88}}\right)_{\text{mix meas}} = \left(\frac{N^{86}}{N^{88}}\right)_{\text{mix meas}} - \left(\frac{N^{86}}{N^{88}}\right)_{\text{sample ic}}$$

$$Q_{86(88)} \cdot \left(\frac{N^{86}}{N^{88}}\right)_{\text{spike}} - Q_{86(88)} \cdot \left(\frac{N^{86}}{N^{88}}\right)_{\text{mix meas}} = \left(\frac{N^{86}}{N^{88}}\right)_{\text{mix meas}} - \left(\frac{N^{86}}{N^{88}}\right)_{\text{sample ic}}$$

$$\text{eq.VI.15} \quad \left(\frac{N^{86}}{N^{88}}\right)_{\text{sample NEW}} = \left(\frac{N^{86}}{N^{88}}\right)_{\text{mix meas}} \cdot (1 + Q_{86(88)}) - \frac{1}{Q_{86(88)}} \cdot \left(\frac{N^{86}}{N^{88}}\right)_{\text{spike}}$$

With the exponential fractionation law a new fractionation factor β_{new} can be calculated (eq.8 in the algorithm flow chart):

$$\left(\frac{N^{86}}{N^{88}}\right)_{sample\ New} = \left(\frac{N^{86}}{N^{88}}\right)_{sample\ ic} \cdot \left(\frac{mSr^{86}}{mSr^{88}}\right)^\beta$$

$$\beta_{new} = \frac{\log\left(\frac{\left(\frac{N^{86}}{N^{88}}\right)_{sample\ New}}{\left(\frac{N^{86}}{N^{88}}\right)_{sample\ ic}}\right)}{\log\left(\frac{mSr^{86}}{mSr^{88}}\right)}$$

eq.VI.16

With β_{new} better isotopic ratios of the sample can be calculated (eq.9 and eq.10 in the algorithm flow chart):

$$\left(\frac{N^{88}}{N^{84}}\right)_{sample\ New} = \left(\frac{N^{88}}{N^{84}}\right)_{sample\ ic} \cdot \left(\frac{mSr^{88}}{mSr^{84}}\right)^\beta$$

$$\left(\frac{N^{87}}{N^{84}}\right)_{sample\ New} = \left(\frac{N^{87}}{N^{84}}\right)_{sample\ ic} \cdot \left(\frac{mSr^{87}}{mSr^{84}}\right)^\beta$$

$$\left(\frac{N^{86}}{N^{84}}\right)_{sample\ New} = \left(\frac{N^{86}}{N^{84}}\right)_{sample\ ic} \cdot \left(\frac{mSr^{86}}{mSr^{84}}\right)^\beta$$

With latter values the algorithm starts again until abortion criteria is reached.

VI.4 Acknowledgements

At first I want to thank Prof. Anton Eisenhauer for intrusting me with the development of the Sr double spike method and his professional support during the whole course of my PhD. Additionally, Toni is kindly acknowledged for providing the great sample set on which our second publication is based. He really was a super-supervisor to me even if we had our disagreements from time to time.

I want to say a special thank you to Jan Fietzke who shared a lot of time with me freezing in front of the IFM-GEOMAR building while having a cigarette and discussing scientific problems. He really has a great share on this PhD-thesis and even if he was busy all the time he was never hesitating to answer my questions and helped me whenever he could.

Furthermore I like to thank Florian Böhm who supported my work with the knowledge of an excellent scientist. Discussion with him always resulted in progress of my work. Whenever I needed to find some literature he was the one who instantaneously advised a good publication.

Volker Liebetrau is acknowledged for his enthusiasm and for supporting me with his pansophy in all areas of my research. Ana Kolevica deserves my special thanks. In the beginning of my work at the IFM-GEOMAR she supported me by introducing me to all laboratory procedures and mass spectrometers. She is always happy and I will remember her as the “good soul” of the institute.

Hauke Vollstaedt of course is acknowledged for the fruitful und always funny discussions which often resulted in new ideas and different views on special problems. We had a great cooperation that accelerated the evolution of stable Sr isotope work to at least Mach 4. He really is one of the best colleagues one can imagine and surely will become a great scientist.

Jazec Raddatz is kindly acknowledged for the great time I had with him during the development of our manuscript and for being a friend. Of course he is also acknowledged for the scientific discussions we had and for developing simple phrases for complicated things like the “Interval of Maximum Calcification” – the “IMCA” – which I am sure will be known to every coral scientist in the future. All the colleagues that shared the office with me are kindly acknowledged for their support, their strong nerves and for the always nice and funny conversations we had. Tonja Soós as well as her lovely kids deserves special thanks because they had to suffer a lot from my unpredictable mood swings while working on this thesis.

Last but not least I will thank my family. They supported me in everything I have done in the past. Without them this work would have never been realized. And, of course I would like to thank all the people I might have forgotten.

Thank you all!

VI.5 Curriculum Vitae

André Krabbenhöft

Diplom Physiker

Personal Details

Address: Schneiderkoppel 22
24109 Melsdorf, Germany

Phone: +49 176 2383296

Email: ankrabbenhoeft@ifm-geomar.de

Date of birth: 12. January 1977

Place of birth: Rendsburg, Germany

Curriculum Vitae

Since 02/2008 PhD-student at the Leibniz Institute of Marine Science at Kiel
University, IFM-GEOMAR

10/2002 – 4/2007 Studies of physics/astronomy at the Ruprecht Karls University of
Heidelberg. Degree: Diplom-Physiker
Diploma Thesis: „Lucky Imaging of Quasar-Host-Galaxies“

10/1998 - 10/2002 Studies of physics at the University of Siegen